Synaptic Targeting of Neurotransmitter Receptors is Regulated by Neurobeachin

PhD Thesis

in partial fulfilment of the requirements
for the degree "Doctor of Philosophy (PhD)"
in the Neuroscience Program
at the Georg August University Göttingen,
Faculty of Biology

Submitted by

Ramya Nair

Born in
Mumbai, India

March 2011

Declaration

I hereby declare that this thesis has been written independently, with no other sources and aids than those cited.

Ramya Nair
Goettingen 14th March 2011

To my family

Table of Contents

List of Figures and Tables

Abstract

In neuronal network, information is transferred mainly via chemical synapses. Typically, a neuron receives thousands of inputs, which are transmitted by the activation of a large number of receptors present at postsynapses. Therefore, the functional integrity of synapses is tightly dependent on the localization and function of postsynaptic receptors. The receptor transport, anchoring, and turnover at postsynaptic sites all contribute to synaptic strength and are controlled by multiple trafficking, sorting, motor, and scaffolding proteins. In this study, Neurobeachin (Nbea), a neuron specific BEACH domain protein, was identified as a novel essential regulator of the trafficking of neurotransmitter receptors to postsynapses. The deletion of Nbea leads to a reduction in GABAergic and glutamatergic synaptic transmission due to reduced surface expression of $GABA_A$ and glutamate receptors. AMPA- type glutamate receptors are trapped in the endoplasmic reticulum and the Golgi apparatus of the Nbea KO neurons, and kainate, NMDA, and $GABA_A$ receptors do not reach the synapses in Nbea KO neurons. However, the total expression levels of pre- and postsynaptic proteins, the maturation and surface expression of membrane proteins, as well as presynaptic function and synapse formation are unperturbed upon Nbea loss. Thus, under resting conditions Nbea organizes the synaptic delivery of neurotransmitter receptors directly from the endoplasmic reticulum to synapses and thereby exerts a major influence on synaptic transmission.

1 Introduction

1.1 Information Processing in the Brain

The human brain is an extremely complex organ that functions as the information-processing unit of the central nervous system. The major building blocks of this unit are neurons and glial cells, each estimated to amount to 10^{11} or more in number (Azevedo et al., 2009). Neurons are polarized cells that possess a soma, multiple dendrites and typically one axon. For information transfer, the axon of a neuron forms presynaptic terminals or boutons (signal sender), which are typically in contact with the dendrites or somata of other neurons (signal receiver). These specialized contacts between the two cells were first shown towards the end of the 19th century by the Spanish anatomist Santiago Ramón y Cajal, who provided evidence for the neuron doctrine, according to which neurons are discrete cells that contact one another only at specialized junctions (Katz-Sidlow, 1998; Lopez-Munoz et al., 2006). These specialized junctions were termed ‘synapses’ by Sir Charles Sherrington in 1897. Through synapses, neurons form networks in the brain to relay information in the form of electrochemical signals, which control all conscious and unconscious behavior. Glial cells, on the other hand provide support and protection to neurons in the central nervous system and modulate synapse function (Edgar and Nave, 2009).

The brain contains two fundamentally different types of synapses, electrical and chemical synapses. At electrical synapses or gap junctions, the cytoplasm of the connecting cells is continuous via channels, allowing direct and fast electrical or chemical signaling (Bennett and Zukin, 2004). At chemical synapses, on the other hand there is no cytoplasmic continuity since pre- and postsynaptic compartments are separated by a synaptic cleft. In the vertebrate nervous system, most neurons communicate via chemical synapses since chemical synaptic transmission is very amenable to signal amplification or modulation (Waites et al., 2005).

1.2 Chemical Synaptic Transmission

The chemical synapse contains a presynaptic bouton, which is the site for neurotransmitter release, and a structurally separated postsynaptic compartment, which converts the chemical signal from neurotransmitter release back into an electrical signal. Chemical synaptic transmission is initiated by the invasion of an action potential (AP) in the presynaptic bouton, leading to opening of voltage gated Ca^{2+} channels and influx of Ca^{2+} ions into the presynaptic terminal. This transient elevation of Ca^{2+} ion concentration in the presynaptic terminal facilitates binding of Ca^{2+} to specific Ca^{2+} sensors, leading to the fusion of neurotransmitter-containing synaptic vesicles (SVs) with the plasma membrane (Sudhof, 2004). This process of membrane fusion occurs at specialized domains called active zones, which are equipped with SVs and contain a dense network of protein complexes that are essential in defining the release sites and regulating fast synchronous transmitter release and mobilization and refilling of SVs (Sudhof, 2004; Wojcik and Brose, 2007).

The neurotransmitter released from the presynaptic site diffuses through the synaptic cleft to bind neurotransmitter receptors present at the postsynaptic membrane. Similar to the active zone, the postsynaptic membrane is associated with a dense network of proteins collectively called postsynaptic density (PSD), which is rich in neurotransmitter receptors, ions channels, and scaffold and signaling molecules (Sheng, 2001).

The major neurotransmitters employed in the central nervous system are glutamate, GABA, glycine, dopamine, serotonin, and acetylcholine. These neurotransmitters are synthesized in the cytosol and loaded into SVs of presynaptic neurons by vesicular neurotransmitter transporters. Upon release, they can mediate various responses in the postsynaptic cell, depending on the receptors activated. The postsynaptic receptors can be ligand-gated ion channels, which, on activation, produce direct and fast forms of synaptic transmission, or they can be metabotropic receptors, which, upon activation, trigger second messenger cascades to produce slow forms of synaptic

transmission (Nicoll et al., 1990).

1.3 Synaptogenesis

Selective formation and stabilization of synapses is critical in determining the connectivity and functionality of neuronal networks. Synaptogenesis, the formation of functional synapses, requires the ability of an axon to grow and form appropriate connections with target neurons. Molecules like netrins, ephrinA, and semaphorins are essential in guiding axons to their target cell (Bagri and Tessier-Lavigne, 2002; Pascual et al., 2004; Tessier-Lavigne, 1995). Subsequently, contact formation is initiated by cell adhesion molecules (CAMs). Such CAMs include members of the cadherin, neuroligin, neurexin, SynCAM, and LRRTM protein families (Biederer et al., 2002; Garner et al., 2002; Graf et al., 2004; Linhoff et al., 2009; Scheiffele et al., 2000; Takai et al., 2003). Next, the newly formed contact sites recruit presynaptic and postsynaptic molecules to generate fully functional synapses.

Presynaptic active zone components such as Piccolo, Bassoon and RIM, as well as proteins of the release machinery like syntaxin and SNAP25 are first transported along axons on Piccolo-Bassoon transport vesicles (PTV) and delivered to presynaptic compartments (Shapira et al., 2003; Zhai et al., 2001). Subsequently, postsynaptic differentiation begins with the gradual accumulation of PSD proteins (Bresler et al., 2001; Friedman et al., 2000). Synapse maturation is the next phase of synaptogenesis, where the pre and postsynaptic elements undergo development in size and shape as well as in their number of presynaptic vesicles and postsynaptic receptors (Harris and Stevens, 1989; Pierce and Mendell, 1993; Schikorski and Stevens, 1997). The final phase of synaptogenesis involves activity dependent changes in the composition or number of synapses (Hashimoto and Kano, 2003; Knott et al., 2002; LeVay et al., 1980). However neuronal activity is not a prerequisite for synapse formation during development since synapse morphology and density are initially unaffected in the absence of neurotransmitter release (Verhage et al., 2000).

1.4 Excitatory and Inhibitory Signal Transmission

In the mammalian brain, there are two functionally different classes of chemical synapses, excitatory synapses and inhibitory synapses. At excitatory synapses, glutamate is employed as the major neurotransmitter. It typically acts on receptors that produce depolarization of the postsynaptic cell. On the other hand, at mature inhibitory synapses, GABA or glycine is released to activate receptors that produce hyperpolarization of the postsynaptic cell. These two classes of synapses can be distinguished by their morphology (Gray, 1959). Type I synapses are excitatory glutamatergic synapses that mainly form between an axon and a dendritic spine or dendritic shaft. These synapses contain predominantly round or spherical SVs and form distinct contacts that are distinguished by a thick postsynaptic density and prominent active zones. Type II synapses are inhibitory GABAergic synapses, which primarily form on dendritic shafts and neuronal cell bodies. SVs at these synapses are flattened or elongated in their appearance, and the synapse contains smaller active zones and less prominent postsynaptic densities.

Besides the morphological differences, there are major disparities between these synapses at the molecular level. For example, synaptic vesicles are defined as excitatory or inhibitory by their ability to sequester glutamate or GABA/glycine respectively. At excitatory synapses, vesicular glutamate transporter (VGLUT) mediate glutamate uptake into synaptic vesicles (Takamori et al., 2000; Wojcik et al., 2004) and at inhibitory synapses, VIAAT (vesicular inhibitory amino acid transporter) is responsible for the uptake of both GABA and glycine into SVs (Wojcik et al., 2006). In addition, major differences are observed in protein composition and assembly of PSDs between these two classes of synapses.

The PSD is a multiprotein complex comprising receptors, signaling molecules, ion channels, cell adhesion molecules, and scaffolding proteins. Excitatory PSDs contains two major types of ionotropic glutamate receptors: AMPA (α-amino-3-hydroxy-5-methyl-4- isoxazolepropionic acid) receptors and NMDA

(N-methyl-D-aspartic acid) receptors (Bekkers and Stevens, 1989; Okabe, 2007), which are indirectly linked to each other via proteins of the postsynaptic scaffold (Wenthold et al., 2003). These receptors are absolutely essential for maintaining the basic synaptic function of neurons but are dispensable for the maintenance of the basic PSD morphology (Kuriu et al., 2006; Meng et al., 2003; Zamanillo et al., 1999). Another important component of the PSD is the cytoplasmic signaling molecule calcium-calmodulin-dependent protein kinase II (CaM kinase II) (Kennedy et al., 1983), which has been implicated in structural modification of the cytoskeleton (Costa et al., 1999; Shen and Meyer, 1999; Shen et al., 1998) and in maintaining postsynaptic receptor function and number (Gardoni et al., 1998; Hayashi et al., 2000; Lisman and Zhabotinsky, 2001; Nicoll and Malenka, 1999). Other prominent PSD proteins include scaffolding molecules of the membrane-associated guanylate kinase (MAGUK) family of proteins, composed of three PDZ domains, a src homology (SH3) domain and a guanylate kinase (GK) domain (Kim and Sheng, 2004). The best-characterized member of this family of proteins is PSD-95, which can directly interact via its PDZ domains with the NR2 subunit of the NMDA receptor (Kornau et al., 1995) and voltage gated potassium channels (Kim et al., 1995). Other important binding partners of PSD-95 are the postsynaptic adhesion molecules of the neuroligin family (Irie et al., 1997), which reach into the synaptic cleft and interact with neurexin (present on the presynaptic side). AMPA receptor recruitment into the PSD is also regulated indirectly by PSD-95 via its interaction with stargazin, which is a member of the transmembrane AMPA receptor regulatory protein (TARP) family (Chen et al., 2000). In addition to this, AMPA receptors also bind directly to other PSD proteins with PDZ domains like glutamate receptor-interacting protein (GRIP), AMPA receptor-binding protein (ABP), and protein interacting with C kinase 1 (PICK1) (Barry and Ziff, 2002; Dong et al., 1997; Xia et al., 1999). These interactions are critical for receptor function and clustering at the excitatory PSD. Therefore, regarding glutamatergic synapses, the complex interplay between the various PSD proteins is essential for the regulation of excitatory postsynaptic transmission.

At inhibitory synapses, the PSD is composed of an entirely different set of proteins. Glycine receptors and γ-aminobutyric type A ($GABA_A$) receptors are the major inhibitory receptors in the central nervous system, and, unlike the PSD of excitatory synapses, inhibitory synapses do not contain an elaborate network of proteins belonging to the MAGUK family. Gephyrin is the major scaffolding protein of inhibitory synapses, which interacts directly with glycine receptors, thereby facilitating synaptic clustering of glycine receptors (Meyer et al., 1995). In the case of $GABA_A$ receptors, a direct interaction with gephyrin had not been demonstrated even though different isoforms of $GABA_A$ receptors colocalize with gephyrin (Sassoe-Pognetto et al., 2000) and deletion of gephyrin affects $GABA_A$ receptor clusters at the synapse (Levi et al., 2004). $GABA_A$ receptor-associated protein (GABARAP), which is a microtubule linker protein, interacts with both gephyrin (Kneussel et al., 2000) and $GABA_A$ receptors (Wang et al., 1999). However GABARAP is not localized at inhibitory synaptic sites (Kneussel et al., 2000) and deletion of GABARAP has no effect on synaptic function of $GABA_A$ receptor (O'Sullivan et al., 2005) indicating that the interaction of GABARAP with $GABA_A$ receptors and gephyrin is not important for receptor anchoring. It is clear that the excitatory and inhibitory synapses are very distinct in the central nervous system. The factors responsible for the differences in function and organization of excitatory and inhibitory PSD act already at the level of biosynthesis, assembly, and cellular trafficking of PSD proteins to the postsynaptic membrane.

1.5 Neuronal Protein Trafficking

Much of the current knowledge on intracellular protein trafficking is derived from genetic analyses of *Saccharomyces cerevisiae* (Antonny and Schekman, 2001; Lee et al., 2004). These mechanisms of protein trafficking also apply to neurons since the same major organelles are involved in the secretory pathway of neurons and yeast. Given the immense size and complex architecture of neurons, trafficking of membrane proteins and lipids to the appropriate subcellular locations is a major challenge. Most proteins

destined for cell membranes are translated at the ER, where they undergo major conformational changes as well as posttranslational modifications to ensure exit of correctly synthesized and folded proteins (Kleizen and Braakman, 2004). Protein cargo leaves the ER in COPII-coated vesicles. These deliver this cargo to the Golgi apparatus, where newly synthesized proteins undergo further modifications, like glycosylation, as they advance to the trans Golgi network (TGN), where they are sorted and transported to various membrane compartments (Kennedy and Ehlers, 2006; Kuehn and Schekman, 1997).

In neurons, ER and Golgi compartments are not restricted to somata but also present in dendrites, thus providing postsynapses with the ability to control synaptic strength by localized protein synthesis and sorting (Gardiol et al., 1999; Kacharmina et al., 2000; Spacek and Harris, 1997; Torre and Steward, 1996). However, Golgi outposts are not found along all dendrites, indicating that bulk protein trafficking occurs via the somatic Golgi (Horton and Ehlers, 2003; Kennedy and Ehlers, 2006).

Along axons, transport of vesicles containing preassembled AZ components to presynaptic compartments has been reported (Shapira et al., 2003; Zhai et al., 2001). However recruitment of proteins into the PSD is fundamentally different from the AZ assembly since the trafficking of postsynaptic receptors and their scaffolding molecules appears to be regulated differentially.

1.6 AMPA Receptor Trafficking

AMPA receptors are tetrameric molecules, composed of different combinations of GluA1, GluA2, GluA3, and GluA4 receptor subunits (Hollmann and Heinemann, 1994; Rosenmund et al., 1998), which can form homomeric and heteromeric functional receptors. The dimerization of AMPA receptors starts early in the ER, and in mature neurons of the hippocampus most of the AMPA receptors are composed of GluA1/2 or GluA2/3 combinations (Wenthold et al., 1996b). AMPA receptors composed of GluA1/2 subunits exit the ER rapidly, and undergo glycosylation in the Golgi network,

unlike GluA2/3 heteromers, which are retained longer in the ER. In fact studies on glycosylation patterns of AMPA receptors subunits revealed the presence of a stable GluA2 subunit pool retained in the ER, which is controlled by Arg607 at the channel pore region of the GluA2 subunit (Greger et al., 2002). In addition, ER exit and trafficking of the AMPA receptors subunits requires the interaction of the C terminal domain of AMPA receptor subunits with PDZ domain containing proteins like SAP97 and PICK1, which bind GluA1 and GluA2 subunits, respectively. It has been suggested that the selective interaction of GluA1 with SAP97 regulates faster ER export of GluA1/2 receptor subunits (Greger et al., 2002; Sans et al., 2001).

The majority of AMPA receptors are synthesized far away from postsynaptic compartments. Therefore, precise targeting of AMPA receptors is achieved by long-range dendritic transport of receptors along microtubules via interactions with motor proteins (Kennedy and Ehlers, 2006). Two possible mechanisms have been postulated for AMPA receptor trafficking along dendrites, both involving the PDZ domain protein GRIP1. GRIP1 can interact directly with kinesin (KIF5) and indirectly with KIF1 via liprin-α to form GluA2-GRIP1-Kinesin complex, allowing dendritic transport of GluA2 to postsynaptic compartments (Setou et al., 2002; Shin et al., 2003; Wyszynski et al., 2002). The postsynaptic compartments of neurons are rich in actin. Therefore, AMPA receptor containing transport vesicles need to be transferred from the microtubular system to an actin based cytoskeletal system for final transport to the PSD. A possible adaptor between AMPA receptors and the actin cytoskeleton are the 4.1 family proteins, which can interact directly with GluA1 and GluA4 and regulate their surface expression (Coleman et al., 2003; Shen et al., 2000). Finally, efficient postsynaptic assembly is achieved by synaptic anchoring and stabilization of AMPA receptors. This is again regulated via direct interaction of AMPA receptors with PDZ domain proteins like GRIP1/ABP and PICK1 (Barry and Ziff, 2002; Dong et al., 1997; Osten et al., 2000; Xia et al., 1999) and indirect interaction of AMPA receptors with PSD-95 via stargazin (Chen et al., 2000).

The levels of AMPA receptors in postsynaptic compartments is tightly regulated by synaptic activity (Kessels and Malinow, 2009). AMPA receptors can be inserted into synapses by two different pathways, depending on the subunit composition. GluA2/3 receptors are inserted continuously in an activity independent manner into synapses whereas GluA1/2 receptors as well as GluA4 containing receptors are inserted into synapses in an activity dependent manner, which depends on NMDA receptor activation (Shi et al., 2001; Wenthold et al., 1996b; Zhu et al., 2000). The constitutive pathway involving continuous cycling of GluA2/3 receptors is essential in preserving the numbers of AMPA receptors at synapses. Instead, the regulated pathway involving activity dependent trafficking of GluA1/2 is involved in plasticity-induction, leading to enhancement of synaptic strength also called long-term potentiation (LTP) (Durand et al., 1996; Hayashi et al., 2000; Shi et al., 2001).

Similar to the constitutive and regulated mechanisms of receptor delivery to synapses, AMPA receptors are also trafficked out of synapses via constitutive regulated pathways. The regulated removal of AMPA receptors leads to long-term depression (LTD) of synaptic strength, which, unlike LTP, affects all AMPAR subunits (Bhattacharyya et al., 2009; Lee et al., 2002). The signaling cascade mediating the regulated delivery and removal of AMPAR involves a complex interplay between many signaling pathways, involving PKA (Esteban et al., 2003), PKC (Kim et al., 2001), CaMKII (Lee et al., 2000) and the mitogen-activated protein kinase (MAPK)(Zhu et al., 2002).

1.7 NMDA Receptor Trafficking

NMDA receptors are tetrameric complexes formed by the assembly of GluN1, GluN2, and GluN3 subunits. There are eight different GluN1 subunits generated by alterative splicing from single gene, four different GluN2 subunits (GluN2A, GluN2B, GluN2C, GluN2D), which originate from different genes, and two different GluN3 subunits, which are also generated from different genes (Wenthold et al., 2003). In the brain, the majority of NMDA receptors are composed of two GluN1 and two GluN2 subunits (Dingledine et

al., 1999). In the forebrain, GluN2A and 2B are the most abundantly expressed GluN2 subunits. The GluN2B subunit is expressed early in development and its levels gradually decrease with age, whereas expression of GluN2A is low shortly after birth and increases with age (Williams et al., 1993). GluN1 and GluN2A subunits assemble in the ER to form functional NMDA receptors. In fact, GluN1 and GluN2 subunits, when expressed alone in heterologous cells, are retained in the ER and not efficiently targeted to the plasma membrane (McIlhinney et al., 1996; Okabe et al., 1999). Thus, the correct stoichiometry and assembly of NMDA receptors in neurons is a prerequisite for NMDA receptor export. Retention of non-assembled subunits is ensured by ER retention motifs at the C termini of the NMDA receptor subunits (Scott et al., 2001).

Similar to AMPA receptors, most of the NMDA receptors are delivered from the somatic Golgi apparatus to the dendritic spines (Kennedy and Ehlers, 2006). Two independent pathways have been proposed for long-range dendritic transport of NMDA receptors. mLin10, which is a constituent of a complex associated with cargo carrying NMDA receptors, can interact with the kinesin molecule KIF17 to directly transport NMDA receptors along microtubules to synapses (Setou et al., 2000). In addition, NMDA receptors interact with SAP102, a MAGUK family protein, and with the exocyst complex component sec8 (Hsu et al., 1999), indicating another possible transport mechanism by which NMDARs and PSD-95 family of proteins are delivered together to synapses (Sans et al., 2003).

The synaptic organization of NMDA receptors can be influenced by several additional proteins, most of which belong to the MAGUK family (Kim and Sheng, 2004; Wenthold et al., 2003). In fact, deletion of the C terminal PDZ binding domain of NR2A inhibits synaptic localization of NMDA receptors, indicating PDZ domain binding is essential for synaptic targeting of NMDA receptors (Steigerwald et al., 2000). However, deletion or overexpression of individual PDZ domain proteins does not affect the delivery of NMDA receptors to synapses (El-Husseini et al., 2000; McGee et al., 2001; Schnell et

al., 2002) indicating that different synaptic PDZ proteins operate in a redundant manner to control the synaptic targeting of NMDA receptors.

NMDA receptors play a pivotal role in inducing activity dependent LTP and LTD (Malenka and Bear, 2004). At resting membrane potential, NMDARs are inactive due to the presence of Mg^{2+} ions that block the receptor channel pore. Activation of NMDARs requires the depolarization of the postsynaptic membrane (Ascher and Nowak, 1988; Mayer et al., 1984; Nowak et al., 1984) and simultaneous binding of glycine, which binds to the GluN1 subunit, and of glutamate, which binds to the GluN2 subunit (Furukawa et al., 2005; Johnson and Ascher, 1987). Once activated, these receptor channels are permeable to Ca^{2+} ions (besides Na^{+} and K^{+} ions), which leads to neuronal depolarization and activation of downstream signaling pathways, ultimately affecting synaptic AMPA receptor density (Hayashi et al., 2000; Lee et al., 2003) and NMDA receptor population (Grosshans et al., 2002; Harney et al., 2008; Montgomery et al., 2005).

1.8 Kainate Receptor Trafficking

Kainate receptors (KARs) are tetrameric glutamate receptors composed of GluK1, GluK2, GluK3, GluK4, and GluK5. GluK1-3 can form functional homomeric and heteromeric receptors, whereas GluK4 ad GluK5 cannot form functional homomeric receptors and generally co-assemble with other KARs subunits (Coussen, 2009). KARs are widely distributed in the mammalian brain and unlike AMPA and NMDA receptors, operate in different subcellular compartments. Indeed, KARs are localized at both presynaptic and postsynaptic sites and play an essential role in modulating synaptic activity (Bettler and Mulle, 1995; Lerma, 2003).

The molecular mechanisms accounting for polarized targeting of KARs are largely unknown. Presynaptic KARs are observed at both excitatory and inhibitory synapses. They play an essential role in modulating the release of glutamate (Lauri et al., 2001; Schmitz et al., 2001) and GABA (Clarke et al., 1997; Rodriguez-Moreno et al., 1997) and facilitate short-term and long-term

plasticity (Bortolotto et al., 1999; Contractor et al., 2001). Postsynaptic KARs function like AMPA and NMDA receptors as carriers of excitatory currents, leading to depolarization of postsynaptic membrane compartments (Castillo et al., 1997; Vignes and Collingridge, 1997).

Like most membrane proteins, KARs are assembled in the ER and undergo quality control for efficient delivery to their subcellular locations. GluK1-3 subunits of KARs undergo alterative splicing to generate splice variants that differ in the sequence of their cytoplasmic C-termini and which exhibit differential rates of intracellular trafficking and surface expression (Jaskolski et al., 2004; Jaskolski et al., 2005; Ren et al., 2003b). An intact ligand-binding site of GluK2 is essential for membrane expression of KARs expressing this subunit (Mah et al., 2005). In addition, ER retention signals have been identified on the GluK5 subunits, and oligomerization of GluK5 and GluK2 is critical to sterically shield these ER retention signals (Hayes et al., 2003; Ren et al., 2003a).

KAR subunits exhibit diverse interactions with proteins due to differences in their C terminal domain. The microtubule motor protein KIF17 interacts with GluK2 and GluK5 to form a GluK2-GluK5-KIF17 complex that is essential for dendritic transport of KARs (Kayadjanian et al., 2007). In addition several PDZ domain proteins such as PSD95, GRIP, and PICK1 interact with the C terminal domain of GluK2. However, these interactions regulate synaptic anchoring but not trafficking of KARs from ER to plasma membrane (Garcia et al., 1998; Hirbec et al., 2003).

1.9 Glycine Receptor Trafficking

Glycine receptors (GlyRs) are pentameric and function as inhibitory receptors in mature neurons (Betz, 1990). In the CNS, GlyRs are expressed most prominently in spinal chord, retina, and brainstem, and less in higher brain regions (Fujita et al., 1991; Malosio et al., 1991; Watanabe and Akagi, 1995). GlyRs are assembled from α subunits and β subunits (Langosch et al., 1988)

in the ER to form functional homo-oligomers of α subunits or hetero-oligomers of α and β subunits with a 3:2 stochiometry (Hoch et al., 1989; Langosch et al., 1988; Takahashi et al., 1992). The mouse genome contains four GlyR α subunit genes and one β subunits gene. Like other membrane proteins, GlyRs undergo multiple posttranslational maturation steps, and the extracellular N terminal domains of the subunits are required for the formation and ER exit of functional GlyRs (Griffon et al., 1999; Kuhse et al., 1993).

Unlike the glutamate receptors, which interact with the cytoskeleton via PDZ proteins, GlyRs interact directly with microtubule-associated proteins (Sheng and Pak, 2000). Gephyrin, a microtubule binding protein, is a key component of the inhibitory postsynaptic scaffold and a binding partner of GlyRs. The interaction with gephyrin is mediated mainly with the β subunit of GlyRs (Meyer et al., 1995). GlyR-gephyrin complexes are known to interact with motor proteins such as KIF5 and Dynein, indicating a direct involvement of gephyrin in anterograde and retrograde trafficking of GlyRs between the soma and the synaptic plasma membrane (Maas et al., 2009; Maas et al., 2006). Moreover, deletion studies in mice showed that Gephyrin plays a crucial role in GlyR clustering at synapses (Feng et al., 1998; Levi et al., 2004).

1.10 $GABA_A$ Receptor Trafficking

In the mammalian brain, $GABA_A$ receptors mediate most of the inhibitory synaptic transmission (Sieghart and Sperk, 2002). Similar to GlyR, $GABA_A$ receptors are pentamers. They are assembled from seven different classes of subunits, of which some have multiple isoforms that are generated from different genes: α (1-6), β (1-3), γ (1-3), δ, ε (1-3), π and θ. Structurally, $GABA_A$ receptors can thus be very diverse, but in the brain, the majority of them are composed of two α, two β and one γ (or δ) subunits (Rudolph and Mohler, 2004). The different subunit compositions of $GABA_A$ receptors provides them with different physiological and pharmacological properties. For example, receptors composed of α1-3 along with β and γ subunits are benzodiazapine-sensitive and localized synaptically, mediating phasic

inhibition (Rudolph and Mohler, 2004), whereas the receptors containing the α5 subunit are localized extrasynaptically (Brunig et al., 2002). Receptors composed of α4 or α6 along with β and δ subunits are benzodiazapine-insensitive extrasynaptic receptors, mediating tonic inhibition (Brunig et al., 2002).

Theoretically, $GABA_A$ receptors can be assembled in many different combinations of receptor subunits, but only a few of those can exit the ER and reach the plasma membrane. ER-chaperone molecules like immunoglobulin heavy chain binding protein (BiP) and calnexin retain $GABA_A$ receptors, that are assembled incorrectly in the ER (Connolly et al., 1996). The fate of $GABA_A$ receptors subunits can also be modulated by activity dependent ubiquitination and degradation at the level of the ER to regulate the efficacy of synaptic inhibition (Saliba et al., 2007). After their assembly, $GABA_A$ receptors are inserted into the plasma membrane and several proteins like $GABA_A$R-associated protein (GABARAP) (Wang et al., 1999), Brefeldin-A-inhibited GDP/GTP exchange factor 2 (BIG2) (Charych et al., 2004), GABAAR-interacting factor 1 (GRIF1) (Smith et al., 2006) and *N*-ethylmaleimide-sensitive factor (NSF) (Goto et al., 2005) are known binding partners of $GABA_A$ receptor subunits. However a clear molecular mechanism of $GABA_A$ receptor transport has not emerged yet. Depending on the subunit composition, $GABA_A$ receptors are delivered either to the synapse or to extrasynaptic membrane domains (Brunig et al., 2002).

A candidate molecule implied in $GABA_A$ receptor clustering at inhibitory synapses is gephyrin. Gephyrin colocalizes with the majority of synaptic $GABA_A$ receptor subunits in the brain (Sassoe-Pognetto et al., 2000) and deletion of gephyrin affects synaptic $GABA_A$ receptor clustering (Levi et al., 2004), supporting the idea of gephyrin promoting the stability of synaptic $GABA_A$ receptor subunits. However, unlike GlyRs, complete loss of $GABA_A$ receptor subunits is not observed in gephyrin KO mice, indicating the existence of gephyrin independent mechanisms of $GABA_A$ receptor clustering at inhibitory postsynapses (Kneussel et al., 2001).

1.11 Neurobeachin, BEACH Domain Protein and AKAP

Neurobeachin (Nbea) is very large (327 kDa) cytosolic protein expressed exclusively in neuronal and endocrine cells (Wang et al., 2000). Its isoform LPS-responsive beige-like anchor protein (LRBA) is expressed ubiquitously in all cell types and is upregulated in cancer cells and stimulated immune cells (Wang et al., 2001). In neurons, Nbea is localized in association with tubulovesicular endomembranes of the Golgi complex and distributed throughout the cell body and dendrites. Association of Nbea with the Golgi complex is stimulated by GTPγS and inhibited by brefeldinA indicating a possible involvement of Nbea in neuronal trafficking (Wang et al., 2000). Studies in *C. elegans* mutants lacking the Nbea homolog SEL-2 indicated that Nbea/SEL-2 might be a negative regulator of lin/Notch activity affecting endosomal trafficking of LET-23/EGFR (de Souza et al., 2007). Similarly, mutations in DAKAP550/rugose, an Nbea homolog of *Drosophila*, lead to phenotypic changes arising from abnormalities in Notch and EGFR signaling (Shamloula et al., 2002). All these findings indicate an essential role of Nbea during early nerve cell development. In mice, Nbea expression starts at E10.5 and increases progressively with age (Su et al., 2004). Homozygous deletion of Nbea in mice leads to perinatal lethality, confirming that neurobeachin is crucial for proper development (Medrihan et al., 2009; Su et al., 2004). Functional analyses of the neuromuscular junction (NMJ) and brainstem of Nbea KO mice indicate a possible involvement of Nbea in presynaptic regulation and release of neurotransmitters (Medrihan et al., 2009; Su et al., 2004).

The human neurobeachin (NBEA) gene contains a region of chromosomal instability on chromosome13, which was identified in linkage studies as a candidate region of autism (Savelyeva et al., 2006), and rearrangements in the NBEA gene have been observed in patients suffering from idiopathic, non-familial autism (Castermans et al., 2003). Based on these results NBEA is considered a candidate gene for autism.

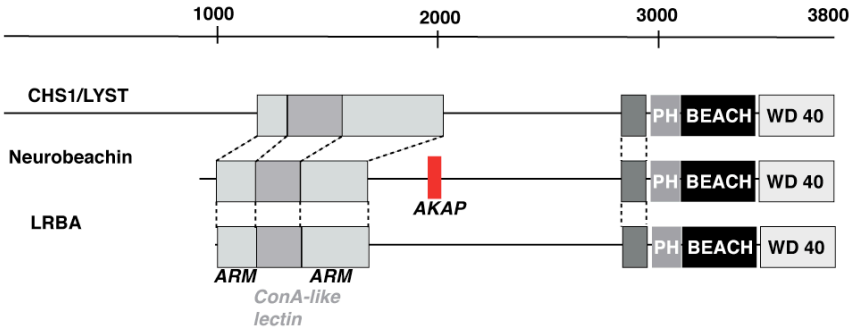

Figure 1.1: Domain structure of BEACH proteins.

The C termini of LYST, Nbea, and LRBA contain a PH and a BEACH domain, and multiple WD40 repeats. The N termini end contains Armadillo Repeats (ARM) and a ConA-like lectin domain. An AKAP motif is present only in Nbea. (Modified from Burgess et al., 2009).

Nbea and LRBA belong to the family of BEACH proteins. At their C termini they contain PH and BEACH domains, which are followed by WD40 repeats (Figure 1.1). Structural analyses of Nbea and LRBA have shown the BEACH domain to interact with the PH domain, but the molecular function of this interaction is unknown (Gebauer et al., 2004; Jogl et al., 2002). The BEACH domain is an evolutionarily ancient domain, and a well-characterized protein containing this domain is LYST. Mutations in the LYST gene are causing the *beige* mouse phenotype and Chediak-Higashi syndrome (CHS) in humans, which is characterized by severe immunological deficiencies accompanied by abnormalities in pigmentation and blood clotting (Spritz, 1998). At the cellular level, this mutation affects sorting of proteins, leading to enlargement of lysosomes (Burkhardt et al., 1993).

At their N termini, Nbea contains a ConcavalinA (ConA)-like lectin domain (Figure 1.1), which may be involved in binding and sorting oligosaccharide side chains of proteins. In Nbea this domain is flanked on either side by HEAT/ Armadillo (ARM) repeats (Burgess et al., 2009). In addition to the C terminus sequence homology, the upstream sequences of LYST also resemble those of Nbea in length, and amino acid composition, and certain

sequences of LYST resemble the ARM repeats of Nbea (Nagle et al., 1996). Due to these similarities in structure, Nbea might be functionally related to LYST. Moreover, functional analysis of LvsA, another member of the BEACH protein family in *Dictyostelium* revealed a critical role of BEACH domain proteins in plasma membrane dynamics during cell division (Wang et al., 2002). Therefore, it is conceivable that Nbea might be involved in sorting and trafficking of neuron specific proteins to the plasma membrane.

Apart from containing a BEACH domain, Nbea functions as an A-kinase anchoring protein (AKAP) due to its ability to bind the type II regulatory subunit (RII) of protein kinase A (PKA) (Colledge and Scott, 1999; Wang et al., 2000). AKAPs are molecules involved in recruiting PKA to different subcellular locations (Wong and Scott, 2004), and this interaction is essential in modulating synaptic function (Rosenmund et al., 1994). In neurons, type II isoforms of PKA are expressed exclusively along somata and dendrites (De Camilli et al., 1986; Zhong et al., 2009). The dendritic targeting of PKA is mediated by microtubule-associated protein MAP2 (Zhong et al., 2009).

Phosphorylation is a key mechanism regulating glutamate receptor localization at synapses, and AKAP79/150 is a major PKA binding protein at the excitatory PSD modulating the expression of AMPA receptors in an activity-dependent manner (Bhattacharyya et al., 2009). In neurons, the distribution of Nbea and the RII isoform of PKA are similar (De Camilli et al., 1986; Wang et al., 2000). Therefore, it is possible that Nbea is involved in recruiting and targeting PKA to specific substrate proteins.

2 Aim of the Study

The present study was aimed at elucidating the function of Neurobeachin in nerve cells. For this purpose, I planned to study the phenotypic consequences of Neurobeachin loss-of-function in mouse neurons, focusing on

- changes in synaptic transmission,

- morphological changes in cultured neurons,

- cell biological changes in protein trafficking in cultured neurons, and

- biochemical changes in protein processing in cultured neurons.

In addition, I planned to investigate the role of individual Neurobeachin domains by employing over-expression studies in cultured neurons.

3 Materials and methods

3.1 Materials

3.1.1 Chemicals and Reagents

Agarose	Sigma-Aldrich GmbH
Albumine, Bovine	Sigma-Aldrich GmbH
Ammonium Persulfate (APS)	Sigma-Aldrich GmbH
Aprotinin	Roche Diagnostics GmbH
ATP/GTP	Sigma-Aldrich GmbH
B-27 Supplement	Life Technologies Gibco BRL GmbH
BSA	Pierce Biotechnology
Calcymicin	Calbiochem
Cell Culture Flasks	Firms Greiner, Costar, Falcon, Nunc
Collagen	BD Biosciences
Cysteine	Sigma-Aldrich GmbH
DMEM (Dulbecco's MEM)	Life Technologies Gibco BRL GmbH
DMSO	Sigma-Aldrich GmbH
dNTPs	Pharmacia Biotech GmbH
Dry Milk	Nestle
ECL Films and Reagent	Amersham-Buchler GmbH & Co
Electroporation Cuvettes	BioRad Laboratories GmbH
EZ-Link NHS-SS Biotin	Pierce Biotechnology
Ethidium Bromide	Sigma-Aldrich GmbH
FBS	Life Technologies Gibco BRL GmbH
FM1-43	Molecular Probes
GABA	Sigma-Aldrich GmbH
Glucose	Sigma-Aldrich GmbH
Glutamate	Sigma-Aldrich GmbH
GlutaMAX TM I	Life Technologies Gibco BRL GmbH
Glycine	Sigma-Aldrich GmbH

Goat serum	Life Technologies Gibco BRL GmbH
HBSS (Hank's balanced salt solution	Life Technologies Gibco BRL GmbH
Hepes	Sigma-Aldrich GmbH
Kainic Acid	Sigma-Aldrich GmbH
L-Glutamine	Life Technologies Gibco BRL GmbH
Luria Broth (LB) Medium	Sigma-Aldrich GmbH
Leupeptin	Roche Diagnostics GmbH
MITO	BD Biosciences
MK-801	Sigma-Aldrich GmbH
Neurobasal Medium	Life Technologies Gibco BRL GmbH
Neutravidin	Pierce Biotechnology
Papain	Worthington Biomedical Corporation
PBS	PAA Chemical Company
Penicillin/Streptomycin	Life Technologies Gibco BRL GmbH
Plastic Tubes	Greiner, Falcon und Brandt
PMSF	Roche Diagnostics GmbH
Poly-D-Lysine / Poly-L-Lysine	Sigma-Aldrich GmbH
Polyacrylamide (AMBA solution)	BioRad Laboratories GmbH
Ponceau S	Sigma-Aldrich GmbH
Protein Assay	BioRad Laboratories GmbH
Protein Molecular Weight Standard	Fermentas GmbH
Reaction Eppendorf Tubes	Eppendorf
SDS Roche	Diagnostics GmbH
Sodium Cholate	Sigma-Aldrich GmbH
Sucrose	Sigma-Aldrich GmbH
TEMED	BioRad Laboratories GmbH
Tris Base	Sigma-Aldrich GmbH
Triton X-100	Roche Diagnostics GmbH
Trypsin EDTA	Life Technologies Gibco BRL GmbH
Trypsin Inhibitor	Sigma-Aldrich GmbH
TTX	Tocris Cookson Inc.

Tween 20	Sigma-Aldrich GmbH
Whatman 3MM	Whattmann International Ltd
Whatmann-Cellulose Filter Nr.1	Biometra GmbH

3.1.2 Kits and Apparatus

1.5 ml Eppendorf Shaker	Eppendorf GmbH
Centrifuges	Eppendorf GmbH, Heraeus GmbH
Developer	Agfa-Gevaert GmbH
Electroporation Apparatus	BioRad Laboratories GmbH
Electroporation system agarose gels	Life-Technologies Gibco-BRL GmbH
Electroporation system SDS-PAGE	BioRad Laboratories GmbH
Endofree Maxi Kit	Qiagen
Freezer/ Refrigerators	Libherr
Gel Photography	Apparatus Intas GmbH
Heating Block	Eppendorf GmbH
Hoeffer electrophoresis unit	Amersham pharmacia biotech
Incubators	Heraeus GmbH
Nexttex DNA Extraction Kit	Nexttex Biotechnology
PCR Machine	Biometra GmbH
pH Meter	Knick, Schuett GmbH
Pipettes, Pipetteboy	Gilson and Brandt GmbH
Shaking Incubator	New Brunswig Scientific GmbH
Spectrophotometer	Pharmacia
Transfection Kit	Clontech
Tris Acetate gels 3-8%	Invitrogen
Water Bath	Biometra GmbH

3.1.3 Antibodies

Antibodies	**Source**	**WB**	**ICC**

Actin	Ms Sigma Aldrich	1:4000	
β-Tubulin	Ms Sigma Aldrich	1:30000	
GABA-A γ2	Rb Abcam/GPFritschy	1:1000	1:5000
GABA-A α1	Rb chemicon	1:1000	
GABA-A α5	G.P Fritschy		1:5000
GluR1	Rb, Upstate	1:1000	
GluR2	Ms, Chemicon		1:200
GluR2/3	Rb, Chemicon	1:1000	1:500
GluR6/7	Rb, Upstate	1:1000	
Gephyrin	Ms (3B11) SySy		1:3000
MAP2	Chicken Novus		1:4000
Munc-13-1	Rb Dr. Varoqueaux	1:1000	
Neurobeachin	Rb, SySy	1:2000	1:1000
Neuroligin1	Ms Dr. Varoqueaux		1:5000
NR1	Ms(M68) SySy	1:1000	
NR2A	Rb Chemicon	1:1000	1:500
PSD95	Ms, AbCam	1:2000	1:1000
Rab3a	Ms SYY	1:4000	
Synapsin	Ms, SySy		1:2000
Synaptophysin	Ms (7.2), SySy	1:20000	
Synaptotagmin 1	Rb, SySy	1:1000	
TfR	Ms Zymed	1:2000	
VIAAT	Rb SySy	1:2000	1:2000
VGLUT1	Rb SySy	1:2000	1:2000
Anti-mouse. Anti-Guinea Pig, ,Anti-Rabbit (from Goat)	Horse Radish peroxidase Conjugate	1:5000	
Anti-mouse. Anti-Guinea Pig, Anti-Rabbit, Anti-	Alexa Fluor 488/555/633 Molecular Probes		1:2000

chicken (from Goat)			

3.2 Methods

3.2.1 Astrocyte Culture for Mouse Neuronal Autaptic Cultures

The microisland astrocyte feeder cells were prepared two days before plating neurons. In order to culture astrocytes in a microisland, sterilized coverslips were first coated with agarose, which forms a non-permissive substrate where cells are reluctant to attach. Following this, the PDL/acetic acid/collagen coating solution (3:1:1 acetic acid, PDL, collagen) was stamped onto the agarose to form 'islands' using custom-made stamp (200 x 200 µm). Before usage the plates were sterilized under UV for 20mins.

To obtain astrocytes, mouse cortices from newborn WT animals were digested for 20 minutes in Trypsin/EDTA at 37°C with gentle agitation (1 ml/cortex). The supernatant was carefully discarded, and FBS (10% FBS, MITO, Pen/Strep, in DMEM) was added and incubated for 15 min at 37°C. After discarding the supernatant, 0.2 ml of prewarmed FBS was added, and brains were triturated following which the supernatant was transferred to prewarmed FBS Medium. Cells were plated into a T-75 culture flask. The medium was exchanged the day after plating and cells were left to grow in a monolayer until confluence was reached (normally a week to 10 days). Cells from the T-75 culture flask were then treated with Trypsin (5ml Trypsin/EDTA), counted and plated at a density of 12.000 cells per well of 6-well plates containing microdot-coated coverslips.

3.2.2 Treatment of Coverslips for Culturing Primary Neurons (Continental Cultures)

To ensure adhesion of cultured neurons, the surface of coverslips was coated

with PLL under sterile conditions. The coverslips were incubated with PLL for one hour (usually overnight) at 37°C, washed twice with sterile water, once with HBSS and then incubated with Neurobasal medium at 37°C.

3.2.3 Mouse Neuronal Cultures and Transfection

The neuron cultures were prepared as per (Jockusch et al., 2007) . The Papain solution (1 ml of solution contains 2 mg Cystein, 10 ml DMEM, 1 mM $CaCl_2$, 0.5 mM EDTA) was prepared by addition of 20-25 units of papain. This solution was mixed and bubbled with carbogen (95% oxygen, 5% carbon dioxide) for 20 minutes (until the solution was clear). The papain solution was sterilized by filtration through a 0.2 mm filter just before use. The brains of E18 embryos were quickly removed (Nbea deletion mutant, or wild-type mice) and collected in HBSS at room temperature following which the hippocampi were dissected out and transferred immediately to 0.5 ml Papain solution, pre-warmed at 37°C, and incubated for approximately 45-50mins at 37°C with gentle agitation. Papain was removed and the hippocampi were incubated with pre-warmed Stop Solution (25 mg albumine, 25 mg trypsin inhibitor, 9 ml Dulbecco's MEM (DMEM), 1 ml FCS. The solution was kept in a water bath at 37°C until use) for 15-20 minutes at 37°C with gentle agitation. Further, the supernatant was removed and the tissue was rinsed in 500 µl of pre-warmed NBA Medium (100 ml Neurobasal, 2 mM GlutaMAX TM I, 2 ml 1x B-27 supplement, Pen/Strep 1:100), following which, fresh NBA medium 200 µl was added. The hippocampi were gently triturated and the supernatant was transferred to 1 ml of pre-warmed NBA Medium. Cells were counted using the Naubauer Counting Chamber (4x4 grid x 1000 cells/ml) and approximately 90.000-240.000 were plated out per well in 6 well plate for continental cultures, while 4.000 cells were plated per well in 6 well astrocyte-plate for autaptic cultures. The medium was not changed. In the case of Nbea mutant neurons, genotyping was performed after the preparation of neuronal cultures. The Nbea mutant mice at E18 were clearly identified based on their characteristic anatomical abnormalities (see 3.4.1). Genotypes were confirmed by sequencing after the preparation. For tranfection of mouse

autaptic neurons the calcium phosphate method was used (Kohrmann et al., 1999). DNA (5mg) was mixed with 2M $CaCl_2$ solution and same volume of 2X HBS. The DNA solution was incubated for 20 mins and added to the neurons at 37ºC in 5% CO_2 until a fine precipitate formed (this step normally takes between 15-20 mins). The resulting precipitate formed is washed using acidified HBSS and cultured in the original medium at 37°C at 5% CO_2. All the DNAs used for transfection were obtained from Amsterdam (Prof. Matthijs Verhage) and the plasmids were amplified using the Endofree Maxi Prep (as per the istuctions of the manual). For all the experiments, cells were transfected at DIV4.

3.2.4 Genotyping PCR

All the primers were produced by by D. Schwerdfelger, I. Thanhaeuser and F. Benseler at the MPI for Experimental Medicine, using the department-owned Oligo Synthesizer, ABI 5000 DNA/RNA Synthesizer, and the Applied Biosystems 373 DNA Sequencer and are given in the 5' to 3' direction.

Primer 1 TTTCGTACTAGCAAAGGAGTG
Primer 2 GACTAAAAGATGGCAGCTCTC
Primer 3 TTTGAGCACCAGAGGACATC
Nbea genotyping was performed on mouse genomic DNA by separate amplification of wild-type and knock-out alleles. The wild-type allele was amplified with primers number 1 and 2, and the knock-out allele with primers 1 and 3. The amplification conditions used were identical for both amplifications and were as follows:
Step 1: 95°C for 5 minutes
Step 2: 95°C for 30 seconds
Step 3: 58°C for 45 seconds
Step 4: 72 °C for I minute (34cycles from step 2)
Step 5: 72°C for 10 minutes
Reaction mixture for 1 tail prep (Final volume set to 25 µl with H_2O)
1 µl Tail DNA

0.75 µl 5' Primer 1 (5 pmol)
0.75 µl 3' Primer 2 (5 pmol)
0.75 µl 3' Primer 3 (5 pmol)
0.75 µl dNTP-Mix (2.5 mM each)
2.5 µl 10x Polymerase Buffer (Sigma)
0.75 µl Red Taq Polymerase (Sigma)

3.2.5 Agarose Gel Electrophoresis

Agarose gel electrophoresis was used to separate, identify and purify negatively charged DNA fragments based on their size. DNA bands were made visible with ethidium bromide, and can be photographed in UV-Light (254 or 314 nm). Usually 0.7 to 2% gels are used. Agarose was dissolved by heating in 100 ml of the required 1x TBE buffer, and 0.5 mg/ml Ethidium Bromide was added. Samples were mixed with 6x Probe Buffer (0.25% Bromophenol Blue, 40% Sucrose in H_2O) to a final 1x concentration, and loaded into the wells. DNA fragments are separated at constant voltage (80-120 V) in TBE running buffer (50 mM Tris-Base, 50 mM Boric Acid, 2mM EDTA pH8.0).

3.2.6 DNA Constructs

All the DNA constructs used in the experiments were generated in Amsterdam (Prof. Matthijs Verhages's Lab). The full-length Nbea was generated by using a yeast-two-hybrid cDNA library (Clontech CAT# ML408AH) and a partial image clone (Kazusa mKIAA1544). First, the N-terminal part of Nbea was obtained from the yeast-two-hybrid cDNA library and subcloned in pCR-Script (Stratagene Cat# 211190) using the following primers: rz62 5'TGCACAGCTCCTCAGCAGCG'3; rz63r 5'GCTGGGTGTTCTGACATTAGAGCC'3 and rz64 5'CAGCTCATATTAAAGGATCGAGG'3; rz65r 5'GGATGAGGGATAGATGGTATGACC'3. The resulting subclones were merged using PstI and ScaI. Then, the C-terminal part from the Kazusa image clone was connected to the N-terminal part using NotI and SpeI

resulting in a full-length Nbea in a pCR-Script backbone. For creating the Nbea-IRES$_2$EGFP construct the full-length Nbea script clone was digested with NdeI and SalI. After modifying the NdeI site with Klenow polymerase, (New England Biolabs CAT #M0210S) the Nbea-containing fragment was ligated into the pIRES$_2$EGFP (Clontech PT3267-5), which was digested with SmaI and SalI. A fusion of EYFP and Nbea was made by digesting the Nbea full length pCR-Script with SalI & KspI and ligating it into the pEYFP-C1 digested with the same enzymes. Digesting with AflII and self-ligating resulted in an EYFP-N-terminal Nbea fusion construct contaning the first 710 amino acids (AA) of Nbea after the EYFP. For creating the EGFP-Nbea C-terminal fusion the Kazusa image clone was used as template and a C-terminal Nbea fragment containing AA 1956 - 2936 was amplified using rz106 5'AAAGAATTCACCATGGCGGAAGGAAGGTTGTTGTGCCATGC'3 (adding a EcoRI site) and rz118r 5'TTTGGATCCCACTTGAATGTGGCTTCTGCTGC'3 (adding BamHI site) which was subcloned into pCR-Script. EcoRI and BamHI sites were used for cloning into pEGFP-C3. pEGFP was both purchased from Clontech (CAT#PT2039-5, CAT#PT3973-5).

3.2.7 Electrophysiology

3.2.7.1 Whole-Cell Patch Clamp Recording from Cultured Neurons

Whole cell patch clamp was performed on neurons of DIV11-15 at room temperature. The recording setup consists of a microscope, a pharmacological manipulation system and a data acquisition module. An inverted microscope (Olympus) was used to visualize and position the neurons and the microelectrode. Microelectrode movements were controlled by custom made manipulators. All the pharmacological applications of drugs were performed using custom made flow pipe system (pipette shifting in 100ms range). Finally the signals recorded were digitalized (Digidata 1440A) and amplified using an Axon 700B amplifier (Axon Instruments). The data was stored on a Windows PC and the recordings were analysed using the Axograph 4.9 and KaleidoGraph 4.0 software. Statistical analyses were

performed using the Instat software. Statistical analyses were performed using unpaired Student's T Test unless stated otherwise. *, $p<0.05$; **, $p<0.01$; ***, $p<0.001$. Electrodes were made using a Sutter 2000 filament-based horizontal puller and filled with internal solution. In order to clamp a neuron, pipette was first placed in contact with the cell, following which a negative pressure was applied to obtain a Giga seal. The membrane potential was held constant (clamped) at- 70 mV and the membrane patch in contact with the tip of the electrode was ruptured allowing measurement of the current flowing through the cell. The series resistance was compensated to 50 % and cells with series resistances below 15 MΩ were analyzed. EPSCs/IPSCs were evoked by depolarizing the cells from -70 to 0 mV for 2ms.

3.2.7.2 Solutions Used for Physiology

Extracellular Solution I (Used for most of the experiments)

140 mM NaCl, 2.4 mM KCl, 10 mM Hepes, 10 mM Glucose, 4 mM $CaCl_2$, 4 mM $MgCl_2$.

Extracellular Solution II (Used for NMDA receptor experiments)

(Extracellular solution I, without $CaCl_2$ and $MgCl_2$) along with 2.5 mM $CaCl_2$ and 10μM glycine

KCl internal Solution (Used for most of the experiments)

136mM KCl, 17.8mM Hepes, 1 mM EGTA, 1X ATP/GTP regeneration system

ATP/GTP Regeneration System (10x)

6 mM $MgCl_2$, 40 mM ATP-Mg^{2+}, 3 mM GTP-Na_2, 150 mM Phosphocreatine, 50 U/ml Creatinephosphokinase.

QX-314 Internal Solution (Used in postsynaptic cells of paired recording)

5mM QX-314, 138mM Cesium-methane-sulfonate, 10mM Hepes, 5mM TEA-Cl, 4mM NaCl, 1mM $MgCl_2$, 0.25mM EGTA, 4mM ATP-Mg salt, 0.3mM GTP-Na salt

K-Gluconate Internal Solution (Used for NMDA receptor experiments)

143mM K-Gluconate, 17.8mM Hepes, 1 mM EGTA, 1X ATP/GTP regeneration system

Hypertonic Sucrose Solution

0.5 M Sucrose in Base Plus Solution

Drugs were used at the following concentrations:

Drugs	**Final concentration**
TTX	300 nM
Kainate	10 µM
GABA	3 µM
Glutamate	30 µM
NMDA	100 µM
Calcymicin	10 µM
MK-801	3 µM
Glycine	10 µM

3.2.8 Immunocytochemistry on Autaptic Hippocampal Neurons

Neurons were fixed by incubation in 4% paraformaldehyde (Sigma) in phosphate buffered saline (PBS) for 20 minutes. Subsequently, they were permeabilized for 5 minutes in PBS containing 0.5% Triton X-100, followed by a 30 minutes incubation in PBS containing 0.1% Triton X-100 and 2% normal goat serum to block non-specific binding. The same solution was used for diluting antibodies. Neurons were incubated for 2 hours in primary antibodies at room temperature or overnight at 4°C, washed 3 times with PBS and incubated in secondary antibodies for 1 hour. After additional 3 washes the coverslips were mounted using ProLong®Gold (Invitrogen) or Dabco-Mowiol on slides. This protocol was followed for all the standard immunocytochemistry, except for PSD95 when cells were fixed for 20 minutes in methanol at -20°C. The WT and KO analysis for a given set was treated in parallel and the images were taken with the same settings. For morphological analysis of WT and KO cells, neurons were stained with antibodies against gephyrin, VIAAT, and MAP2 or alternatively, with antibodies against PSD95, VGLUT1 and MAP2. Immunofluoroscent labelings were observed at high

magnification (40×) with an upright epifluorescence Olympus BX-61 microscope. Images were acquired with a digital camera (F-View II) and analyzed using AnalySIS software (Soft-Imaging Systems). Synapses were counted as described previously(Varoqueaux et al., 2002). For receptor colocalization experiments, confocal images were acquired with a Leica confocal microscope (TCS SP2 equipped with AOBS) with a 63X objective lens and analyzed using AnalySIS software (Soft-Imaging Systems).

For fixable FM1-43 labeling, hippocampal neurons were grown for 14 days and then stained at 30°C for 10 s with 20 µM fixable FM1-43 (Molecular Probes) in modified depolarizing external medium containing 86 mM K^+ and 83.5 mM Na^+, immediately followed by an incubation for 30 s with the same dye concentration in standard external medium (Na^+, 167 mM; K^+, 2.4 mM, HEPES, 10 mM; glucose, 10 mM; Ca^{2+}, 4 mM; Mg^{2+}, 4 mM. 330 mOsm/l, pH 7.3). All further procedures were performed at room temperature. The cells were washed several times with external medium, fixed for 5 min with 2.5% formaldehyde in external medium, and then incubated for 15 min with 5% formaldehyde in PBS. Reactive sites were blocked with 25 mM glycine in PBS for at least 30 min. Then, cell membranes were permeabilized under mild conditions to avoid the formation of dispersive aggregates from membrane contents and the membrane staining dye. For this purpose, the cells were kept for 20 min in 1 mM sodium cholate in an otherwise salt free 300 mM sucrose solution. Before and after the permeabilization, cells were carefully washed with 300 mM sucrose to remove salt and detergent residues. To identify all synapses independently of their exocytotic activity, the cultures were immunolabeled with antibodies VGLUT1 and MAP-2 (Jockusch et al., 2007).

The dendrites arborisation was measured using the Sholl Analyses of the MAP2 labeling of the neurons. Concentric circles at intervals of 7.5 µm were drawn around the neurons using Meta Imaging Series 6.1 (Universal Imaging). The number of dendritic processes intersecting along each circle was calculated manually in order to measure the dendritic arborisation of WT

and Nbea KO neurons(Sholl, 1953).

3.2.9 Surface Receptor Labeling in Large Density Culture

Live hippocampal neurons at DIV 16 were labeled for 10 min at 37°C with an antibody directed against the extracellular N-terminal domain of the AMPA receptor subunit GluA2 (Chemicon, 1:200) or the $GABA_A$ receptor subunit $GABA_A\gamma2$ (1:2000). The synaptic localization of GluA2 and $GABA_A\gamma2$ was quantified by their apposition to VGLUT1 and VIAAT, respectively. The cells were then mounted and observed at high magnification (63×) with an upright epifluorescence Olympus BX-61 microscope. For the receptor internalization assay, live neurons were labeled with an anti-GluA2 antibody for 10 min at 37°C and then washed and placed back into the medium of the cells at 37°C for 0, 10, 30, or 60 min. The neurons were then fixed in 4% paraformaldehyde and stained with Alexa-488 labeled anti-mouse antibodies under non-permeabilizing conditions. Subsequently, the neurons were permeabalized and stained with Alexa-555-labeled anti-mouse antibodies to stain endocytosed receptors. Confocal images were acquired with a Leica confocal microscope (TCS SP2 equipped with AOBS) with a 63X objective lens. Red fluorescence intensities indicative of internalization were divided by total (red + green) fluorescence intensities to control for cell density. Units of internalization were measured as red/total fluorescence(Lin et al., 2000; Varoqueaux et al., 2006)

3.2.10 Image Analyses

All the image analyses were conducted on the AnalySIS image acquisition software (Olympus). Synaptic staining of various pre and postsynaptic markers were analyzed by thresholding the signal and applying a separation filter to separate large puncta. Further, the number and fluorescent intensity of the puncta per cell were measured. The apposition of pre and postsynaptic puncta were measured using intensity correlation analyses on the ImageJ software. Each channel was thresholded to omit pixels coming from the extracellular field. Standard Pearson's correlation coefficient was evaluated in

the thresholded fields using the Intensity Correlation Analysis plugin for ImageJ. For the surface receptor colocalization studies, ROI were drawn manually for each fluorescent puncta in a given channel, superimposed on the complementary channel, and the number of colocalized puncta was determined manually. Statistical analyses were performed using unpaired Student's T Test unless stated otherwise. *, $p<0.05$; **, $p<0.01$; ***, $p<0.001$

3.2.11 Biochemical Experiments

3.2.11.1 Mouse Brain Homogenate

The mouse brain were removed and placed in 0.5-3 ml ice- cold Homogenisation Buffer (320mM sucrose with protease inhibitors (1 mM PMSF, 1 µg/µl Leupeptin and Aprotinin) and homogenised at 900 rpm (ten strokes) with a Glass- Teflon homogeniser. The homogenate was centrifuged for 10 minutes at 900x g_{max} and the nuclear pellet was discarded. The supernatant collected was diluted with 3x Laemmli Loading Buffer (10 % SDS, 140 mM Tris/HCl (pH 6.8), 3 mM EDTA, 30 % Glycerol, 0.1 % Bromophenol Blue, 150 mM DTT before use) to a 1x final concentration, and either used immediately or stored at –20 C for later use.

3.2.11.2 Lysates of Cultured Neurons

High density cultured neurons were washed with ice-cold PBS and lysed with Homogenisation buffer. The cells were removed from the dish using a cell scraper and the lysate was centrifuged at 100x g_{max} for 10 minutes. The supernatant was collected and used directly for Western blotting analysis, or stored at -20°C after addition of Laemmli Buffer.

3.2.11.3 Biotinylation Experiments

Continental cultures of hippocampal neurons were washed with PBS and incubated with 0.5mg/ml of Biotin for 30 mins at 4°C. The unbound biotin was removed with a glycine wash, following which the cells were lysed using RIPA Buffer (50mM Tris, 150mM NaCl, 10mM EDTA, 1%Triton X-100, 0.1% SDS

and protease inhibitors PMSF, Leupeptin and Aprotinin). The cells were scraped out and spun at 13000rpm for 15 mins at 4°C.The supernatant was collected and the protein concentrations were measured using BCA (Pierce). Equal amounts of WT and KO proteins were incubated with streptavidin beads to capture biotinylated proteins. After washing in extraction buffer, biotinylated proteins were eluted from streptavidin beads by boiling in sample buffer, separated by SDS-PAGE and immunoblotted using antibodies against proteins of interest

3.2.11.4 Deglycosylation Experiments

All the enzymes and buffers for the reactions were purchased from New England Biolabs and the reaction were carried out on cell culture lysates as per the protocol provided by the producers. Three samples of each genotype were prepared as follows.

10X Denaturing Buffer	5µl
Protein sample	X µl (50 µg of protein)
Water	50-x

The samples were then boiled at 100°C for 10 mins and were treated as follows:

Samples	Endo-H	PNGase-F	Control
10X EndoH buffer	7µl		7µl
EndoH	1µl		
10X PNgase F buffer		7µl	
10X NP40		7µl	
PNGase F		1µl	

70µl final volume with water

These samples were treated for 2 hrs at 37°C in a shaker and were mixed

with Laemmli Buffer for immediate use or storage at –20 C.

3.2.11.5 Preparation of Proteins Samples for SDS Electrophoresis

Protein concentrations for all the experiments were determined using the BCA protocol, following the instructions provided by Protein Assay from the Bio-Rad company. For all the biochemical analysis, WT and KO samples were standardized to the same concentration and the volumes were equalized in RIPA or homogenizing buffer. The protein samples were first mixed with Laemmli Buffer following which they were boiled for 10 mins.

3.2.11.6 Sodium-Dodecyl-Sulfate-Polyacrylamide-Gel Electrophresis (SDS- PAGE) and Western Blotting

In SDS-PAGE, proteins are separated based on their molecular size as they migrate in an electrical field through pores in the gel matrix towards the anode. Pore sizes decrease with increasing acrylamide concentrations and for most of the experiments 10% or 7.5% SDS-PAGE gels were used. The glass plates were assembled as per Biorad instructions and the separation gel solution of desired concentration was poured between the glass plates. The separating gel solution was covered with water-saturated butanol to obtain a smooth surface of the gel. After the gel polymerization, butanol was washed out and the remaining volume above the gel was filled with stacking gel solution into which the comb was inserted. After polymerization, the gel chamber was filled with SDS running buffer and the electrophoresis was performed at constant voltage of 90-120V until the dye reached the end of the gel. The gel was then removed from the glass plates and processed for Western blotting.

Western Blotting is used to transfer proteins separated on SDS-PAGE gel to nitrocellulose membranes. The proteins were electrophoretically transferred at 250 mA for 2 hours, or overnight at 40 mA, to a nitrocellulose membrane and this process was subsequently monitored by reversible Ponceau-S staining. The transferred proteins are bound to the surface of the membrane, making

them accessible to immunodetection reagents.

For immunoblotting, primary antibodies were used which recognize a specific epitope on the protein of interest. Non-specific binding was inhibited by the use of a blocking solution containing goat serum (5%) and tween 20 (0.1%). To detect the antigen-antibody reaction, a horseradish peroxidase (HRP)-labelled secondary antibody was used, which binds to the first unlabelled antibody. The active components of the ECL system are luminol and H_2O_2. The peroxidase reduces the hydrogen peroxide, and the resulting oxygen oxidises the luminol, which releases light. The chemiluminescence is then enhanced through appropriate enhancers and visualised on Amersham Hyperfilm films. The intensity of bands on the ECL films was quantified using ImageJ software in all the experiments. Statistical analyses were performed using unpaired Student's T Test unless stated otherwise. *, $p<0.05$; **, $p<0.01$; ***, $p<0.001$

4 Results

4.1 Nbea Mutant Mice

Heterozygous Nbea KO mice display no obvious phenotypic changes in their viability or fertility. However, Nbea-deficient mice exhibit hunched posture, show no response to tactile stimuli and die perinatally (Medrihan et al., 2009; Su et al., 2004), most likely due to defective neuromuscular synaptic transmission and concomitant breathing failure (Su et al., 2004). In addition, Nbea KO animals display an omphalocele, which is an abdominal defect where the intestine is not withdrawn into the abdominal cavity during embryonic development (Figure 4.1). Furthermore, a cleft palate was also observed in 30% of Nbea KO embryos.

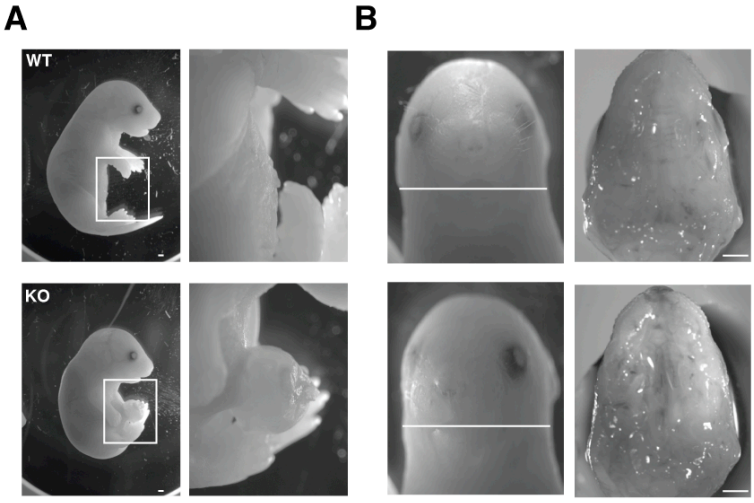

Figure 4.1: Homozygous Nbea KO mice

(A) E18 WT and Nbea KO littermates. Note the omphalocele in the KO in high magnification. (B) Head of the E18 WT and Nbea KO littermates indicating the cross section and the ventral view of upper jaw in WT and Nbea KO newborns. The cleft palate is clearly observed in the KO animals Scale bar= 1mm.

4.2 Glutamatergic and GABAergic Synaptic Transmission in Nbea KO Neurons

To obtain insight into the function of Nbea in glutamatergic and GABAergic nerve cells, I studied synaptic transmission in autaptic cultures of hippocampal and striatal neurons from E18 WT and Nbea KO embryos.

4.2.1 Evoked and Spontaneous Responses

I detected no significant morphological or functional differences between wildtype (WT) and heterozygous Nbea KO neurons. Therefore the data obtained with these genotypes were pooled and designated as control in all experiments. Evoked excitatory postsynaptic current (EPSC) amplitudes in Nbea KO hippocampal neurons and inhibitory postsynaptic current (IPSC) amplitudes in Nbea KO striatal neurons were significantly reduced by 64% and 67%, respectively, as compared to control cells (Cont) (Figure 4.2 A-C and Table 1). Similar phenotypic changes were observed in analyses of postsynaptic responses triggered by hypertonic sucrose solution, which releases all fusion competent SVs and thus allows to assess the readily releasable pool (RRP) of SVs in a calcium independent manner in autaptic neurons, provided that postsynaptic responsiveness is unaltered. The apparent RRP is determined by integrating the total charge transfer of the transient component of the postsynaptic response during the application of 0.5M sucrose solution (Rosenmund and Stevens, 1996). Glutamatergic and GABAergic Nbea KO neurons showed dramatic reductions in apparent RRP sizes of 75% and 70%, respectively (Figure 4.2 D and Table 1). The vesicular release probabilities (P_{vr}) in the two types of neurons, calculated by dividing the charge transferred during an AP- induced postsynaptic response by the charge transferred during RRP release, were slightly reduced in the Nbea KO in comparison to control (Figure 4.2 E and Table 1).

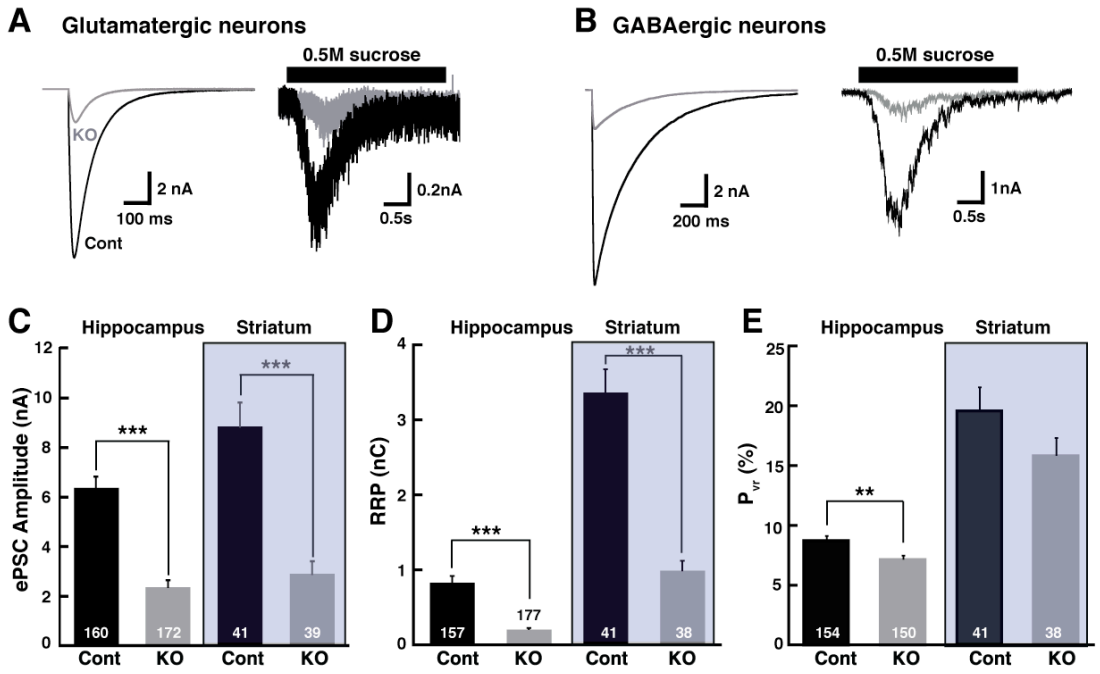

Figure 4.2: Neurons of Nbea KO show dramatic phenotypic differences in evoked synaptic transmission.

(A) EPSCs and responses to stimulation with 0.5M sucrose in glutamatergic hippocampal neurons. (B) IPSCs and responses to stimulation with 0.5M sucrose in GABAergic striatal neurons. (C) Mean EPSC and IPSC amplitudes measured in control (Cont) and KO glutamatergic and GABAergic neurons. (D) Mean RRP size measured in Cont and KO glutamatergic and GABAergic neurons. (E) Mean P_{vr} measured in Cont and KO glutamatergic and GABAergic neurons. Numbers in or above the bars indicate cell numbers. Error bars indicate SEM.

The spontaneous activities of Nbea KO and control neurons were also analyzed for 100s in the presence of 300nM tetrodotoxin (TTX), which blocks propagation of action potentials by blocking Na^+ channels. Unlike evoked EPSCs/IPSCs, amplitudes of miniature EPSCs and IPSCs (mEPSCs/mIPSCs) triggered by the release of single synaptic vesicles were reduced only slightly in KO as compared to control cells (Figure 4.3 A-C and Table 1), and the kinetics of the events were unaffected in the KO (Figure 4.3 E-F). However, the corresponding mEPSC/mIPSC frequencies were reduced by 60% in KO cells (Figure 4.3 D and Table 1), i.e. by a similar degree as evoked

EPSC/IPSC amplitudes and the corresponding responses to hypertonic sucrose solution (Fig 4.2).

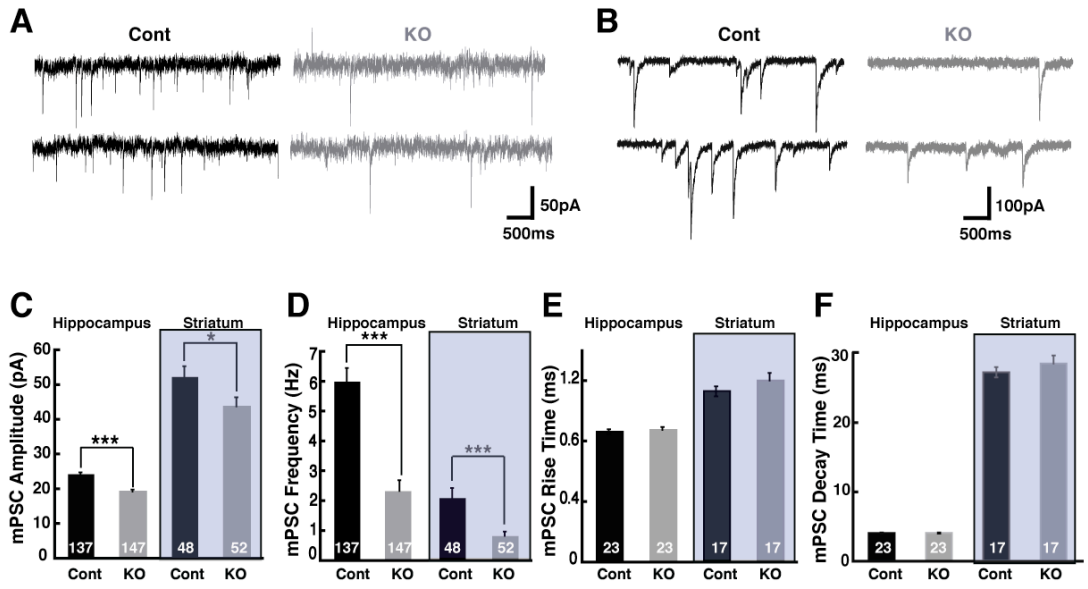

Figure 4.3: Spontaneous synaptic transmission is impaired in Nbea KO neurons

(A) mEPSC trace recorded at -70mV holding potential in the presence of 300nM TTX. (B) mIPSC trace recorded at -70mV holding potential in the presence of 300nM TTX. (C) Mean miniature event amplitude measured in glutamatergic and GABAergic neurons. (D) Mean miniature event frequency measured in glutamatergic and GABAergic neurons. (E) Mean miniature event rise time (10-90%) measured in glutamatergic and GABAergic neurons. (D) Mean miniature event decay time measured in glutamatergic and GABAergic neurons. Numbers in the bar indicate cell numbers. Error bars indicate SEM.

4.2.2 Unaltered Presynaptic Release Machinery

In the next set of experiments, I used the Ca^{2+} ionophore calcimycin to activate all functional presynapses in autaptic neurons independently of action potentials and Ca^{2+} channels (Jockusch et al., 2007). Irrespective of the genotype and transmitter type of the tested neurons, elevation of intracellular Ca^{2+} levels ($[Ca^{2+}]_i$) by 10 μM calcimycin, which was applied for 2 min,

triggered a massive release of synaptic vesicles, leading to the complete depletion of all releasable synaptic vesicles. Importantly, calcimycin responses in Nbea KO cells were reduced to a similar degree as the responses to hypertonic sucrose solution (Figure 4.4 A-B and Table 1). These findings indicate that synaptic transmission is severely perturbed in Nbea KO neurons and that the dominant defect is downstream of action potential propagation or presynaptic Ca^{2+} signaling.

In addition, to directly monitor release of active presynapses in glutamatergic Nbea KO neurons, 20µM fixable FM1-43 was used. The neurons were first stimulated with 86mM K^+ for 10s in the presence of fixable FM1-43. Subsequently, the cells were washed, and in order to identify all synapses present, neurons were fixed and immunostained for VGLUT1. The proportion of active synapses, which was determined by calculating the number of FM1-43 positive puncta colocalizing with VGLUT1, was similar between the Nbea KO and control neurons (Figure 4.4 C-D and Table 3). Taken together, these findings indicate that Nbea KO neurons have functionally intact presynapses although the frequency of mPSCs in Nbea deficient neurons was reduced considerably.

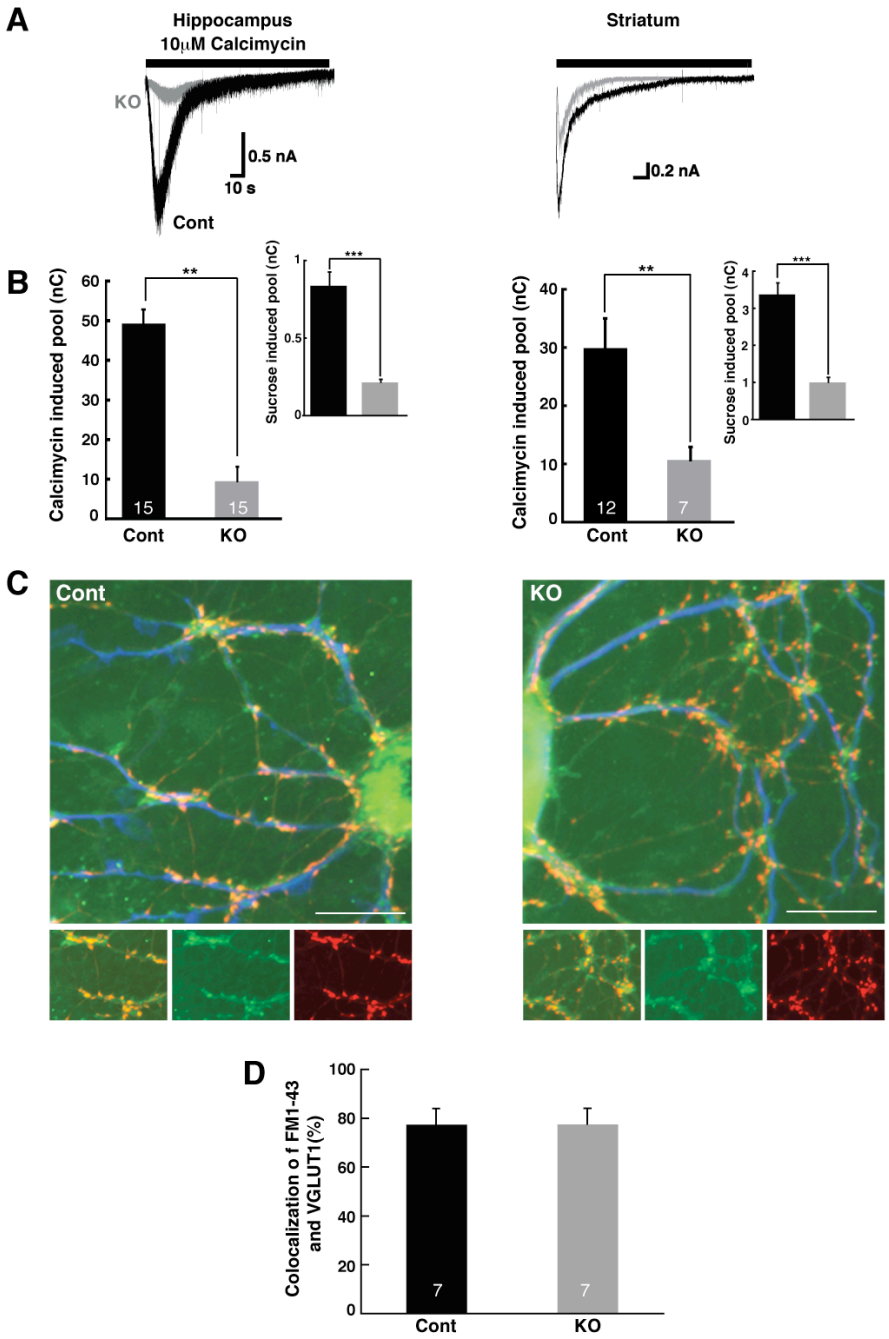

Figure 4.4: Intact presynaptic activity in Nbea KO neurons

(A) Representative traces of release induced by 10μM calcimycin in hippocampal glutamatergic and striatal GABAergic control (Cont) and KO neurons. (B) Total charge transfer induced by application of calcimycin measured in glutamatergic and GABAergic neurons. Insets show the RRP sizes induced by sucrose application (C) Examples of fluorescence staining in autaptic neurons with FM1-43 (green), VGLUT1 (red) and MAP2

(blue). Scale bar=10μM (D) Quantification of VGLUT1 and FM1-43 colocalization. Numbers in the bar indicate cell numbers. Error bars indicate SEM.

4.3 Nbea localization and Morphology of Nbea KO Neurons

4.3.1 Synapse Formation in Nbea KO Neurons

To study the effects of Nbea loss on synapse formation, immunolabeling analyses were performed with antibodies directed against the presynaptic markers VGLUT1 and VIAAT (Wojcik et al., 2006; Wojcik et al., 2004), which are specific for glutamatergic and GABAergic nerve terminals, respectively, and against PSD95 and gephyrin (Fritschy et al., 2008; Schluter et al., 2006), which are specific for glutamatergic and GABAergic postsynaptic densities, respectively. The number of glutamatergic and GABAergic nerve terminals were counted for each cell. No differences between control and Nbea KO neurons were observed in the number of synapses per cell. Also, the number of properly apposed pre- and postsynaptic structures was very similar in control and KO Nbea neurons (Figure 4.5 and Table 3). These results show that Nbea loss does not affect synapse formation.

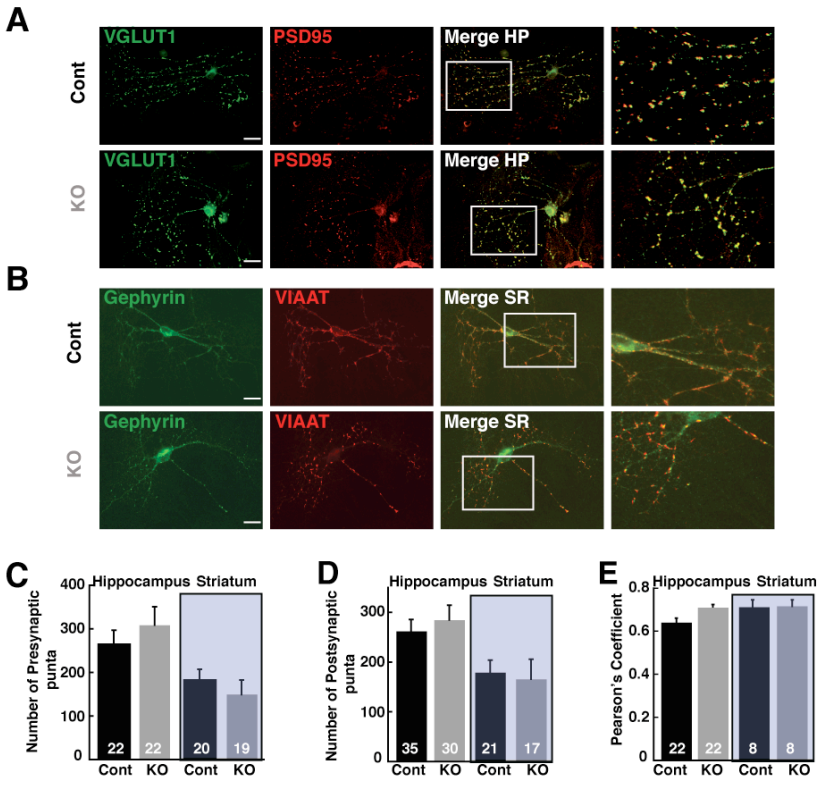

Figure 4.5: Synapse formation is unaltered in Nbea KO neurons

(A) Double staining of glutamatergic hippocampal neurons from control (Cont) and KO at DIV15 using antibodies to presynaptic and postsynaptic markers. (B) Double staining of GABAergic striatal neurons from Cont and KO at DIV15 using antibodies to presynaptic markers and postsynaptic markers. Scale bar=20μM (C) Average number of synapses determined by VGLUT1 positive puncta and VIAAT positive puncta. (D) Average number of synapses determined by PSD95 positive puncta and gephyrin positive puncta. (E) Intensity correlation analysis of VGLUT1/PSD95 and VIAAT/gephyrin in Cont and KO neurons. Numbers in the bar indicate cell numbers. Error bars indicate SEM.

4.3.2 Dendritic Arborization in Nbea KO Neurons

Certain Nbea-related BEACH domain proteins play an important role in the control of membrane dynamics and membrane trafficking, thus contributing to cell maturation and development (Wang et al., 2000). In order to test whether the reduction in synaptic transmission observed in Nbea KO neurons were due to impairment in dendrite development and maturation, dendrites were stained using an anti-MAP2 antibody on fixed autaptic hippocampal neurons of DIV14. The dendrite complexity was analyzed using Sholl analysis (Sholl,

1953). Nbea KO neurons had larger and more complex dendrites than control neurons. The average number of dendrites was higher in Nbea KO neurons and their dendrites were most complex at a distance of 30 μm from their the cell bodies, while the dendrites of control neurons were most complex at a distance of 37.5 μm from their cell bodies (Figure 4.6). These results show that the reduced synaptic transmission in Nbea KO neurons is not due to impaired dendrite growth. The increased dendrite complexity in Nbea KO neurons may be attributed to compensatory mechanisms or reflects an inhibitory effect of Nbea on neurite development.

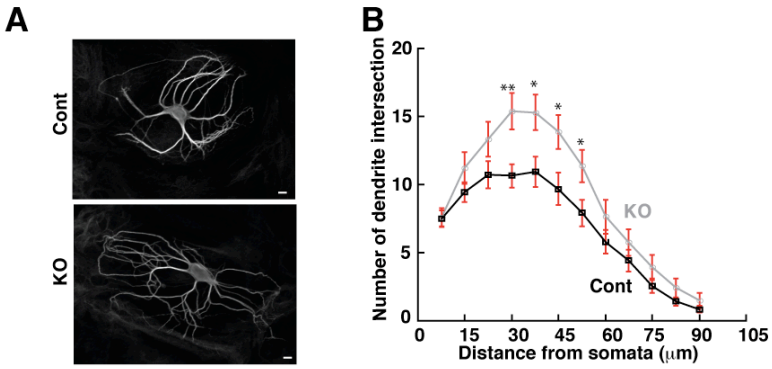

Figure 4.6: Increase in dendritic arborization in Nbea KO

(A) Representative staining of control (Cont) and KO neurons using antibody to dendritic marker MAP2. Scale bar=10μm. (B) Quantification by Sholl analysis conducted on Nbea KO (n=26) and Cont neurons (n=26). Error bars indicate SEM.

4.3.3 Nbea Localization in WT neurons

To examine the subcellular distribution of Nbea in neurons, a novel Nbea-specific antibody was used. The specificity of the antibody was tested using KO brain tissues and neurons as negative control (data from our collaborators). In WT neurons, Nbea is detectable abundantly in discrete compartments throughout the somata and in dendrites (Figure 4.7), and is reminiscent of a Golgi apparatus.

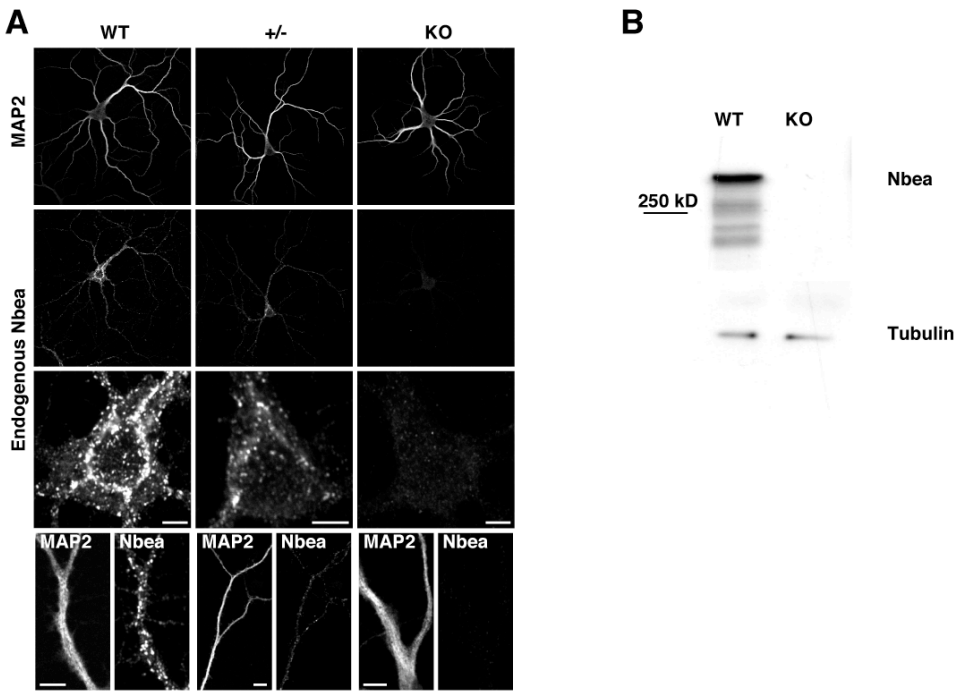

Figure 4.7: Nbea antibody specificity

Immunostaining of Nbea and MAP2 in DIV14 WT, heterogyzous and KO hippocampal neurons. Scale bar = 5μm. (Data from J Lauks). (B) Western blot of Nbea in DIV14 WT and KO hippocampal neurons.

To analyze the Nbea subcellular localization in detail, neurons were colabeled for Nbea and an ER marker (KDEL) or a cis Golgi marker (GM130). Nbea immunopositive structures are juxtaposed to cis Golgi compartments (Figure 4.8) but do not colocalize with the ER marker KDEL. A similar pattern of distribution was observed in studies using cells line, where Nbea localization in association with the Golgi complex was stimulated with GTPγS and inhibited by brefeldinA, indicating a possible role of Nbea in trafficking proteins along the secretory pathway (Wang et al., 2000).

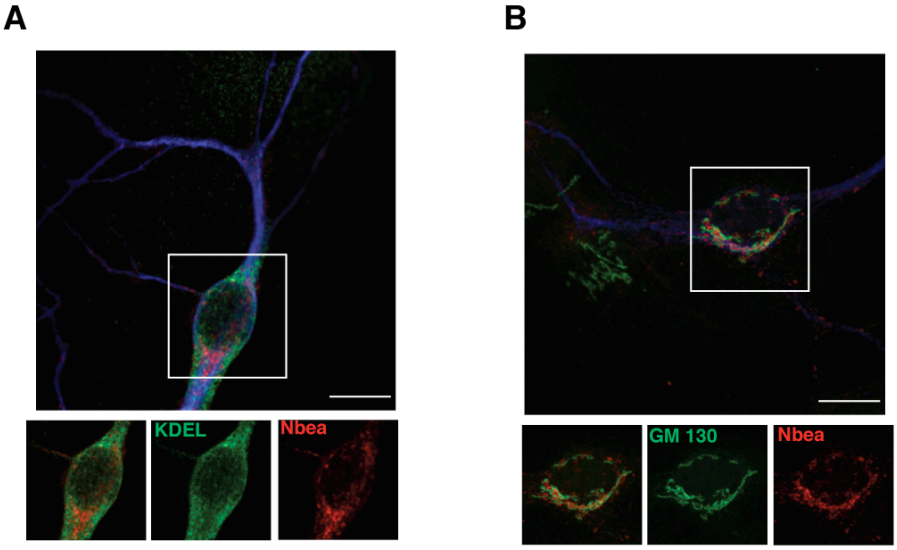

Figure 4.8: Nbea localization in WT neurons

(A) DIV 14 hippocampal WT neurons stained for endogenous Nbea (red), ER marker KDEL (green) and MAP2 (blue). (B) DIV 14 hippocampal WT neurons stained for endogenous Nbea (red), cis-Golgi marker GM130 (green) and MAP2 (blue). Scale bar=10μM.

4.4 Reduction in Functional Neurotransmitter Receptors in Nbea KO Neurons

4.4.1 Exogenous Application of Receptor Agonist

To further investigate the causes of the reduced synaptic transmission in Nbea KO neurons, surface glutamate and $GABA_A$ receptors were assessed by exogenous application of glutamate or $GABA_A$ receptor agonists to control and Nbea KO neurons (Jones and Westbrook, 1996). Compared to control cells at DIV11-15, Nbea KO neurons exhibited dramatic reductions in their responses to exogenous application of 10μM kainate, 30μM glutamate or 3μM GABA (Figure 4.9 and Table 1).

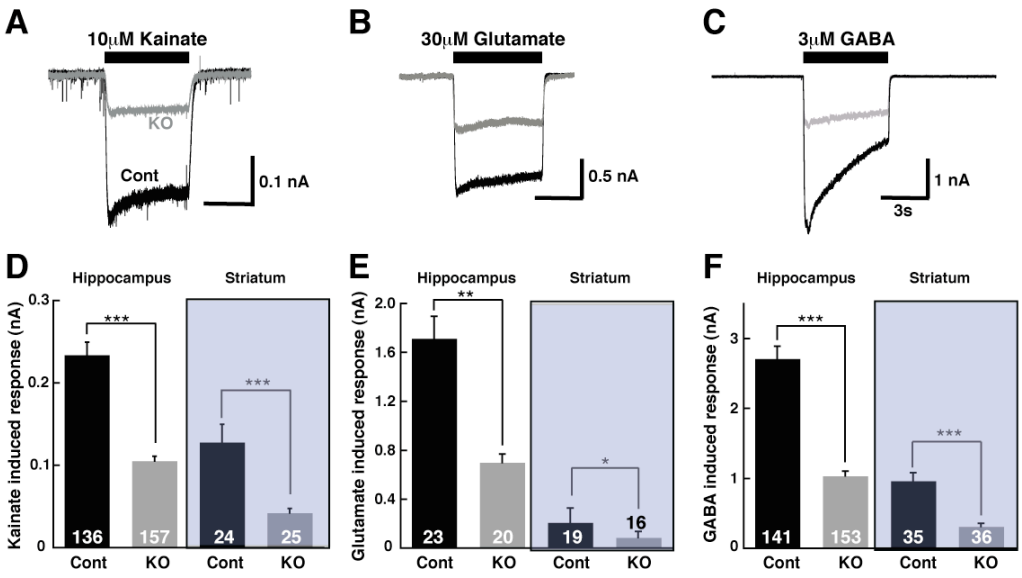

Figure 4.9: Exogenous applications of Kainate, Glutamate and GABA receptor agonists in autaptic control and Nbea KO neurons.

(A-C) Representative traces of responses to Kainate (A), Glutamate (B) and GABA (C) receptor agonist application measured in control (Cont) and KO neurons (D) Mean amplitudes induced by exogenous application of 10μM kainate measured in hippocampal glutamatergic and striatal GABAergic neurons. (E) Mean amplitude induced by exogenous application of 30μM glutamate measured in glutamatergic and GABAergic neurons. (F) Mean amplitude induced by exogenous application of 3μM GABA measured in glutamatergic and GABAergic neurons. Numbers in or above the bars indicate cell numbers. Error bars indicate SEM.

Interestingly, the same patterns of reduced glutamatergic responses were seen in GABAergic KO cells and reduced GABAergic responses were seen in glutamatergic KO cells, and the extent of these reductions (approximately 65%) was similar in both glutamatergic and GABAergic Nbea KO neurons. Furthermore, the dramatic reductions in the responses were also observed in high-density cultures of Nbea KO neurons (Figure 4.10 and Table 1).

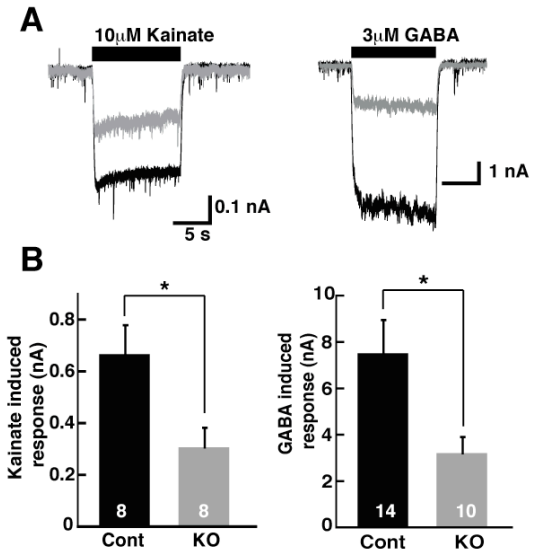

Figure 4.10: Reduced functional receptors in high density cultures

(A) Representative traces of response to kainate and GABA receptor agonist application in presence of TTX in DIV14-15 hippocamapal neurons. (B) Mean responses triggered by exogenous application of kainate and GABA induced in control (Cont) and KO neurons. Numbers in the bars indicate cell numbers. Error bars indicate SEM.

However, unlike neurons from DIV11-15, Nbea KO neurons at DIV3-4 did not exhibit impaired responses to exogenously applied receptor agonists (Figure 4.11). Given that neurons at DIV3-4 do not have functional synapses, these findings indicate that Nbea plays a role specifically in receptor trafficking as neurons mature and form synapses. Taken together, above data indicate that the dramatic loss of synaptic transmission in the absence of Nbea is caused by severe defects in the number of functional transmitter receptors at the cell surface.

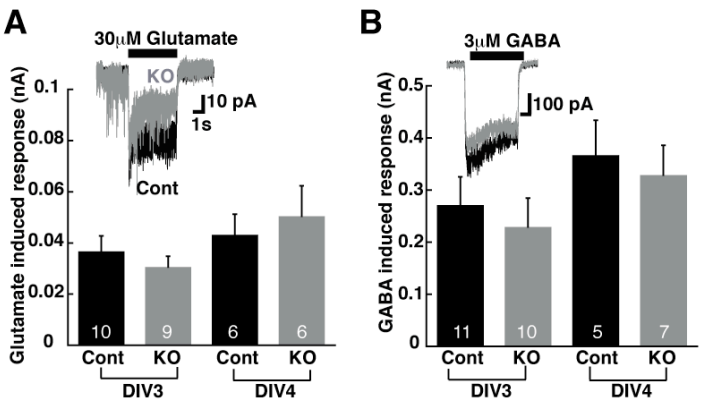

Figure 4.11: Functional receptors intact before synapse formation in Nbea KO neurons

(A) Example traces (inset) and mean amplitudes of responses to exogenously applied glutamate in DIV3-DIV4 control (Cont) and KO neurons. (B) Example traces (inset) and mean amplitudes of responses to exogenously applied GABA in DIV3-DIV4 Cont and KO neurons. Numbers in the bar indicate cell numbers. Error bars indicate SEM.

4.4.2 Reduction of Synaptic Functional Receptors

For NMDA receptors, it is possible to functionally distinguish between synaptic and extrasynaptic receptor populations. The exogenous application of 100μM NMDA in the presence of Mg^{2+} free and glycine containing bath solution revealed a reduction in the number of functional NMDA receptors on the plasma membrane of KO neurons. Following this treatment the synaptic NMDA receptors were blocked by application of a 0.33Hz stimulus train in the presence of the irreversible open-channel blocker MK-801 (Huettner and Bean, 1988). In this regimen, synaptic NMDA receptors become selectively blocked by MK-801 (Rhee et al., 2002). Subsequent application of NMDA to these neurons reveals only the functional extrasynaptic NMDA receptors. The ratio between the second response to exogenous NMDA application after MK801 blockade and the first response to exogenous NMDA application before MK801 blockade can be used to assess the distribution of NMDA receptors between synaptic and extrasynaptic membrane domains. The corresponding ratios obtained in control cells indicate that typically about 80% of all functional NMDA receptors are at synapses. In contrast, Nbea KO neurons have much less synaptic NMDA receptors while the number of

functional extrasynaptic receptors is unaffected (Figure 4.12 A and Figure 4.12 C-E and Table 1). The synaptic release probability, which can be estimated on the basis of the decay time course of the synaptic NMDA receptor current during the 0.33 Hz train in the presence of MK-801, was similar between Nbea KO and control cells, indicating that the synaptic release machinery is not affected in Nbea KO neurons. The synaptic NMDA/AMPA response ratios were also similar in Nbea KO and control cells (Figure 4.12 B and Table 1) providing indirect evidence for reduced synaptic localization of AMPA receptors.

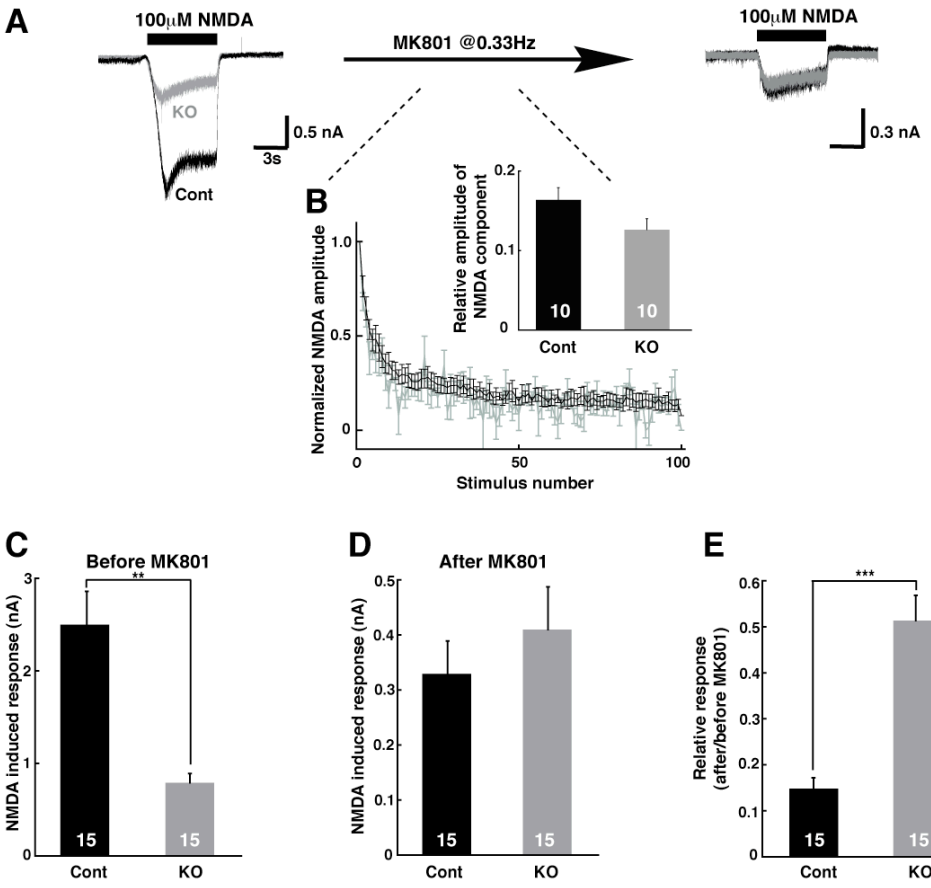

Figure 4.12: Reduced synaptic localization of NMDAR in Nbea KO neurons

(A) Representative traces of responses triggered by 100μM NMDA before and after MK801 treatment on control (Cont) and KO neurons. (B) Synaptic NMDA EPSCs were blocked by eliciting a series of 100 EPSCs at 0.3 Hz in the presence of MK-801. Averaged normalized NMDA-mediated amplitudes plotted against the stimulus number during the application of MK-

801 (Cont n=10 and KO n=10). The inset shows the mean NMDA component relative to the AMPA component. (C) Mean NMDA induced response before MK801 application. (D) Mean NMDA induced response after MK801 application. (E) Relative NMDA induced response after/before MK801 application. Numbers in the bar indicate cell numbers. Error bars indicate SEM.

4.4.3 Intact Assembly of AMPA Receptor Subunits in KO Neurons

To test whether the composition of AMPA receptor subunits at the synapse is altered by Nbea expression, the rectification indices and the I-V curve of synaptic AMPA responses were recorded by paired recordings from microislands containing two cells. Although the Nbea KO neurons show dramatic reduction in the EPSC amplitude mediated by AMPA receptors, Nbea KO neurons show rectifications of I-V curves that are similar to those in control neurons (Figure 4.13). This indicates that the reduced responses to exogenous application of glutamate in Nbea KO neurons are primarily due to the loss of functional AMPA receptors in synapses without changes in the composition of AMPA receptor subunits.

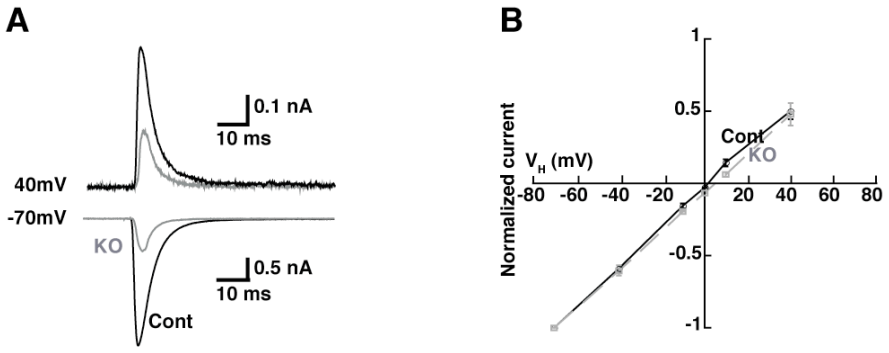

Figure 4.13: AMPA receptor subunit assembly intact in Nbea KO neurons

(A) I-V curves of control (Cont) (n=75) and Nbea KO neurons (n=5) obtained by measuring evoked EPSC amplitudes at different holding potentials. The EPSC amplitudes at different potentials were normalized to the amplitude obtained at -70. Error bars indicate SEM.

Table 1. Synaptic transmission in control (Cont) and Nbea KO neurons

	Glutamatergic neurons		GABAergic neurons	
	$Cont_{hipp}$	KO_{hipp}	$Cont_{stri}$	KO_{stri}
PSC(nA)	6.4 ± 0.42, n=160	2.3 ± 0.19, n=172	8.8 ± 0.96, n= 41	2.89 ± 0.44, n=39
RRP size(nC)	0.83 ± 0.080, n=157	0.21 ± 0.01, n= 177	3.4 ± 0.30, n=41	1.0± 0.12, n=38
Pvr(%)	8.7 ± 0.37, n=154	7.1 ± 0.32, n=150	19.6 ± 2, n=41	15.8 ±1.5, n=38
mPSC amplitude(pA)	24.2 ± 0.60, n=137	19.2± 0.59, n= 147	52.1 ± 3.15, n=48	43.7 ± 2.7, n=52
mPSc frequency (Hz)	6 ± 0.45, n=137	2.3± 0.37, n=147	2.1 ± 0.33, n=48	0.82 ± 1.500, n=52
10μM Calcimycin induced pool (nC)	48.9 ± 12.15, n=15	8.0 ± 1.80, n= 15	29.87± 5.130, n=12	10.6 ± 2.26, n=7
30μM Glutamate response (nA)	1.71 ± 0.3, n=23	0.7 ± 0.140, n=20	0.20 ± 0.040, n=19	0.08 ±0.010, n=16
3μM GABA response (nA)	2.7 ± 0.18, n=141	1.03 ± 0.06, n=153	0.96 ± 0.120, n=35	0.30 ±0.050, n=36
10μM Kainate response (nA)	0.23 ± 0.015, n=136	0.10 ± 0.006,n=157	0.12 ± 0.020, n=24	0.042 ± 0.005,n=25
100μM NMDA response (nA) before MK801 application	2.49 ± 0.365, n=15	0.787 ± 0.10, n=15		
100μM NMDA response (nA) after MK801 application	0.33 ± 0.06, n=15	0.41 ± 0.078, n=15		
Relative ratio of NMDA response after/before MK801	0.148 ± 0.023, n=15	0.51 ± 0.055, n=15		
Normalized NMDA to AMPA ratio	0.17 ± 0.020, n=10	0.14 ± 0.020, n=10		
Continental cultures 100μM Glutamate response (nA)	0.79 ± 0.082, n=11	0.364 ± 0.12, n=11		
Continental	0.67 ± 0.110,	0.30 ± 0.075,		

cultures 10μM Kainate response (nA)	n=8	n=8		
Continental cultures 3μM GABA response (nA)	7.5 ± 1.43, n=14	3.2 ± 0.69, n=10		
PSC in presence of 10μM Forskolin (nA)	7.38 ± 1.26, n=16	3.93 ± 0.471, n=27	7.97 ± 1.08, n=15	2.24 ± 0.41, n=14

4.5 Nbea Overexpression in WT and KO

4.5.1 Rescue of Nbea KO Phenotype by Nbea Overexpression

To examine if the phenotypic changes seen in the Nbea KO neurons are a direct consequence of Nbea loss, full length Nbea was transfected into autaptic glutamatergic and GABAergic Nbea KO neurons. The effects of Nbea loss on evoked EPSC and IPSC amplitudes and on responses to exogenous agonist application were fully rescued by re-expression of full length Nbea (Figure 4.14 and Table 2), indicating that the phenotypic effects of loss of Nbea in neurons are cell autonomous and that Nbea loss does not lead to complex secondary effects that cannot be reverted by Nbea re-expression.

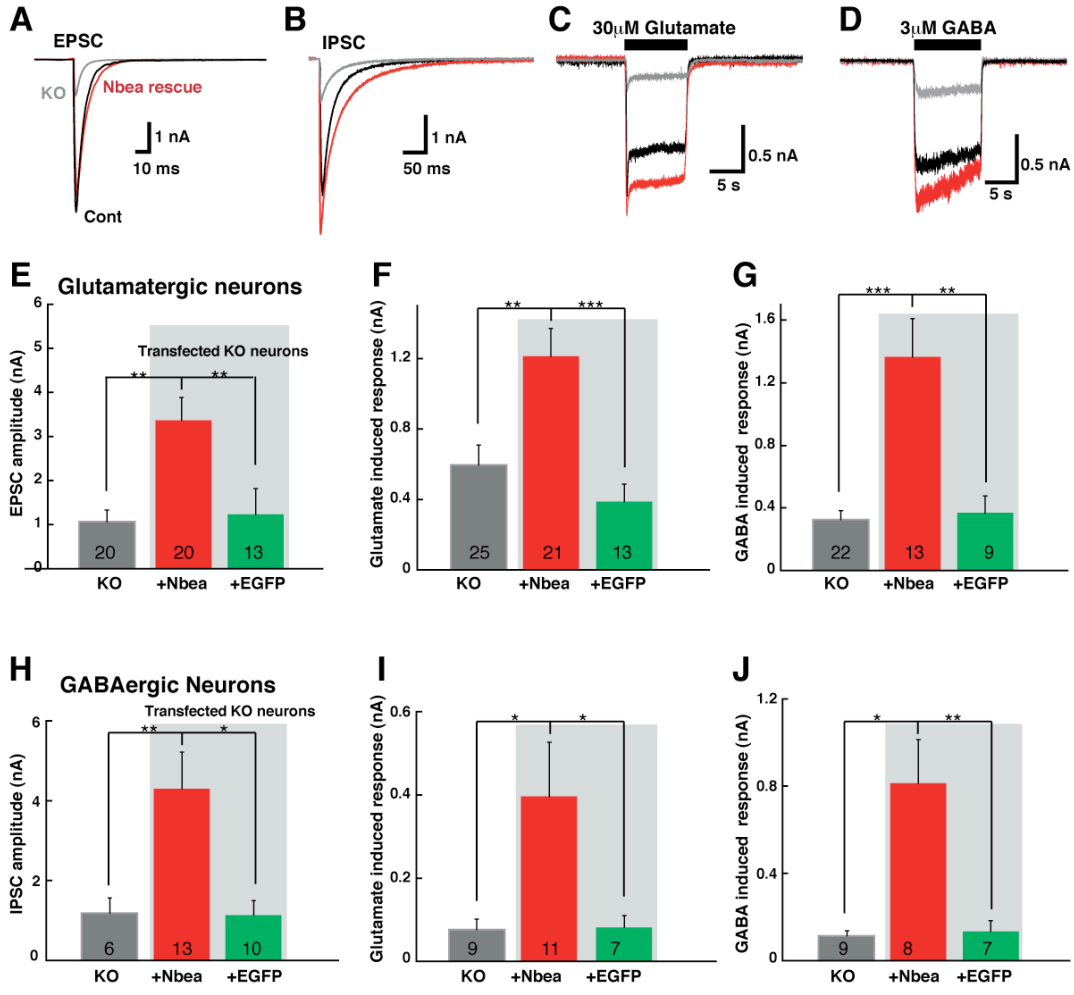

Figure 4.14: Nbea overexpression rescues the phenotype of Nbea KO neurons.

(A) Representative traces of EPSCs in glutamatergic neurons. (B) Representative traces of IPSCs in GABAergic neurons. (C) Representative traces of responses triggered by exogenous application of glutamate. (D) Representative traces of responses triggered by exogenous application of GABA. (E-G) Mean evoked EPSC amplitude (E), response induced by exogenous application of glutamate (F) and GABA (G) measured in glutamatergic neurons with indicated genotypes after calcium phosphate transfection at DIV4. (H-J) Mean evoked IPSC (H), response induced by exogenous application of glutamate (I) and GABA (J) measured in GABAergic neurons with indicated genotypes after calcium phosphate transfection at DIV4. Numbers in the bars indicate cell numbers. Error bars indicate SEM. The statistical significance of changes was tested using nonparametric ANOVA followed by Dunn's multiple comparison tests.

Re-expression of only the N-terminal domain of Nbea containing the ARM repeats and the ConA-like lectin domain or of only the C- terminal domain of

Nbea containing the domain of unknown function (DUF), PH, BEACH and WD40 domains did not rescue the phenotypic changes seen in Nbea KO neurons (Figure 4.15 A-D and Table 2).

Nbea is a putative AKAP protein. In order to circumvent the loss of a possible AKAP function and consequent defect in cAMP signaling in Nbea KO neurons, cells were treated with the adenylate cyclase activator forskolin. However, forskolin treatment did not rescue the reduced evoked EPSC/IPSC amplitudes in Nbea KO neurons (Figure 4.15 E Table 1). These rescue data indicate that the Nbea KO phenotypic is cell autonomous, and requires the AKAP as well as N- and C-terminal part of the protein.

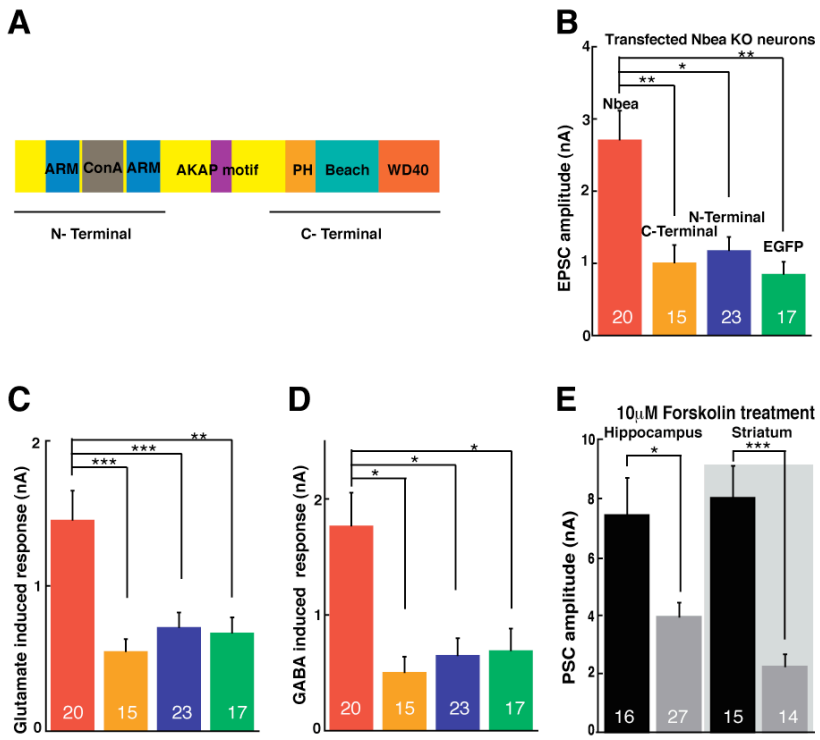

Figure 4.15: Structure function analysis of Nbea

(A) Structure of N and C- terminal constructs of Nbea. (B) Mean EPSC amplitudes measured from Nbea KO neurons over-epressing Nbea full-length, N-terminal domain, C-terminal domain and empty EGFP. (C) Mean response triggered by exogenous application of

glutamate in Nbea KO neurons overepressing Nbea full-length, N-terminal domain, C-terminal domain and empty EGFP. (D) Mean response triggered by exogenous application of GABA measured from Nbea KO neurons overexpressing Nbea full-length, N-terminal domain, C-terminal domain of Nbea and empty EGFP. The statistical significance of changes was tested neurons using nonparametric ANOVA followed by Dunn's multiple comparison tests. (E) Mean evoked glutamatergic and GABAergic responses measured from autaptic neurons treated with 10 μM forskolin. Numbers in the bars indicate cell numbers. Error bars indicate SEM.

4.5.2 Nbea Overexpression in WT Neurons

Next, the effects of overexpression of Nbea in WT neurons were tested. Interestingly, overexpression of full length Nbea in autaptic WT hippocampal neurons caused approximately 50% increase of evoked responses and of responses triggered by application of glutamatergic and GABAergic receptor agonists (Figure 4.16 and Table 2).

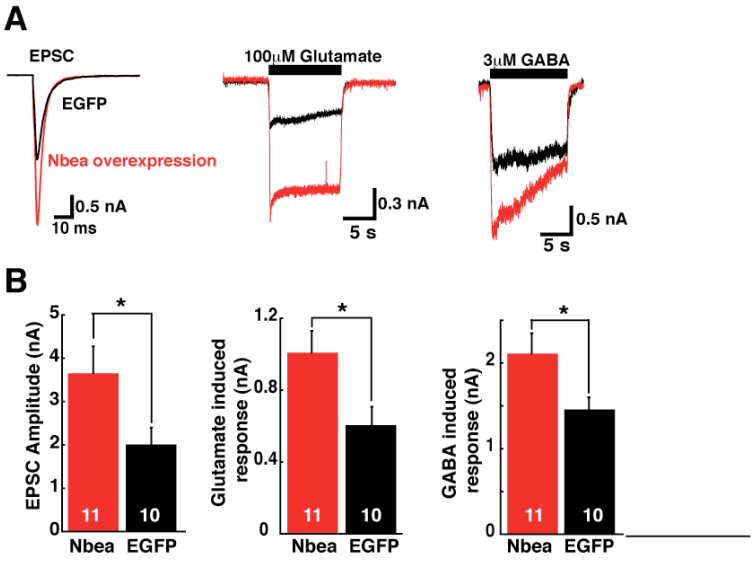

Figure 4.16: Over-expression of Nbea in WT neurons increases synaptic strength

(A) Representative traces of EPSC and of responses triggered by exogenous application of glutamate and GABA induced responses in WT autaptic neurons overexpressing EGFP (black) and full length Nbea (red). (B) Mean EPSC, mean response triggered by exogenous application of glutamate, and GABA in autapses. Numbers in the bars indicate cell numbers. Error bars indicate SEM.

Table 2. Nbea overexpression in WT and KO neurons

	EGFP in WT	Nbea Full length in KO	EGFP in KO	KO empty
EPSCamplitude (nA)	4.2 ± 0.94 n=20	3.4 ± 0.53 n=20	1.23 ± 0.58 n=13	1.06 ± 0.27 n=20
IPSC amplitude (nA)	3.32 ± 0.72 n=10	4.32 ± 0.93 n=13	0.92 ± 0.356 n=6	1.12 ± 0.383 n=10
Glutamate induced response in hippocampal neurons (nA)	1.24 ± 0.197 n=27	1.21± 0.155 n=21	0.39 ± 0.098 n=13	0.59 ± 0.11 n=25
GABA induced response in hippocampal neurons (nA)	0.90 ± 0.144 n=21	1.36 ± 0.25 n=13	0.37± 0.107 n=9	0.32 ± 0.06 n=22
Glutamate induced response in straital neurons (nA)	0.23 ± 0.051 n=10	0.4 ± 0.13 n=11	0.081 ± 0.028 n=9	0.076 ±0.026 n=7
GABA induced response in straital neurons (nA)	0.53 ± 0.133 n=9	0.81 ± 0.197 n=8	0.132 ± 0.052 n=9	0.112 ± 0.025 n=7

	Nbea Full length in KO	Nbea C-terminal in KO	Nbea N-terminal in KO	EGFP in KO
EPSC amplitude (nA)	2.72 ± 0.396, n=20	1.01 ± 0.243 n=15	1.18 ± 0.182 n=23	0.85 ± 0.1662 n=17
Glutamate induced response (nA)	1.45 ± 0.202 n=20	0.55 ± 0.079 n=15	0.72 ± 0.96 n=23	0.68 ± 0.106 n=17
GABA induced response (nA)	1.769 ± 0.290 n=19	0.506 ± 0.135 n=15	0.65 ± .15 n=23	0.7 ± 0.19 n=17

	Nbea Full length in WT	EGFP in WT
EPSC amplitude (nA)	3.6 ± 0.62 n=11	2 ± 0.40 n=10
Glutamate induced response (nA)	1.0 ± 0.12 n=9	0.6 ± 0.10 n=9
GABA induced response (nA)	2.11 ±0.23 n=11	1.45 ± 0.14 n=10
Glutamate induced response in high density culture (pA)	460.5 ± 42.95 n=57	690±58.3 n=55

4.6 Localization of Receptor Proteins in Nbea KO Neurons

4.6.1 Unaltered Total Protein Composition in Brain and Cultured Neurons

To test if the reduced synaptic localization of functional neurotransmitter receptors in Nbea KO neurons is paralleled by changes in total receptor protein expression, Western blotting was employed to compare total expression levels of proteins in Nbea KO and control neurons from both whole brain homogenates (E18) and DIV19 hippocampal cultures (Figure 4.17). The total expression levels of glutamate and GABA receptor subunits were similar in Nbea KO and control samples irrespective of the preparation. Earlier studies performed on brainstem indicated that deletion of Nbea affected the expression levels of presynaptic components of the transmitter release machinery (Medrihan et al., 2009). However, no such changes were observed here in cultures or brain homogenates prepared from Nbea KO animals (Figure 4.17).

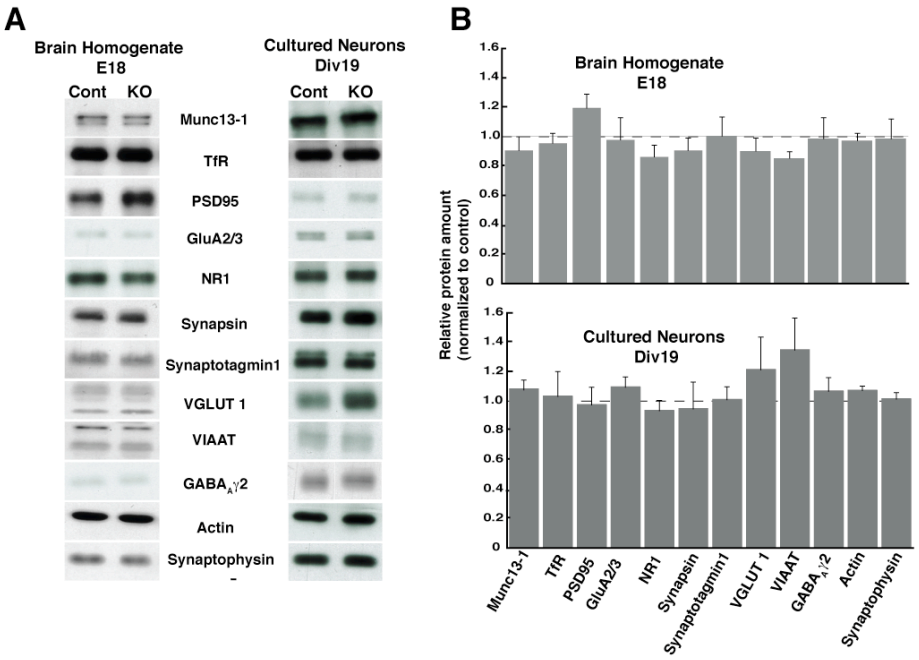

Figure 4.17: Protein expression levels in Nbea KO show no significant differences

(A) Expression levels of synaptic proteins from E18 brain homogenates and DIV19 cultured neurons in control (Cont) and KO mice. (B) Quantification of total expression of proteins in Nbea KO neurons from three independent experiments (normalized to Cont levels). Error bars indicate SEM.

4.6.2 Reduction in Surface Expression of Neurotransmitter Receptors

Since massive reductions were observed in the number of functional receptors at postsynapses while no alterations in total expression levels of receptor proteins were detectable in the Nbea KO neurons, cell surface biotinylation assays were conducted on high-density hippocampal cultures (DIV19) to measure surface expression of subunits of AMPA, NMDA and $GABA_A$-receptors. Nbea KO cells showed a 60% reduction in the cell surface level of GluA2/3 and a 40% reduction of GluA1, GluN1, GluN2A, GluK2/3, $GABA_A\gamma2$ and $GABA_A\alpha1$ (Figure 4.18). The cell surface expression of other membrane proteins, such as neuroligin 1 or transferrin receptor, were unaffected or even slightly increased in Nbea KO neurons. Also, the cell surface expression of the extrasynaptic $GABA_A$ receptor subunit $GABA_A\alpha5$

(Brunig et al., 2002) was slightly increased in Nbea KO cells (Figure 4.18). Hence, Nbea loss exclusively affects surface expression of neurotransmitter receptors that are recruited to synapses.

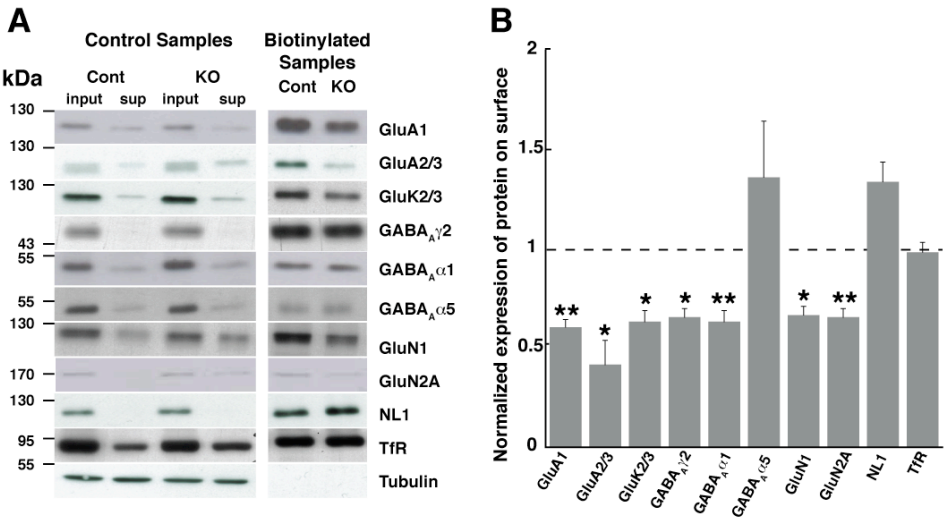

Figure 4.18: Receptor surface expression analysis using biotinylation assay

(A) Biotinylation assays were performed on DIV19 control (Cont) and KO hippocampal neurons to measure the surface expression of the indicated proteins. Input indicates total protein levels before biotinylation, and supernatant (sup) indicates cytosolic proteins after biotinylation. Immunolabeled bands were visualized by enhanced chemoluminescence. (B) Quantification of surface expression of proteins in Nbea KO neurons (normalized to Cont levels) from at least three independent experiments. Error bars indicate SEM.

4.6.3 Absence of Synaptic GluA2 and $GABA_A\gamma2$ Subunits in Nbea KO Neurons

To confirm that the synaptic phenotype of Nbea KO was caused by the absence or reduction of neurotransmitter receptors on postsynapses, live immunostaining of surface-exposed receptors was performed with antibodies directed against the extracellular N-terminal domains of GluA2 and $GABA_A\gamma2$. GluA2 labeled neurons were fixed and co-labeled for VGLUT1, while $GABA_A\gamma2$ labeled neurons were fixed and co-stained for VIAAT. Nbea KO neurons showed a 60% reduction in the number of live-stained GluA2 positive puncta apposed to VGLUT1 positive puncta (Figure 4.19 A, C and Table 3).

Along with reduced GluA2 expression on the cell surface, Nbea KO neurons displayed higher intracellular accumulation of GluA2/3 in the cell body as compared to control neurons (Figure 4.19 B) This finding is in accordance with the biochemical data described above, which showed that the overall expression levels of AMPA receptor subunits are not changed in Nbea KO cells (Figure 4.17), and supports the notion that AMPA receptor subunits are produced normally in Nbea KO cells but are not transported properly to synapses.

To test whether the loss of functional AMPA receptors in Nbea KO synapses is due to altered receptor endocytosis, the cells were fixed at different time points after live-staining with anti-GluA2 antibodies. In order to stain the surface population of GluA2 receptor subunits, the cells were first treated with secondary antibody (Alexa Goat anti mouse 555) under non-permeabilizing conditions, and were then permeabilized and stained with another secondary antibody ((Alexa Goat anti mouse 488) to assess the internalized population of receptors in control and KO neurons. The population of GluA2 receptor subunit internalized was indistinguishable between control and Nbea KO cells, suggesting that Nbea does not affect receptor endocytosis (Figure 4.19 D).

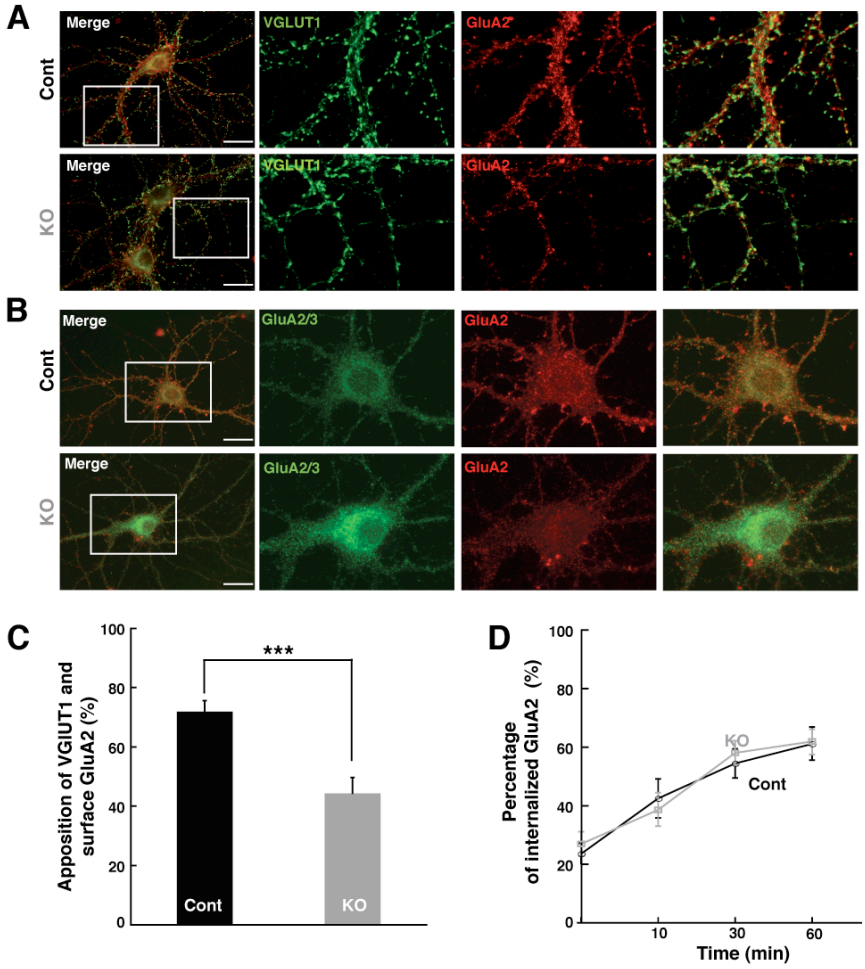

Figure 4.19: Surface staining of AMPA receptors

(A) Surface staining of GluA2 costained with presynaptic synaptic marker VGLUT1 in control (Cont) and Nbea KO neurons. (B) Surface staining of GluA2 costained with GluA2/3 in Cont and Nbea KO neurons. Scale bar=20μM. (C) Quantification of ratios of surface GluA2 puncta apposing VGLUT1 in Cont (n=8) and Nbea KO neurons (n=8). (D) GluA2 endocytosis activity monitored over 1 h in Cont (n=8) and Nbea KO (n=8) neurons. Error bars indicate SEM.

As was the case for AMPA receptors, the number of $GABA_A\gamma2$-positive puncta apposing VIAAT-positive puncta was reduced by 20% in glutamatergic and by 30% in GABAergic neurons (Figure 4.20 and Supplementary Table 3). This finding confirms that Nbea KO neurons form excitatory and inhibitory synapses but the surface expression of receptors is impaired severely in these neurons, especially in synapses.

Table 3. Morphological analysis of control (Cont) and Nbea KO neurons

	Glutamatergic neurons		GABAergic neurons	
	$Cont_{hipp}$	**KO_{hipp}**	**$Cont_{stri}$**	**KO_{str}**
Number of VGLUT1 puncta per cell	266 ± 29.8, n=22	308 ± 42.34, n=22		
Number of PSD95 puncta per cell	261.4 ± 23.64, n=20	284.3 ± 29.8, n=19		
Number of VIAAT puncta per cell			184.2 ± 22.04, n=35	148.7 ± 33.40, n=30
Number of Gephyrin puncta per cell			178.4 ± 24.70, n=21	165.18 ± 40.15,n=17
Apposition between pre and post synapses	0.64 ± 0.016, n=22	0.71 ± 0.013, n=22	0.71 ± 0.030, n=8	0.715 ± 0.026, n=8
Percentage of surface GluA2 puncta apposing VGLUT1(%)	71.8 ± 3.67, n=8	44.2 ±5.29, n=8		
Number of FM1-43 puncta colocalizing with VGLUT1	77.3 ± 6.42, n=7	77.4 ± 6.46, n=7		
Percentage of surface $GABA_A\gamma2$ puncta apposing VIAAT (%)	74.0 ± 2.86, n=5	55 ± 4.5, n=5	90 ± 2.4, n=10	60 ± 4.4, n=10
Number of somatic GluA2/3 puncta per unit μm^2	1.8 ± 0.44, n=7	5.2 ± 0.53, n=7		
Number of dendritic	1.41± 0.138, n=7	0.66 ± 0.11, n=7		

GluA2/3 puncta per unit μm^2				
Number of somatic $GABA_A\gamma2$ puncta per unit μm^2			3.8 ± 0.32, n=7	4.4 ± 0.33, n=7
Number of dendritic $GABA_A\gamma2$ puncta per unit μm^2			2.1 ± 0.15, n=7	1.93 ±0.320, n=7
Number of somatic GluN2A puncta per unit μm^2	3.05 ± 0.41, n=10	3.68 ± 0.33, n=10		
Number of dendritic GluN2A puncta per unit μm^2	2.73 ± 0.25, n=10	2.57 ± 0.29, n=10		

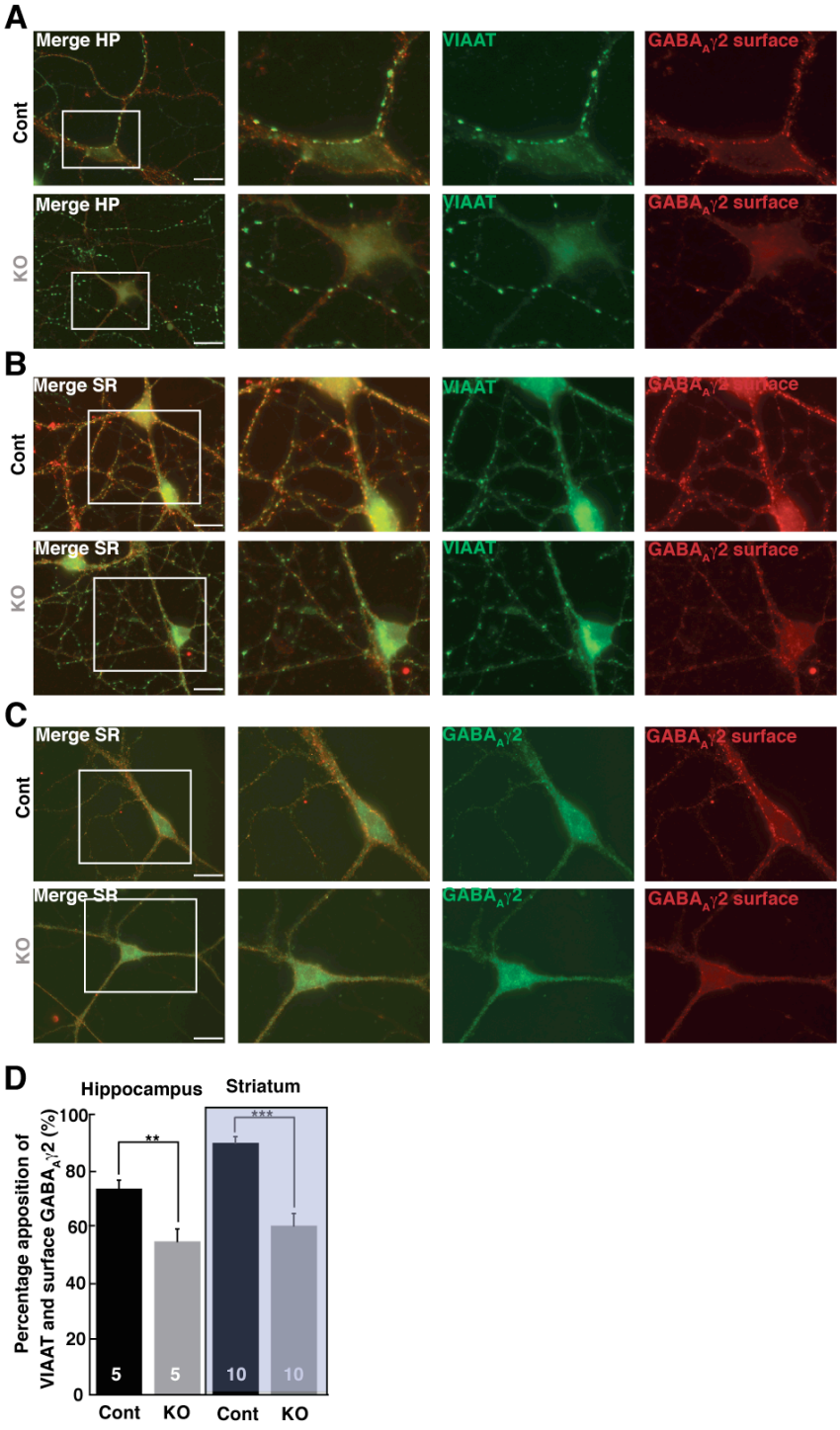

Figure 4.20: Reduced level of GABAγ2R at synapses.

(A-B) Examples of fluorescence staining of surface GABAγ2R (red) and the presynaptic marker VIAAT (green) in hippocampal neurons (A) and striatal neurons from control (Cont) and KO neurons (B). (C) Examples of fluorescence staining of surface GABAγ2R (red) with total GABAγ2R (green) in Cont and KO neurons. Scale bar= 20μM (D) Quantification of ratios

of surface GABAγ2R puncta apposing VIAAT. Numbers in the bars indicate cell numbers. Error bars indicate SEM.

4.6.4 Glycosylation Pattern of Receptor Proteins

To obtain independent evidence for the compromised receptor targeting in Nbea KO neurons and to identify the step in the secretory pathway affected by deletion of Nbea, the trafficking status of receptor subunits in neurons was analyzed by assessing their sensitivity to endoglycosidase H (EndoH) and PNGase F treatment. EndoH is an enzyme that specifically recognizes and cleaves high mannose type sugars, which are present on proteins resident in ER and cis-Golgi. These high mannose type sugars are processed along the secretory pathway such that most glycoproteins become EndoH insensitive as they mature into the medial-Golgi. PNGaseF on the other hand removes all sugar moieties of a glycoprotein irrespective of its state of maturation. EndoH and PNGaseF were employed to determine the receptor maturation levels in the absence of Nbea. Nbea deficient neurons showed 50% reduction in the levels of glycosylated GluA2/3 subunits, but not of GluK2/3, $GABA_A\alpha1$, extrasynaptic $GABA_A$ receptors ($GABA_A\alpha5$) or the synaptic adhesion protein neuroligin-1 (Figure 4.21). This indicates that Nbea deletion compromises GluA2/3 subunit trafficking from the ER to the Golgi while other receptor subunits can reach the Golgi and are probably arrested here, given their reduced surface expression.

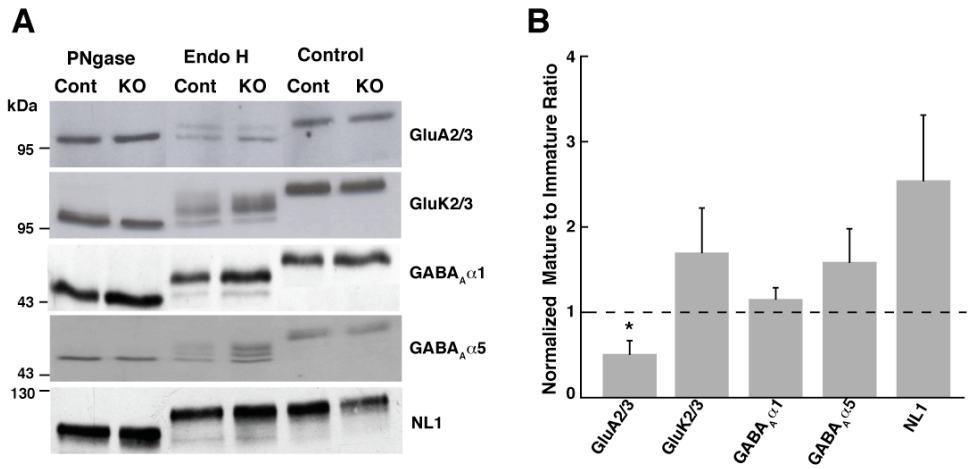

Figure 4.21: Glycosylation pattern of receptors in Nbea KO neurons.

(A) Western blot of indicated proteins from control (Cont) and Nbea KO DIV19 neurons after different enzyme treatments (PNGase F, Endo-H, Control with no enzyme treatment), (B) Quantification of ratios between mature and immature protein levels measured by Endo-H treatment in Nbea KO neurons (normalized to Cont levels). At least three independent experiments were conducted for each protein indicated. Error bars indicate SEM.

4.6.5 Intracellular Localization of Neurotransmitter Receptor

To confirm that receptors are differentially affected along the secretory pathway in Nbea KO neurons the localization of receptor proteins was compared to those of the Golgi marker GM130 and the ER marker KDEL. Confocal images of double staining for GluA2/3 staining and these markers showed a marked increase in somatic GluA2/3 puncta in KO neurons in comparison to control (Figure 4.22 A). Quantification of the number of somatic vs. dendritic puncta revealed an imbalance in the distribution of GluA2/3 in the KO neurons (Figure 4.22 B and Table 3). However, the immunostaining of $GABA_A\gamma2$ subunit and the GluN2A subunit revealed no intracellular accumulation in the Nbea KO neurons (Figure 4.22 C-F and Table 3) demonstrating the differential regulation of AMPA, NMDA and $GABA_A$-receptor subunits by Nbea along the secretory pathway.

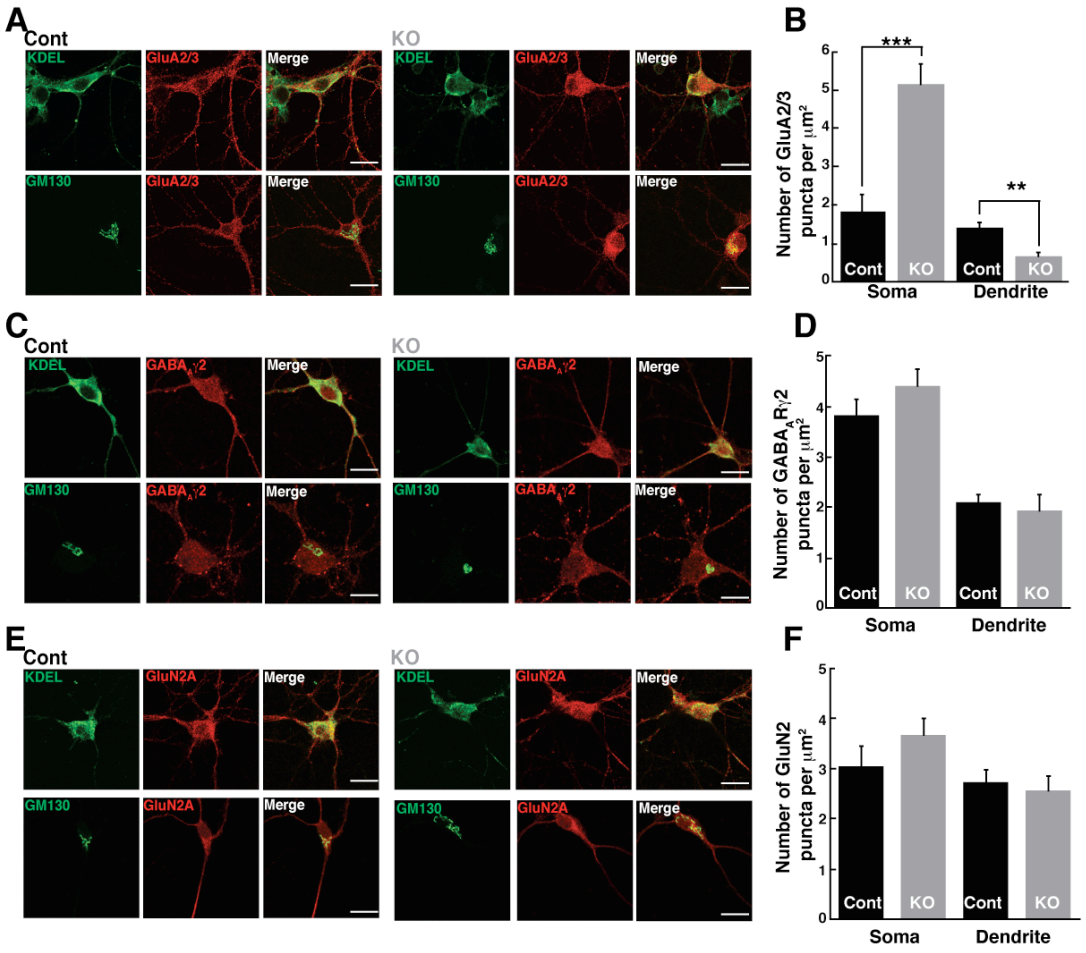

Figure 4.22: Receptor subunit distribution in Nbea KO neurons

(A) Examples of fluorescence staining in control (Cont) and KO glutamatergic hippocampal neurons at DIV15 using antibodies to GluA2/3 and the ER marker KDEL (top panel) or the cis-Golgi marker GM130 (lower panel). (B) Quantification of the number somatic and dendritic GluA2/3 puncta (n=7). (C) Examples of fluorescence staining in control (Cont) and KO GABAergic striatal neurons at DIV15 using antibodies to GABAγ2R and the ER marker KDEL (top panel) or the cis-Golgi marker GM130 (lower panel). (D) Quantification of the number of somatic and dendritic GABAγ2R puncta (n=7). (E) Examples of fluorescence staining in control (Cont) and KO glutamatergic hippocampal neurons at DIV15 using antibodies to GluN2A and the ER marker KDEL (top panel) or the cis-Golgi marker GM130 (lower panel). (F) Quantification of the number of somatic and dendritic GluN2A puncta (n=10). Error bars indicate SEM. Scale bar=10µM

5 Discussion

5.1 Functional Consequences of Nbea Loss

In WT embryos Nbea is expressed robustly, starting as early as E10.5. At E18.5 homozygous Nbea KO embryos display no gross abnormalities in brain development but have a hunched back posture and are immobile (Medrihan et al., 2009; Su et al., 2004). Moreover, Nbea KO pups also display an omphalocele and in some cases a cleft palate (Figure 4.1), which is similar to the phenotype of homozygous KO mice lacking VIAAT, which is a vesicular transporter responsible for filling of synaptic vesicles at GABAergic and glycinergic synapses (Wojcik et al., 2006). Also, mice lacking 67 kDa isoform of the GABA-synthesizing enzyme glutamic acid decarboxylase or the $GABA_A\beta3$ receptor subunit have a cleft palate (Asada et al., 1997; Homanics et al., 1997), and mice lacking the essential vesicle priming proteins Munc13-1 and 2 and CAPS or the KCC2 channel, whose expression determines the developmental switch of GABAergic transmission from excitatory to inhibitory, exhibit perinatal lethality along with the same hunched posture that is seen in the Nbea KO mice. In addition, KCC2 KO animals also show an omphalocele (Hubner et al., 2001; Jockusch et al., 2007; Varoqueaux et al., 2002). These findings indicate that a cleft palate and omphalocele result from perturbed GABAergic signaling. The underlying mechanisms are unclear, but it is likely that perturbed mobility of the affected embryos is the reason for aberrant palate and abdominal development and hunched body posture.

In the absence of Nbea, synaptic transmission is dramatically pertubed in glutamatergic and GABAergic autaptic neurons. The EPSC and IPSC amplitudes as well as apparent RRP sizes in Nbea KO hippocampal and striatal neurons were significantly reduced by approximately 70% as compared to control cells (Figure 4.2 and Table 1). mEPSCs/mIPSCs amplitudes were reduced only slightly in the Nbea KO neurons with no

changes in their kinetics, but the corresponding mEPSC/mIPSC frequencies were also reduced by 60% in Nbea KO neurons (Figure 4.2 and Table 1).

In principle, these phenotypic changes can be caused by perturbed synapse formation and reduced numbers of functional synapses. However, Nbea deletion does not alter the formation and number of synapses in glutamatergic and GABAergic neurons (Figure 4.5 and Table 3). In addition, no change was observed in the number of active presynapses or in the presynaptic release machinery in the absence of Nbea (Figure 4.4). Also, the overall expression levels of pre- and postsynaptic proteins were normal in Nbea KO neurons (Figure 4.17), and the synaptic release probability was not perturbed (Figure 4.12 B and Table 1). Instead, postsynaptic receptor localization, assessed using exogenous application of receptor agonists, biotinylation assays, and surface labeling, was dramatically reduction in the Nbea KO neurons (Figure 4.9, Figure 4.18, Figure 4.19 and Figure 4.20). These results indicate that synapses are made in the absence of Nbea but the postsynaptic receptors are not properly targeted to the synapses.

The observation that Nbea loss mainly causes postsynaptic defects was unexpected since previously published data on the neuromuscular junction (NMJ) and brainstem of Nbea KOs indicated a presynaptic function of Nbea. In the NMJ of Nbea KOs, evoked responses are completely blocked while spontaneous responses, and AchR expression and localization were unaffected (Su et al., 2004). A possible explanation for this discrepancy may arise from the structural and functional organization of murine NMJ synapses, which are formed between a motor neuron and muscle fibers. Transmitter receptor synthesis and transport in vertebrate muscle cells are profoundly different from the corresponding processes in nerve cells, and it is possible that muscle cells use homologues of Nbea to control AChR trafficking.

In the brainstem analyses of Nbea KOs, evoked and spontaneous synaptic transmission were both affected in a pattern similar to the hippocampal and striatal neurons studied here (Medrihan et al., 2009). However, the phenotypic

changes were attributed to presynaptic dysfunction since abnormalities in synapse formation and expression levels of presynaptic proteins were observed in the brainstem of Nbea KO animals. In cultured neurons and whole brain homogenates of Nbea KO animals, such defects were not seen (Figure 4.17). Also, the number of active synapses as measured by FM1-43 staining and the number of pre- and postsynapses as well as their apposition were normal in Nbea KO autaptic glutamatergic and GABAergic neurons (Figure 4.7 and Table 2). These findings corroborate observations on Nbea KO NMJs, whose morphology is unchanged (Su et al., 2004). In addition, Nbea positive puncta is not detectable in axons and presynaptic terminals of cultured neurons (contributed by Juliane Lauks). Taken together, these findings clearly indicate that Nbea functions postsynaptically. Since synaptic vesicle pool sizes, synaptic release probability, and postsynaptic receptor expression were not analyzed in the Nbea KO brainstem (Medrihan et al., 2009), postsynaptic deficits could still provide a possible explanation for the phenotypic changes observed in the Nbea KO brainstem.

5.2 A Postsynaptic Function of Nbea

The exogenous application of receptor agonists along with biotinylation experiments revealed dramatic reductions in the surface expression of neurotransmitter receptors in the Nbea KO cells (Figure 4.9 and Figure 4.18), and subsequent immunolabeling of AMPA and $GABA_A$ receptors, and electrophysiological measurements using MK801 provided further evidence for a loss of synaptic receptors in Nbea deficient neurons (Figure 4.12, Figure 4.19 and Figure 4.20). However, the surface expression of the synaptic adhesion molecule NL1 and the expression of scaffolding molecules like PSD95 and gephyrin and of extrasynaptic receptors were unchanged in Nbea KO neurons (Figure 4.5 and Figure 4.18). In addition, the overall expression levels of receptor proteins were unchanged in Nbea KO neurons (Figure 4.17). Thus, the reduction in synaptic transmission observed in Nbea KO neurons is mainly due to deficits in postsynaptic localization of neurotransmitter receptors.

The endocytosis of AMPA receptors was unaffected in Nbea KO neurons (Figure 4.19 D), and the localization studies and analyses of GluA2 receptor maturation revealed that AMPA receptors accumulate in/near the ER upon loss of Nbea, while NMDA, $GABA_A$, and kainate receptors are trapped at the level of the Golgi apparatus (Figure 4.21 and Figure 4.22). Taken together, these findings show that loss of Nbea alters synaptic transmission by affecting glutamate and $GABA_A$ receptor accumulation at synapses by causing aberrant receptor trafficking at distinct stages of the secretory pathway (Figure 5.1).

The spontanous synaptic activity recorded in the presence of TTX from Nbea KO neurons was strongly perturbed in Nbea KO cells. mEPSC and mIPSC frequencies were reduced by 60% and mEPSC and mIPSC amplitudes were reduced by 20% (Figure 4.3 and Table 1). These findings, together with the fact that synapses are formed at normal numbers in the absence of Nbea (Figure 4.5 and Table 3), indicate that deletion of Nbea leads to silencing of synapses due to the absence of postsynaptic receptors. The reduction of mEPSC/mIPSC amplitudes indicates that the remaining functional synapses in Nbea KO neurons are not equipped fully with functional receptors.

Subtle deficits were observed in the vesicular release probability of Nbea KO neurons (Figure 4.2 E and Table 1). Such changes are usually attributed to presynaptic deficits. However, Nbea is absent from axons and axon terminals and the key phenotypic changes in Nbea KO cells are observed at postsynapses. Indeed, the observed changes in apparent vesicular release probability may still be due to postsynaptic deficits. In the present study, the vesicular release probability was assessed by the ratio of the charge transfer induced by an action potential and by hypertonic sucrose application, both of which are affected by postsynaptic receptor expression. During sucrose application, large amounts of neurotransmitter are released into the synaptic cleft, which can spill over and activate neighboring extrasynaptic receptors. In Nbea KO neurons, the levels of extrasynaptic receptors are unchanged, causing an overestimation of the RRP relative to action potential induced

responses (Figure 4.12 D and Table 1). This could be a possible explanation for the reduced apparent P_{vr} observed in the Nbea KO neurons.

The findings in the present study clearly establish a key role of Nbea in trafficking neurotransmitter receptors to synapses. Interestingly, in WT neurons, the exogenous application of receptor agonists revealed the presence of functional $GABA_AR$ on glutamatergic autaptic cells and of functional AMPA receptors on GABAergic autaptic neurons. Nbea deletion resulted in a dramatic reduction of the number of $GABA_AR$ in glutamatergic neurons and of AMPA receptors in inhibitory neurons, indicating a heterogeneity of postsynaptic receptors at the cell surface despite the lack of one type of input (Figure 4.9 and Table 1). This type of receptor mismatch is remniscent of a previous study that identified $GABA_AR$ clusters in glutamatergic synapses and glutamate receptor clusters in GABAergic synapses using immunocytochemistry on cultured neurons (Rao et al., 2000). Functionality of such mismatched receptors has been demonstrated both in hippocampal mossy fiber synapses and in autapses (Bergersen et al., 2003; Takamori et al., 2000). Alternatively, presence of $GABA_A$ receptors on glutamatergic autaptic neurons and of glutamate receptors on GABAergic autaptic neurons may represent orphan postsynapses formed in the absence of any input.

The successful rescue experiments conducted on Nbea KO neurons using full-length Nbea indicate that the phenotypic effects of the Nbea KO are cell autonomous and that Nbea loss does not lead to complex secondary effects that cannot be reverted by Nbea re-expression (Figure 4.14 and Table 2). In contrast, neither the N-terminal and C-terminal Nbea constructs nor treatment of KO neurons with forskolin rescued the KO phenotype, indicating that the whole Nbea protein and not merely its AKAP function is required for targeting and clustering of receptors at synapses (Figure 4.15 and Table 2). Interestingly, overexpression of Nbea in WT neurons leads to an increase of synaptic responses (Figure 4.16 and Table 2), indicating that Nbea function is rate-limiting in the neurons analyzed.

5.3 Nbea Localization in WT Neurons

Nbea expression and distribution in neurons was analyzed using a novel antibody. To test the specificity of the antibody, Western blotting and immunolabelings were performed on WT and Nbea KO samples under identical conditions. The absence of any signal in Western blots and immunostainings of Nbea KO tissues established the specificity of the antibody (Figure 4.7).

In neurons, Nbea is enriched in somata in close apposition to the cis Golgi marker GM130 and along dendrites. However, no colocalization of Nbea was observed with the ER marker KDEL (Figure 4.8). Along the dendrites, Nbea was distributed uniformly and displayed partial overlap with the recycling endosomal markers Rab11, Transferrin, and Transferrin receptor, but not with early endosomal (EEA1, Rab5-GFP), mitochondrial (Hsp70), lysosomal (Lamp1), and postsynaptic markers (PSD95) (contributed by Juliane Lauks). Nbea is absent from axons and presynaptic terminals (contributed by Juliane Lauks). Previous studies had described an association of Nbea with the Golgi complex, which is stimulated in the presence of GTPγS and antagonized by BFA, indicating a possible involvement of Nbea in the generation of transport organelles (Wang et al., 2000). The localization of Nbea in neurons is nicely compatible with the postsynaptic changes seen in the Nbea KOs and with a potential role of Nbea in regulating protein trafficking in the secretory pathway.

5.4 Role of Nbea in Receptor Trafficking

Key mechanism by which neurotransmitter receptors are recruited to postsynapses involved diffusion and synaptic clustering of receptors from extrasynaptic locations (Bogdanov et al., 2006; Newpher and Ehlers, 2008). In Nbea KO neurons, experiments using MK801, revealed no differences in the expression and function of extrasynaptic NMDA receptors (Figure 4.12 D and Table 1). Unfortunately corresponding methods to functionally assess

synaptic vs. extrasynaptic $GABA_A$ and AMPA receptors could not be performed due to lack of corresponding tools. However, biotinylation experiments on the extrasynaptic $GABA_A\alpha5$ receptor subunit also failed to reveal changes in surface expression, unlike data on the synaptically localized $GABA_A$, NMDA, and AMPA receptor subunits (Figure 4.18). Moreover, trafficking of receptors to the plasma membrane prior to synaptogenesis is not affected by Nbea loss, unlike the scenario in mature neurons where surface expression of all major receptor subunits localized at synapses is reduced in the absence of Nbea (Figure 4.11). Taken together, these data indicate that the majority of synaptically localized receptors are trafficked directly from the Golgi apparatus to synapses and that Nbea is essential in mediating this process.

Cellular processes involving lateral diffusion of receptors between extrasynaptic and synaptic locations appear to operate downstream of Nbea targeting and may contribute to the remaining functional synaptic receptors observed in Nbea KO neurons. Indeed, some 30% of synapses are still operating rather normally in the absence of Nbea, contributing to the remaining evoked responses observed in the KO (Figure 4.2 and Table 1). Since the extrasynaptic receptor levels seem to be unperturbed in Nbea KO neurons, lateral diffusion of glutamate and $GABA_A$ receptors from extrasynaptic to synaptic sites could contribute to the remaining EPSC and IPSCs. However, mEPSC and mIPSC amplitudes are reduced in Nbea KO neurons in comparison to control cells, indicating that lateral diffusion alone is not sufficient to fully equip synapses with receptors (Figure 4.3 C and Table 1). Therefore, Nbea is a central organizer of postsynaptic receptors at synapses, and in its absence 60% of synapses are postsynaptically silent and the remaining 40% functional synapses contain fewer postsynaptic receptors.

Immunostaining data as well as surface biotinylation data showed that the trafficking of postsynaptic scaffolding proteins and of the synaptic adhesion molecule NL1 to synapses are not affected by Nbea loss (Figure 4.5, Figure 4.18 and Table 3), as is the case for extrasynaptic receptor trafficking (Figure

4.18). It thus appears that proteins destined for postsynapses under resting conditions can be recruited via atleast two pathways. One pathway is Nbea-dependent and transports the majority of neurotransmitter receptors from intracellularly compartments directly to the synapses. The other pathway is Nbea independent and targets the scaffold and adhesion proteins to synapses. In addition, an Nbea independent pathway also regulates the insertion of transmitter receptors into the extrasynaptic plasma membrane and is probably contributing to the remaining postsynaptic receptor population in Nbea KO by allowing receptor redistribution between extrasynaptic and synaptic sites.

AMPA receptor trafficking and their synaptic localization and function have been studied extensively because activity dependent changes of AMPA receptor expression at hippocampal synapses form the basis learning and memory. Synaptic activity differentially affects AMPA receptor subunits. In particular, predominantly expressed AMPA receptor subunits, GluA1 and GluA2/3, are recruited via different mechanisms to synapses. GluA2 homomers and GluA2/3 receptors are constitutively recruited to synapses whereas synaptic clustering of GluA1 receptor subunits is activity-driven (Hayashi et al., 2000; Shi et al., 2001; Wenthold et al., 1996a). Strikingly, Nbea regulates the synaptic expression of both GluA1 and GluA2/3 under basal conditions (Figure 4.18), indicating that Nbea acts upstream of the activity dependent AMPA-receptor trafficking, which is also consistent with the fact that AMPA receptors are immature and accumulate early in the biosynthetic route in the absence of Nbea (Figure 4.21 and Figure 4.22 A-B).

ER retention factors ensure the exit of properly assembled receptor complexes from the ER. Under basal conditions, a stable pool of GluA2 is retained in the ER (Greger et al., 2002), and in the absence of Nbea there is an increase in the number of ER resident GluA2 receptor subunits. Moreover, immunolabeling of GluA2 receptor subunits revealed a massive intracellular accumulation of AMPA receptors in Nbea KO neurons (Figure 4.22 A-B). ER assembly of AMPA receptors appears to be normal in Nbea KO neurons since

the total protein expression level of GluA2 receptor subunits was unaffected (Figure 4.17). Thus, the deglycosylation experiments and subcellular localization analyses of GluA2 receptor subunits indicate that Nbea regulates the transport of AMPA receptors already downstream of ER/cis-Golgi compartments. In contrast, no such maturation deficits and no intracellular accumulation are observed in the case of kainate, NMDA, and $GABA_A$ receptors (Figure 4.21 and Figure 4.22 C-F), indicating that these receptors reach the Golgi apparatus in Nbea KO cells and are probably arrested there since their cell surface expression is dramatically reduced (Figure 4.18). In this manner, Nbea differentially regulates synaptic AMPA, NMDA, kainate, and $GABA_A$ receptor trafficking from the endoplasmic reticulum.

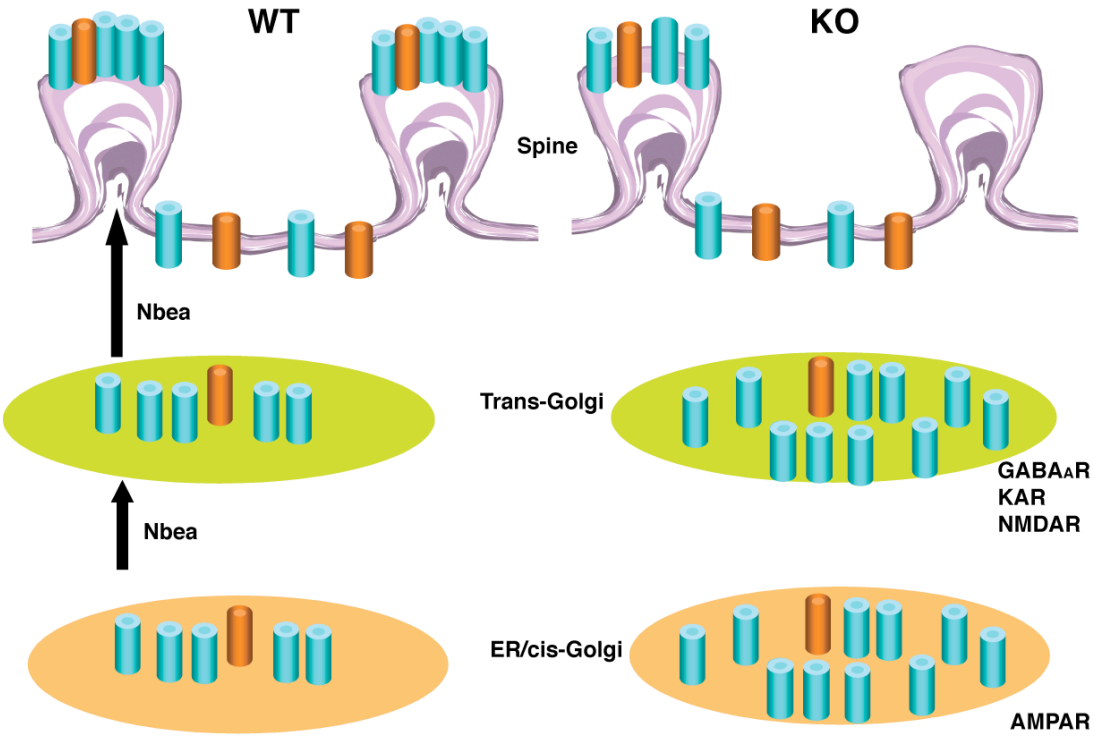

Figure 5.1: Receptor distribution in the presence and absence of Nbea in neurons

The model describes the difference in distribution of receptors in control and Nbea KO neurons. Nbea is essential for trafficking receptors directly to synapses. In its absence, AMPARs are retained in the ER/cis-Golgi while $GABA_AR$, KAR, NMDAR at the level of trans-Golgi network. The remaining receptors at the synapses of Nbea KO neurons are recruited in an Nbea independent manner, probably via lateral diffusion of receptors from extrasynaptic sites.

Several studies have established the essential role played by the C-terminal domain of receptor subunits in synaptic targeting of glutamate receptor subunits. The C-terminal domain of AMPA and NMDA receptor subunits contains a PDZ interacting domain, which binds proteins containing PDZ domains, thereby influencing receptor trafficking. Along the secretory pathway, AMPA receptor trafficking is regulated by interactions of their C-termini with PDZ domain proteins like GRIP1, PICK1, and SAP97 (Greger et al., 2002; Sans et al., 2001; Setou et al., 2002). Similarly, NMDARs were shown to form a complex with in the brain with the PDZ domain protein SAP102 and with sec8, and this complex was shown to be involved in the synaptic delivery of NMDA receptors (Sans et al., 2003). However $GABA_A$ receptors do not associate with PDZ proteins. Several proteins, like $GABA_AR$-associated protein (GABARAP) (Wang et al., 1999), Brefeldin-A-inhibited GDP/GTP exchange factor 2 (BIG2) (Charych et al., 2004), GABAAR-interacting factor 1 (GRIF1) (Smith et al., 2006), and *N*-ethylmaleimide-sensitive factor (NSF) (Goto et al., 2005) are known interaction partners of $GABA_AR$ receptor subunits.

Nbea has a direct effect on the trafficking of AMPA, NMDA, kainate, and $GABA_A$ receptors. Taking into account that the assembly, transport synaptic recruitment, and anchoring of these receptors types varies fundamentally between these receptor families, it is difficult to postulate a common molecular pathway by which Nbea might regulate receptor trafficking (Elias and Nicoll, 2007; Greger and Esteban, 2007; Hirokawa and Takemura, 2004; Jacob et al., 2008; Kneussel and Loebrich, 2007; Prybylowski and Wenthold, 2004). Pulldown and mass spectrometry analyses revealed possible binding partners

of Nbea (unpublished observation Juliane Lauks), but the association of Nbea with these proteins, in vivo still needs to be investigated.

Nbea contains two very distinct domains with a potential role in cellular trafficking. Nbea functions as an AKAP due to its high affinity binding site for the RII subunit of PKA, and at its C-terminal end, it contains a BEACH domain followed by WD40 repeats. LYST, which is also a member of the BEACH domain family of proteins, plays an essential role in membrane trafficking, and mutations in LYST affect the biogenesis of lysosomes, leading to defects in the immune system (Burkhardt et al., 1993; Introne et al., 1999; Nagle et al., 1996; Zhao et al., 1994). Similarly loss of function of SEL-2, which is the Nbea ortholog in *C. elegans*, leads to abnormalities in LIN12/Notch and LET23/EGFR signaling, compromising endocytic trafficking events in polarized cells (de Souza et al., 2007). Furthermore, *Drosophila* mutants of DAKAP 550/rugose also display defects in Notch-EGFR signaling, affecting eye development in flies (Shamloula et al., 2002). In addition, knockdown of AKAP150 affects NMDA triggered endocytosis of synaptic AMPA receptor (Bhattacharyya et al., 2009; Jurado et al.). Thus, BEACH and AKAP proteins are central regulators of signaling and trafficking in cells. However, Nbea only affects the trafficking of receptors from ER/Golgi to synapses, without disturbing the morphology of organelles and development of neurons, indicating that Nbea has a specific function in neurons (Figure 5.1).

In humans, the NBEA gene has been linked to an idiopathic case of non-familial autism (Castermans et al., 2003; Savelyeva et al., 2006). Autism spectrum disorders (ASD) are often interpreted as early neurodevelopmental disorders resulting from an imbalance between excitatory and inhibitory synaptic activity and mutation in proteins associated with ASDs such as neuroligin, neurexin, and shank 3 generally affect synapse function and often lead to abnormal synaptic homeostasis, which is a risk factor for ASDs (Persico and Bourgeron, 2006). In the absence of Nbea, excitatory and inhibitory transmissions are both equally affected due to severe deficits in the targeting of postsynaptic receptors, indicating that the Nbea related autism

cases might not be due to a general imbalance between excitatory and inhibitory synapses but may be due to general synaptic dysfunction.

6 Summary

In the present study, the function of Nbea was characterized in GABAergic and glutamatergic neurons. Loss of Nbea in neurons leads to severe deficits in synaptic transmission, which is observed in both the evoked and spontaneous responses in both cell types. However, no changes were observed in pre- and postsynapse numbers or in overall presynaptic function. In addition, expression of presynaptic proteins and postsynaptic receptors estimated by Western blotting was unaltered in the absence of Nbea. However, the deletion of Nbea dramatically affects the localization of neurotransmitter receptors at synapses as assessed by various methods such as exogenous application of receptor agonists, surface staining of receptors, and surface biotinylation assays. Moreover, the phenotypic changes arising from Nbea loss are rescued by re-introducing full length Nbea, and over-expression of Nbea in WT neurons leads to an increase in synaptic responses. Thus, Nbea function is a major determinant of synaptic strength.

Interestingly, although Nbea appears to be a general and essential regulator of $GABA_A$ and glutamate receptor trafficking, Nbea differentially affects the trafficking of different neurotransmitter receptor types, since the absence of Nbea leads to accumulation of AMPA receptors in the endoplasmic reticulum and/or cis-Golgi, whereas $GABA_A$, NMDA, and kainate receptors in Nbea KO neurons are trapped at the level of the trans-Golgi network. Surprisingly, the synaptic targeting of postsynaptic scaffolding proteins, like PSD95 and gephyrin, and of adhesion molecules, like NL1, are unaffected by Nbea loss, indicating that Nbea acts independently of these scaffolding and adhesion proteins and that these molecules are targeted to synapses in an Nbea-independent manner. Only the synaptic targeting of postsynaptic neurotransmitter receptors clearly depends on Nbea.

Until now, lateral diffusion of receptors from extrasynaptic sites has been proposed to be the major mechanism for synaptic accumulation of

neurotransmitter receptors. However, the present study shows that Nbea is the first identified protein involved in transporting and clustering functional postsynaptic neurotransmitter receptors directly from the secretory pathway.

7 Acknowledgements

I would like to express my sincere gratitude towards all the people, who contributed to the success of this work. At first, I would like to thank my supervisor Dr. JeongSeop Rhee, for the time he has invested on me. I have learnt a lot from him in the last three years.

I am indebted to Prof. Nils Brose, head of my thesis committee, for providing constant support and interest in the project. I am also truly grateful to my thesis committee members Prof. Tobias Moser and Prof. Erwin Neher, for their guidance and suggestions during the course of this study.

I especially thank the coordinators of the IMPRS Neuroscience Program, Prof. Michael Hörner and Sandra Drube, for their invaluable help and support over these years.

I thank my external collaborators Prof. Matthijs Verhage, Prof. Manfred Kiliman,n and Juliane Lauks, for providing material and for sharing their valuable expertise.

I would like to acknowledge the technical support provided by Anja Günther and Ines Beulhausen. I am grateful to all the members of the Neurobiology Department, especially Mrinalini Hoon, Noa Lipstein, Mika-Kishimoto Suga, Christoph Bredack, Christoph Beisemann, Dr. Sonja Wojcik, Dr. Benjamin Cooper and Dr. Hiroshi Kawabe.

Also, I would like to thank my friends, Chao Hua, Larissa, Auyon, Nandana and Gowri for always being there for me. Special thanks go to Gabriel, with whom I share all my up and downs.

Last but not the least, I would like to thank my parents for all the love and support they gave me.

This study was financially supported by the IMPRS.

8 References

Antonny, B., and Schekman, R. (2001). ER export: public transportation by the COPII coach. Curr Opin Cell Biol *13*, 438-443.

Asada, H., Kawamura, Y., Maruyama, K., Kume, H., Ding, R.G., Kanbara, N., Kuzume, H., Sanbo, M., Yagi, T., and Obata, K. (1997). Cleft palate and decreased brain gamma-aminobutyric acid in mice lacking the 67-kDa isoform of glutamic acid decarboxylase. Proc Natl Acad Sci U S A *94*, 6496-6499.

Ascher, P., and Nowak, L. (1988). The role of divalent cations in the N-methyl-D-aspartate responses of mouse central neurones in culture. J Physiol *399*, 247-266.

Azevedo, F.A., Carvalho, L.R., Grinberg, L.T., Farfel, J.M., Ferretti, R.E., Leite, R.E., Jacob Filho, W., Lent, R., and Herculano-Houzel, S. (2009). Equal numbers of neuronal and nonneuronal cells make the human brain an isometrically scaled-up primate brain. J Comp Neurol *513*, 532-541.

Bagri, A., and Tessier-Lavigne, M. (2002). Neuropilins as Semaphorin receptors: in vivo functions in neuronal cell migration and axon guidance. Adv Exp Med Biol *515*, 13-31.

Barry, M.F., and Ziff, E.B. (2002). Receptor trafficking and the plasticity of excitatory synapses. Curr Opin Neurobiol *12*, 279-286.

Bekkers, J.M., and Stevens, C.F. (1989). NMDA and non-NMDA receptors are co-localized at individual excitatory synapses in cultured rat hippocampus. Nature *341*, 230-233.

Bennett, M.V., and Zukin, R.S. (2004). Electrical coupling and neuronal synchronization in the Mammalian brain. Neuron *41*, 495-511.

Bergersen, L., Ruiz, A., Bjaalie, J.G., Kullmann, D.M., and Gundersen, V. (2003). GABA and GABAA receptors at hippocampal mossy fibre synapses. Eur J Neurosci *18*, 931-941.

Bettler, B., and Mulle, C. (1995). Review: neurotransmitter receptors. II. AMPA and kainate receptors. Neuropharmacology *34*, 123-139.

Betz, H. (1990). Ligand-gated ion channels in the brain: the amino acid receptor superfamily. Neuron *5*, 383-392.

Bhattacharyya, S., Biou, V., Xu, W., Schluter, O., and Malenka, R.C. (2009). A critical role for PSD-95/AKAP interactions in endocytosis of synaptic AMPA receptors. Nat Neurosci *12*, 172-181.

Biederer, T., Sara, Y., Mozhayeva, M., Atasoy, D., Liu, X., Kavalali, E.T., and Sudhof, T.C. (2002). SynCAM, a synaptic adhesion molecule that drives synapse assembly. Science *297*, 1525-1531.

Bogdanov, Y., Michels, G., Armstrong-Gold, C., Haydon, P.G., Lindstrom, J., Pangalos, M., and Moss, S.J. (2006). Synaptic GABAA receptors are directly recruited from their extrasynaptic counterparts. Embo J *25*, 4381-4389.

Bortolotto, Z.A., Clarke, V.R., Delany, C.M., Parry, M.C., Smolders, I., Vignes, M., Ho, K.H., Miu, P., Brinton, B.T., Fantaske, R.*, et al.* (1999). Kainate receptors are involved in synaptic plasticity. Nature *402*, 297-301.

Bresler, T., Ramati, Y., Zamorano, P.L., Zhai, R., Garner, C.C., and Ziv, N.E. (2001). The dynamics of SAP90/PSD-95 recruitment to new synaptic junctions. Mol Cell Neurosci *18*, 149-167.

Brunig, I., Scotti, E., Sidler, C., and Fritschy, J.M. (2002). Intact sorting, targeting, and clustering of gamma-aminobutyric acid A receptor subtypes in hippocampal neurons in vitro. J Comp Neurol *443*, 43-55.

Burgess, A., Mornon, J.P., de Saint-Basile, G., and Callebaut, I. (2009). A concanavalin A-like lectin domain in the CHS1/LYST protein, shared by members of the BEACH family. Bioinformatics *25*, 1219-1222.

Burkhardt, J.K., Wiebel, F.A., Hester, S., and Argon, Y. (1993). The giant organelles in beige and Chediak-Higashi fibroblasts are derived from late endosomes and mature lysosomes. J Exp Med *178*, 1845-1856.

Castermans, D., Wilquet, V., Parthoens, E., Huysmans, C., Steyaert, J., Swinnen, L., Fryns, J.P., Van de Ven, W., and Devriendt, K. (2003). The neurobeachin gene is disrupted by a translocation in a patient with idiopathic autism. J Med Genet *40*, 352-356.

Castillo, P.E., Malenka, R.C., and Nicoll, R.A. (1997). Kainate receptors mediate a slow postsynaptic current in hippocampal CA3 neurons. Nature *388*, 182-186.

Charych, E.I., Yu, W., Miralles, C.P., Serwanski, D.R., Li, X., Rubio, M., and De Blas, A.L. (2004). The brefeldin A-inhibited GDP/GTP exchange factor 2, a protein involved in vesicular trafficking, interacts with the beta subunits of the GABA receptors. J Neurochem *90*, 173-189.

Chen, L., Chetkovich, D.M., Petralia, R.S., Sweeney, N.T., Kawasaki, Y., Wenthold, R.J., Bredt, D.S., and Nicoll, R.A. (2000). Stargazin regulates synaptic targeting of AMPA receptors by two distinct mechanisms. Nature *408*, 936-943.

Clarke, V.R., Ballyk, B.A., Hoo, K.H., Mandelzys, A., Pellizzari, A., Bath, C.P., Thomas, J., Sharpe, E.F., Davies, C.H., Ornstein, P.L.*, et al.* (1997). A hippocampal GluR5 kainate receptor regulating inhibitory synaptic transmission. Nature *389*, 599-603.

Coleman, S.K., Cai, C., Mottershead, D.G., Haapalahti, J.P., and Keinanen, K. (2003). Surface expression of GluR-D AMPA receptor is dependent on an interaction between its C-terminal domain and a 4.1 protein. J Neurosci *23*, 798-806.

Colledge, M., and Scott, J.D. (1999). AKAPs: from structure to function. Trends Cell Biol *9*, 216-221.

Connolly, C.N., Krishek, B.J., McDonald, B.J., Smart, T.G., and Moss, S.J. (1996). Assembly and cell surface expression of heteromeric and homomeric gamma-aminobutyric acid type A receptors. J Biol Chem *271*, 89-96.

Contractor, A., Swanson, G., and Heinemann, S.F. (2001). Kainate receptors are involved in short- and long-term plasticity at mossy fiber synapses in the hippocampus. Neuron *29*, 209-216.

Costa, M.C., Mani, F., Santoro, W., Jr., Espreafico, E.M., and Larson, R.E. (1999). Brain myosin-V, a calmodulin-carrying myosin, binds to calmodulin-dependent protein kinase II and activates its kinase activity. J Biol Chem *274*, 15811-15819.

Coussen, F. (2009). Molecular determinants of kainate receptor trafficking. Neuroscience *158*, 25-35.

De Camilli, P., Moretti, M., Donini, S.D., Walter, U., and Lohmann, S.M. (1986). Heterogeneous distribution of the cAMP receptor protein RII in the nervous system: evidence for its intracellular accumulation on microtubules, microtubule-organizing centers, and in the area of the Golgi complex. J Cell Biol *103*, 189-203.

de Souza, N., Vallier, L.G., Fares, H., and Greenwald, I. (2007). SEL-2, the C. elegans neurobeachin/LRBA homolog, is a negative regulator of lin-12/Notch activity and affects endosomal traffic in polarized epithelial cells. Development *134*, 691-702.

Dingledine, R., Borges, K., Bowie, D., and Traynelis, S.F. (1999). The glutamate receptor ion channels. Pharmacol Rev *51*, 7-61.

Dong, H., O'Brien, R.J., Fung, E.T., Lanahan, A.A., Worley, P.F., and Huganir, R.L. (1997). GRIP: a synaptic PDZ domain-containing protein that interacts with AMPA receptors. Nature *386*, 279-284.

Durand, G.M., Kovalchuk, Y., and Konnerth, A. (1996). Long-term potentiation and functional synapse induction in developing hippocampus. Nature *381*, 71-75.

Edgar, J.M., and Nave, K.A. (2009). The role of CNS glia in preserving axon function. Curr Opin Neurobiol *19*, 498-504.

El-Husseini, A.E., Schnell, E., Chetkovich, D.M., Nicoll, R.A., and Bredt, D.S. (2000). PSD-95 involvement in maturation of excitatory synapses. Science *290*, 1364-1368.

Elias, G.M., and Nicoll, R.A. (2007). Synaptic trafficking of glutamate receptors by MAGUK scaffolding proteins. Trends Cell Biol *17*, 343-352.

Esteban, J.A., Shi, S.H., Wilson, C., Nuriya, M., Huganir, R.L., and Malinow, R. (2003). PKA phosphorylation of AMPA receptor subunits controls synaptic trafficking underlying plasticity. Nat Neurosci *6*, 136-143.

Feng, G., Tintrup, H., Kirsch, J., Nichol, M.C., Kuhse, J., Betz, H., and Sanes, J.R. (1998). Dual requirement for gephyrin in glycine receptor clustering and molybdoenzyme activity. Science *282*, 1321-1324.

Friedman, H.V., Bresler, T., Garner, C.C., and Ziv, N.E. (2000). Assembly of new individual excitatory synapses: time course and temporal order of synaptic molecule recruitment. Neuron *27*, 57-69.

Fritschy, J.M., Harvey, R.J., and Schwarz, G. (2008). Gephyrin: where do we stand, where do we go? Trends Neurosci *31*, 257-264.

Fujita, M., Sato, K., Sato, M., Inoue, T., Kozuka, T., and Tohyama, M. (1991). Regional distribution of the cells expressing glycine receptor beta subunit mRNA in the rat brain. Brain Res *560*, 23-37.

Furukawa, H., Singh, S.K., Mancusso, R., and Gouaux, E. (2005). Subunit arrangement and function in NMDA receptors. Nature *438*, 185-192.

Garcia, E.P., Mehta, S., Blair, L.A., Wells, D.G., Shang, J., Fukushima, T., Fallon, J.R., Garner, C.C., and Marshall, J. (1998). SAP90 binds and clusters kainate receptors causing incomplete desensitization. Neuron *21*, 727-739.

Gardiol, A., Racca, C., and Triller, A. (1999). Dendritic and postsynaptic protein synthetic machinery. J Neurosci *19*, 168-179.

Gardoni, F., Caputi, A., Cimino, M., Pastorino, L., Cattabeni, F., and Di Luca, M. (1998). Calcium/calmodulin-dependent protein kinase II is associated with NR2A/B subunits of NMDA receptor in postsynaptic densities. J Neurochem *71*, 1733-1741.

Garner, C.C., Zhai, R.G., Gundelfinger, E.D., and Ziv, N.E. (2002). Molecular mechanisms of CNS synaptogenesis. Trends Neurosci *25*, 243-251.

Gebauer, D., Li, J., Jogl, G., Shen, Y., Myszka, D.G., and Tong, L. (2004). Crystal structure of the PH-BEACH domains of human LRBA/BGL. Biochemistry *43*, 14873-14880.

Goto, H., Terunuma, M., Kanematsu, T., Misumi, Y., Moss, S.J., and Hirata, M. (2005). Direct interaction of N-ethylmaleimide-sensitive factor with GABA(A) receptor beta subunits. Mol Cell Neurosci *30*, 197-206.

Graf, E.R., Zhang, X., Jin, S.X., Linhoff, M.W., and Craig, A.M. (2004). Neurexins induce differentiation of GABA and glutamate postsynaptic specializations via neuroligins. Cell *119*, 1013-1026.

Gray, E.G. (1959). Axo-somatic and axo-dendritic synapses of the cerebral cortex: an electron microscope study. J Anat *93*, 420-433.

Greger, I.H., and Esteban, J.A. (2007). AMPA receptor biogenesis and trafficking. Curr Opin Neurobiol *17*, 289-297.

Greger, I.H., Khatri, L., and Ziff, E.B. (2002). RNA editing at arg607 controls AMPA receptor exit from the endoplasmic reticulum. Neuron *34*, 759-772.

Griffon, N., Buttner, C., Nicke, A., Kuhse, J., Schmalzing, G., and Betz, H. (1999). Molecular determinants of glycine receptor subunit assembly. Embo J *18*, 4711-4721.

Grosshans, D.R., Clayton, D.A., Coultrap, S.J., and Browning, M.D. (2002). LTP leads to rapid surface expression of NMDA but not AMPA receptors in adult rat CA1. Nat Neurosci *5*, 27-33.

Harney, S.C., Jane, D.E., and Anwyl, R. (2008). Extrasynaptic NR2D-containing NMDARs are recruited to the synapse during LTP of NMDAR-EPSCs. J Neurosci *28*, 11685-11694.

Harris, K.M., and Stevens, J.K. (1989). Dendritic spines of CA 1 pyramidal cells in the rat hippocampus: serial electron microscopy with reference to their biophysical characteristics. J Neurosci *9*, 2982-2997.

Hashimoto, K., and Kano, M. (2003). Functional differentiation of multiple climbing fiber inputs during synapse elimination in the developing cerebellum. Neuron *38*, 785-796.

Hayashi, Y., Shi, S.H., Esteban, J.A., Piccini, A., Poncer, J.C., and Malinow, R. (2000). Driving AMPA receptors into synapses by LTP and CaMKII: requirement for GluR1 and PDZ domain interaction. Science *287*, 2262-2267.

Hayes, D.M., Braud, S., Hurtado, D.E., McCallum, J., Standley, S., Isaac, J.T., and Roche, K.W. (2003). Trafficking and surface expression of the glutamate receptor subunit, KA2. Biochem Biophys Res Commun *310*, 8-13.

Hirbec, H., Francis, J.C., Lauri, S.E., Braithwaite, S.P., Coussen, F., Mulle, C., Dev, K.K., Coutinho, V., Meyer, G., Isaac, J.T.*, et al.* (2003). Rapid and differential regulation of AMPA and kainate receptors at hippocampal mossy fibre synapses by PICK1 and GRIP. Neuron *37*, 625-638.

Hirokawa, N., and Takemura, R. (2004). Molecular motors in neuronal development, intracellular transport and diseases. Curr Opin Neurobiol *14*, 564-573.

Hoch, W., Betz, H., and Becker, C.M. (1989). Primary cultures of mouse spinal cord express the neonatal isoform of the inhibitory glycine receptor. Neuron *3*, 339-348.

Hollmann, M., and Heinemann, S. (1994). Cloned glutamate receptors. Annu Rev Neurosci *17*, 31-108.

Homanics, G.E., DeLorey, T.M., Firestone, L.L., Quinlan, J.J., Handforth, A., Harrison, N.L., Krasowski, M.D., Rick, C.E., Korpi, E.R., Makela, R.*, et al.* (1997). Mice devoid of gamma-aminobutyrate type A receptor beta3 subunit have epilepsy, cleft palate, and hypersensitive behavior. Proc Natl Acad Sci U S A *94*, 4143-4148.

Horton, A.C., and Ehlers, M.D. (2003). Neuronal polarity and trafficking. Neuron *40*, 277-295.

Hsu, S.C., Hazuka, C.D., Foletti, D.L., and Scheller, R.H. (1999). Targeting vesicles to specific sites on the plasma membrane: the role of the sec6/8 complex. Trends Cell Biol *9*, 150-153.

Hubner, C.A., Stein, V., Hermans-Borgmeyer, I., Meyer, T., Ballanyi, K., and Jentsch, T.J. (2001). Disruption of KCC2 reveals an essential role of K-Cl cotransport already in early synaptic inhibition. Neuron *30*, 515-524.

Huettner, J.E., and Bean, B.P. (1988). Block of N-methyl-D-aspartate-activated current by the anticonvulsant MK-801: selective binding to open channels. Proc Natl Acad Sci U S A *85*, 1307-1311.

Introne, W., Boissy, R.E., and Gahl, W.A. (1999). Clinical, molecular, and cell biological aspects of Chediak-Higashi syndrome. Mol Genet Metab *68*, 283-303.

Irie, M., Hata, Y., Takeuchi, M., Ichtchenko, K., Toyoda, A., Hirao, K., Takai, Y., Rosahl, T.W., and Sudhof, T.C. (1997). Binding of neuroligins to PSD-95. Science *277*, 1511-1515.

Jacob, T.C., Moss, S.J., and Jurd, R. (2008). GABAA receptor trafficking and its role in the dynamic modulation of neuronal inhibition. Nat Rev Neurosci *9*, 331-343.

Jaskolski, F., Coussen, F., Nagarajan, N., Normand, E., Rosenmund, C., and Mulle, C. (2004). Subunit composition and alternative splicing regulate membrane delivery of kainate receptors. J Neurosci *24*, 2506-2515.

Jaskolski, F., Normand, E., Mulle, C., and Coussen, F. (2005). Differential trafficking of GluR7 kainate receptor subunit splice variants. J Biol Chem *280*, 22968-22976.

Jockusch, W.J., Speidel, D., Sigler, A., Sorensen, J.B., Varoqueaux, F., Rhee, J.S., and Brose, N. (2007). CAPS-1 and CAPS-2 are essential synaptic vesicle priming proteins. Cell *131*, 796-808.

Jogl, G., Shen, Y., Gebauer, D., Li, J., Wiegmann, K., Kashkar, H., Kronke, M., and Tong, L. (2002). Crystal structure of the BEACH domain reveals an unusual fold and extensive association with a novel PH domain. Embo J *21*, 4785-4795.

Johnson, J.W., and Ascher, P. (1987). Glycine potentiates the NMDA response in cultured mouse brain neurons. Nature *325*, 529-531.

Jones, M.V., and Westbrook, G.L. (1996). The impact of receptor desensitization on fast synaptic transmission. Trends Neurosci. *19*, 96-101.

Jurado, S., Biou, V., and Malenka, R.C. A calcineurin/AKAP complex is required for NMDA receptor-dependent long-term depression. Nat Neurosci *13*, 1053-1055.

Kacharmina, J.E., Job, C., Crino, P., and Eberwine, J. (2000). Stimulation of glutamate receptor protein synthesis and membrane insertion within isolated neuronal dendrites. Proc Natl Acad Sci U S A *97*, 11545-11550.

Katz-Sidlow, R.J. (1998). The formulation of the neuron doctrine: the Island of Cajal. Arch Neurol *55*, 237-240.

Kayadjanian, N., Lee, H.S., Pina-Crespo, J., and Heinemann, S.F. (2007). Localization of glutamate receptors to distal dendrites depends on subunit composition and the kinesin motor protein KIF17. Mol Cell Neurosci *34*, 219-230.

Kennedy, M.B., Bennett, M.K., and Erondu, N.E. (1983). Biochemical and immunochemical evidence that the "major postsynaptic density protein" is a subunit of a calmodulin-dependent protein kinase. Proc Natl Acad Sci U S A *80*, 7357-7361.

Kennedy, M.J., and Ehlers, M.D. (2006). Organelles and trafficking machinery for postsynaptic plasticity. Annu Rev Neurosci *29*, 325-362.

Kessels, H.W., and Malinow, R. (2009). Synaptic AMPA receptor plasticity and behavior. Neuron *61*, 340-350.

Kim, C.H., Chung, H.J., Lee, H.K., and Huganir, R.L. (2001). Interaction of the AMPA receptor subunit GluR2/3 with PDZ domains regulates hippocampal long-term depression. Proc Natl Acad Sci U S A *98*, 11725-11730.

Kim, E., Niethammer, M., Rothschild, A., Jan, Y.N., and Sheng, M. (1995). Clustering of Shaker-type K+ channels by interaction with a family of membrane-associated guanylate kinases. Nature *378*, 85-88.

Kim, E., and Sheng, M. (2004). PDZ domain proteins of synapses. Nat Rev Neurosci *5*, 771-781.

Kleizen, B., and Braakman, I. (2004). Protein folding and quality control in the endoplasmic reticulum. Curr Opin Cell Biol *16*, 343-349.

Kneussel, M., Brandstatter, J.H., Gasnier, B., Feng, G., Sanes, J.R., and Betz, H. (2001). Gephyrin-independent clustering of postsynaptic GABA(A) receptor subtypes. Mol Cell Neurosci *17*, 973-982.

Kneussel, M., Haverkamp, S., Fuhrmann, J.C., Wang, H., Wassle, H., Olsen, R.W., and Betz, H. (2000). The gamma-aminobutyric acid type A receptor (GABAAR)-associated protein GABARAP interacts with gephyrin but is not involved in receptor anchoring at the synapse. Proc Natl Acad Sci U S A *97*, 8594-8599.

Kneussel, M., and Loebrich, S. (2007). Trafficking and synaptic anchoring of ionotropic inhibitory neurotransmitter receptors. Biol Cell *99*, 297-309.

Knott, G.W., Quairiaux, C., Genoud, C., and Welker, E. (2002). Formation of dendritic spines with GABAergic synapses induced by whisker stimulation in adult mice. Neuron *34*, 265-273.

Kohrmann, M., Haubensak, W., Hemraj, I., Kaether, C., Lessmann, V.J., and Kiebler, M.A. (1999). Fast, convenient, and effective method to transiently transfect primary hippocampal neurons. J Neurosci Res *58*, 831-835.

Kornau, H.C., Schenker, L.T., Kennedy, M.B., and Seeburg, P.H. (1995). Domain interaction between NMDA receptor subunits and the postsynaptic density protein PSD-95. Science *269*, 1737-1740.

Kuehn, M.J., and Schekman, R. (1997). COPII and secretory cargo capture into transport vesicles. Curr Opin Cell Biol *9*, 477-483.

Kuhse, J., Laube, B., Magalei, D., and Betz, H. (1993). Assembly of the inhibitory glycine receptor: identification of amino acid sequence motifs governing subunit stoichiometry. Neuron *11*, 1049-1056.

Kuriu, T., Inoue, A., Bito, H., Sobue, K., and Okabe, S. (2006). Differential control of postsynaptic density scaffolds via actin-dependent and -independent mechanisms. J Neurosci *26*, 7693-7706.

Langosch, D., Thomas, L., and Betz, H. (1988). Conserved quaternary structure of ligand-gated ion channels: the postsynaptic glycine receptor is a pentamer. Proc Natl Acad Sci U S A *85*, 7394-7398.

Lauri, S.E., Bortolotto, Z.A., Bleakman, D., Ornstein, P.L., Lodge, D., Isaac, J.T., and Collingridge, G.L. (2001). A critical role of a facilitatory presynaptic kainate receptor in mossy fiber LTP. Neuron *32*, 697-709.

Lee, H.K., Barbarosie, M., Kameyama, K., Bear, M.F., and Huganir, R.L. (2000). Regulation of distinct AMPA receptor phosphorylation sites during bidirectional synaptic plasticity. Nature *405*, 955-959.

Lee, H.K., Takamiya, K., Han, J.S., Man, H., Kim, C.H., Rumbaugh, G., Yu, S., Ding, L., He, C., Petralia, R.S.*, et al.* (2003). Phosphorylation of the AMPA receptor GluR1 subunit is required for synaptic plasticity and retention of spatial memory. Cell *112*, 631-643.

Lee, M.C., Miller, E.A., Goldberg, J., Orci, L., and Schekman, R. (2004). Bi-directional protein transport between the ER and Golgi. Annu Rev Cell Dev Biol *20*, 87-123.

Lee, S.H., Liu, L., Wang, Y.T., and Sheng, M. (2002). Clathrin adaptor AP2 and NSF interact with overlapping sites of GluR2 and play distinct roles in AMPA receptor trafficking and hippocampal LTD. Neuron *36*, 661-674.

Lerma, J. (2003). Roles and rules of kainate receptors in synaptic transmission. Nat Rev Neurosci *4*, 481-495.

LeVay, S., Wiesel, T.N., and Hubel, D.H. (1980). The development of ocular dominance columns in normal and visually deprived monkeys. J Comp Neurol *191*, 1-51.

Levi, S., Logan, S.M., Tovar, K.R., and Craig, A.M. (2004). Gephyrin Is Critical for Glycine Receptor Clustering But Not for the Formation of Functional GABAergic Synapses in Hippocampal Neurons. J. Neurosci. *24*, 207-217.

Lin, J.W., Ju, W., Foster, K., Lee, S.H., Ahmadian, G., Wyszynski, M., Wang, Y.T., and Sheng, M. (2000). Distinct molecular mechanisms and divergent endocytotic pathways of AMPA receptor internalization. Nat Neurosci *3*, 1282-1290.

Linhoff, M.W., Lauren, J., Cassidy, R.M., Dobie, F.A., Takahashi, H., Nygaard, H.B., Airaksinen, M.S., Strittmatter, S.M., and Craig, A.M. (2009). An unbiased expression screen for synaptogenic proteins identifies the LRRTM protein family as synaptic organizers. Neuron *61*, 734-749.

Lisman, J.E., and Zhabotinsky, A.M. (2001). A model of synaptic memory: a CaMKII/PP1 switch that potentiates transmission by organizing an AMPA receptor anchoring assembly. Neuron *31*, 191-201.

Lopez-Munoz, F., Boya, J., and Alamo, C. (2006). Neuron theory, the cornerstone of neuroscience, on the centenary of the Nobel Prize award to Santiago Ramon y Cajal. Brain Res Bull *70*, 391-405.

Maas, C., Belgardt, D., Lee, H.K., Heisler, F.F., Lappe-Siefke, C., Magiera, M.M., van Dijk, J., Hausrat, T.J., Janke, C., and Kneussel, M. (2009). Synaptic activation modifies microtubules underlying transport of postsynaptic cargo. Proc Natl Acad Sci U S A *106*, 8731-8736.

Maas, C., Tagnaouti, N., Loebrich, S., Behrend, B., Lappe-Siefke, C., and Kneussel, M. (2006). Neuronal cotransport of glycine receptor and the scaffold protein gephyrin. J Cell Biol *172*, 441-451.

Mah, S.J., Cornell, E., Mitchell, N.A., and Fleck, M.W. (2005). Glutamate receptor trafficking: endoplasmic reticulum quality control involves ligand binding and receptor function. J Neurosci *25*, 2215-2225.

Malenka, R.C., and Bear, M.F. (2004). LTP and LTD: an embarrassment of riches. Neuron *44*, 5-21.

Malosio, M.L., Marqueze-Pouey, B., Kuhse, J., and Betz, H. (1991). Widespread expression of glycine receptor subunit mRNAs in the adult and developing rat brain. Embo J *10*, 2401-2409.

Mayer, M.L., Westbrook, G.L., and Guthrie, P.B. (1984). Voltage-dependent block by Mg2+ of NMDA responses in spinal cord neurones. Nature *309*, 261-263.

McGee, A.W., Topinka, J.R., Hashimoto, K., Petralia, R.S., Kakizawa, S., Kauer, F.W., Aguilera-Moreno, A., Wenthold, R.J., Kano, M., and Bredt, D.S. (2001). PSD-93 knock-out mice reveal that neuronal MAGUKs are not required for development or function of parallel fiber synapses in cerebellum. J Neurosci *21*, 3085-3091.

McIlhinney, R.A., Molnar, E., Atack, J.R., and Whiting, P.J. (1996). Cell surface expression of the human N-methyl-D-aspartate receptor subunit 1a requires the co-expression of the NR2A subunit in transfected cells. Neuroscience *70*, 989-997.

Medrihan, L., Rohlmann, A., Fairless, R., Andrae, J., D√∂ring, M., Missler, M., Zhang, W., and Kilimann, M.W. (2009). Neurobeachin, a protein implicated in membrane protein traffic and autism, is required for the formation and functioning of central synapses. J Physiol *587*, 5095-5106.

Meng, Y., Zhang, Y., and Jia, Z. (2003). Synaptic transmission and plasticity in the absence of AMPA glutamate receptor GluR2 and GluR3. Neuron *39*, 163-176.

Meyer, G., Kirsch, J., Betz, H., and Langosch, D. (1995). Identification of a gephyrin binding motif on the glycine receptor beta subunit. Neuron *15*, 563-572.

Montgomery, J.M., Selcher, J.C., Hanson, J.E., and Madison, D.V. (2005). Dynamin-dependent NMDAR endocytosis during LTD and its dependence on synaptic state. BMC Neurosci *6*, 48.

Nagle, D.L., Karim, M.A., Woolf, E.A., Holmgren, L., Bork, P., and Misumi, D.J. (1996). Identification and mutation analysis of the complete gene for Chediak-Higashi syndrome. Nature Genet *14*, 307-311.

Newpher, T.M., and Ehlers, M.D. (2008). Glutamate receptor dynamics in dendritic microdomains. Neuron *58*, 472-497.

Nicoll, R.A., and Malenka, R.C. (1999). Expression mechanisms underlying NMDA receptor-dependent long-term potentiation. Ann N Y Acad Sci *868*, 515-525.

Nicoll, R.A., Malenka, R.C., and Kauer, J.A. (1990). Functional comparison of neurotransmitter receptor subtypes in mammalian central nervous system. Physiol Rev *70*, 513-565.

Nowak, L., Bregestovski, P., Ascher, P., Herbet, A., and Prochiantz, A. (1984). Magnesium gates glutamate-activated channels in mouse central neurones. Nature *307*, 462-465.

O'Sullivan, G.A., Kneussel, M., Elazar, Z., and Betz, H. (2005). GABARAP is not essential for GABA receptor targeting to the synapse. Eur J Neurosci *22*, 2644-2648.

Okabe, S. (2007). Molecular anatomy of the postsynaptic density. Mol Cell Neurosci *34*, 503-518.

Okabe, S., Miwa, A., and Okado, H. (1999). Alternative splicing of the C-terminal domain regulates cell surface expression of the NMDA receptor NR1 subunit. J Neurosci *19*, 7781-7792.

Osten, P., Khatri, L., Perez, J.L., Kohr, G., Giese, G., Daly, C., Schulz, T.W., Wensky, A., Lee, L.M., and Ziff, E.B. (2000). Mutagenesis reveals a role for ABP/GRIP binding to GluR2 in synaptic surface accumulation of the AMPA receptor. Neuron *27*, 313-325.

Pascual, M., Pozas, E., Barallobre, M.J., Tessier-Lavigne, M., and Soriano, E. (2004). Coordinated functions of Netrin-1 and Class 3 secreted Semaphorins

in the guidance of reciprocal septohippocampal connections. Mol Cell Neurosci *26*, 24-33.

Persico, A.M., and Bourgeron, T. (2006). Searching for ways out of the autism maze: genetic, epigenetic and environmental clues. Trends Neurosci *29*, 349-358.

Pierce, J.P., and Mendell, L.M. (1993). Quantitative ultrastructure of Ia boutons in the ventral horn: scaling and positional relationships. J Neurosci *13*, 4748-4763.

Prybylowski, K., and Wenthold, R.J. (2004). N-Methyl-D-aspartate receptors: subunit assembly and trafficking to the synapse. J Biol Chem *279*, 9673-9676.

Rao, A., Cha, E.M., and Craig, A.M. (2000). Mismatched Appositions of Presynaptic and Postsynaptic Components in Isolated Hippocampal Neurons. J. Neurosci. *20*, 8344-8353.

Ren, Z., Riley, N.J., Garcia, E.P., Sanders, J.M., Swanson, G.T., and Marshall, J. (2003a). Multiple trafficking signals regulate kainate receptor KA2 subunit surface expression. J Neurosci *23*, 6608-6616.

Ren, Z., Riley, N.J., Needleman, L.A., Sanders, J.M., Swanson, G.T., and Marshall, J. (2003b). Cell surface expression of GluR5 kainate receptors is regulated by an endoplasmic reticulum retention signal. J Biol Chem *278*, 52700-52709.

Rhee, J.S., Betz, A., Pyott, S., Reim, K., Varoqueaux, F., Augustin, I., Hesse, D., Sudhof, T.C., Takahashi, M., Rosenmund, C., and Brose, N. (2002). Beta phorbol ester- and diacylglycerol-induced augmentation of transmitter release is mediated by Munc13s and not by PKCs. Cell *108*, 121-133.

Rodriguez-Moreno, A., Herreras, O., and Lerma, J. (1997). Kainate receptors presynaptically downregulate GABAergic inhibition in the rat hippocampus. Neuron *19*, 893-901.

Rosenmund, C., Carr, D.W., Bergeson, S.E., Nilaver, G., Scott, J.D., and Westbrook, G.L. (1994). Anchoring of protein kinase A is required for modulation of AMPA/kainate receptors on hippocampal neurons. Nature *368*, 853-856.

Rosenmund, C., Stern-Bach, Y., and Stevens, C.F. (1998). The tetrameric structure of a glutamate receptor channel. Science *280*, 1596-1599.

Rosenmund, C., and Stevens, C.F. (1996). Definition of the readily releasable pool of vesicles at hippocampal synapses. Neuron *16*, 1197-1207.

Rudolph, U., and Mohler, H. (2004). Analysis of GABAA receptor function and dissection of the pharmacology of benzodiazepines and general anesthetics through mouse genetics. Annu Rev Pharmacol Toxicol *44*, 475-498.

Saliba, R.S., Michels, G., Jacob, T.C., Pangalos, M.N., and Moss, S.J. (2007). Activity-dependent ubiquitination of GABA(A) receptors regulates their accumulation at synaptic sites. J Neurosci *27*, 13341-13351.

Sans, N., Prybylowski, K., Petralia, R.S., Chang, K., Wang, Y.X., Racca, C., Vicini, S., and Wenthold, R.J. (2003). NMDA receptor trafficking through an interaction between PDZ proteins and the exocyst complex. Nat Cell Biol *5*, 520-530.

Sans, N., Racca, C., Petralia, R.S., Wang, Y.X., McCallum, J., and Wenthold, R.J. (2001). Synapse-associated protein 97 selectively associates with a subset of AMPA receptors early in their biosynthetic pathway. J Neurosci *21*, 7506-7516.

Sassoe-Pognetto, M., Panzanelli, P., Sieghart, W., and Fritschy, J.M. (2000). Colocalization of multiple GABA(A) receptor subtypes with gephyrin at postsynaptic sites. J Comp Neurol *420*, 481-498.

Savelyeva, L., Sagulenko, E., Schmitt, J.G., and Schwab, M. (2006). The neurobeachin gene spans the common fragile site FRA13A. Hum Genet *118*, 551-558.

Scheiffele, P., Fan, J., Choih, J., Fetter, R., and Serafini, T. (2000). Neuroligin expressed in nonneuronal cells triggers presynaptic development in contacting axons. Cell *101*, 657-669.

Schikorski, T., and Stevens, C.F. (1997). Quantitative ultrastructural analysis of hippocampal excitatory synapses. J Neurosci *17*, 5858-5867.

Schluter, O.M., Xu, W., and Malenka, R.C. (2006). Alternative N-terminal domains of PSD-95 and SAP97 govern activity-dependent regulation of synaptic AMPA receptor function. Neuron *51*, 99-111.

Schmitz, D., Mellor, J., and Nicoll, R.A. (2001). Presynaptic kainate receptor mediation of frequency facilitation at hippocampal mossy fiber synapses. Science *291*, 1972-1976.

Schnell, E., Sizemore, M., Karimzadegan, S., Chen, L., Bredt, D.S., and Nicoll, R.A. (2002). Direct interactions between PSD-95 and stargazin control synaptic AMPA receptor number. Proc Natl Acad Sci U S A *99*, 13902-13907.

Scott, D.B., Blanpied, T.A., Swanson, G.T., Zhang, C., and Ehlers, M.D. (2001). An NMDA receptor ER retention signal regulated by phosphorylation and alternative splicing. J Neurosci *21*, 3063-3072.

Setou, M., Nakagawa, T., Seog, D.H., and Hirokawa, N. (2000). Kinesin superfamily motor protein KIF17 and mLin-10 in NMDA receptor-containing vesicle transport. Science *288*, 1796-1802.

Setou, M., Seog, D.H., Tanaka, Y., Kanai, Y., Takei, Y., Kawagishi, M., and Hirokawa, N. (2002). Glutamate-receptor-interacting protein GRIP1 directly steers kinesin to dendrites. Nature *417*, 83-87.

Shamloula, H.K., Mbogho, M.P., Pimentel, A.C., Chrzanowska-Lightowlers, Z.M., Hyatt, V., Okano, H., and Venkatesh, T.R. (2002). rugose (rg), a Drosophila A kinase anchor protein, is required for retinal pattern formation and interacts genetically with multiple signaling pathways. Genetics *161*, 693-710.

Shapira, M., Zhai, R.G., Dresbach, T., Bresler, T., Torres, V.I., Gundelfinger, E.D., Ziv, N.E., and Garner, C.C. (2003). Unitary assembly of presynaptic active zones from piccolo-bassoon transport vesicles. Neuron *38*, 237-252.

Shen, K., and Meyer, T. (1999). Dynamic control of CaMKII translocation and localization in hippocampal neurons by NMDA receptor stimulation. Science *284*, 162-166.

Shen, K., Teruel, M.N., Subramanian, K., and Meyer, T. (1998). CaMKIIbeta functions as an F-actin targeting module that localizes CaMKIIalpha/beta heterooligomers to dendritic spines. Neuron *21*, 593-606.

Shen, L., Liang, F., Walensky, L.D., and Huganir, R.L. (2000). Regulation of AMPA receptor GluR1 subunit surface expression by a 4. 1N-linked actin cytoskeletal association. J Neurosci *20*, 7932-7940.

Sheng, M. (2001). Molecular organization of the postsynaptic specialization. Proc Natl Acad Sci U S A *98*, 7058-7061.

Sheng, M., and Pak, D.T. (2000). Ligand-gated ion channel interactions with cytoskeletal and signaling proteins. Annu Rev Physiol *62*, 755-778.

Shi, S., Hayashi, Y., Esteban, J.A., and Malinow, R. (2001). Subunit-specific rules governing AMPA receptor trafficking to synapses in hippocampal pyramidal neurons. Cell *105*, 331-343.

Shin, H., Wyszynski, M., Huh, K.H., Valtschanoff, J.G., Lee, J.R., Ko, J., Streuli, M., Weinberg, R.J., Sheng, M., and Kim, E. (2003). Association of the kinesin motor KIF1A with the multimodular protein liprin-alpha. J Biol Chem *278*, 11393-11401.

Sholl, D.A. (1953). Dendritic organization in the neurons of the visual and motor cortices of the cat. J Anat *87*, 387-406.

Sieghart, W., and Sperk, G. (2002). Subunit composition, distribution and function of GABA(A) receptor subtypes. Curr Top Med Chem *2*, 795-816.

Smith, M.J., Pozo, K., Brickley, K., and Stephenson, F.A. (2006). Mapping the GRIF-1 binding domain of the kinesin, KIF5C, substantiates a role for GRIF-1 as an adaptor protein in the anterograde trafficking of cargoes. J Biol Chem *281*, 27216-27228.

Spacek, J., and Harris, K.M. (1997). Three-dimensional organization of smooth endoplasmic reticulum in hippocampal CA1 dendrites and dendritic spines of the immature and mature rat. J Neurosci *17*, 190-203.

Spritz, R.A. (1998). Genetic defects in Chediak-Higashi syndrome and the beige mouse. J Clin Immunol *18*, 97-105.

Steigerwald, F., Schulz, T.W., Schenker, L.T., Kennedy, M.B., Seeburg, P.H., and Kohr, G. (2000). C-Terminal truncation of NR2A subunits impairs synaptic but not extrasynaptic localization of NMDA receptors. J Neurosci *20*, 4573-4581.

Su, Y., Balice-Gordon, R.J., Hess, D.M., Landsman, D.S., Minarcik, J., Golden, J., Hurwitz, I., Liebhaber, S.A., and Cooke, N.E. (2004). Neurobeachin is essential for neuromuscular synaptic transmission. J Neurosci *24*, 3627-3636.

Sudhof, T.C. (2004). The synaptic vesicle cycle. Annu Rev Neurosci *27*, 509-547.

Takahashi, T., Momiyama, A., Hirai, K., Hishinuma, F., and Akagi, H. (1992). Functional correlation of fetal and adult forms of glycine receptors with developmental changes in inhibitory synaptic receptor channels. Neuron *9*, 1155-1161.

Takai, Y., Shimizu, K., and Ohtsuka, T. (2003). The roles of cadherins and nectins in interneuronal synapse formation. Curr Opin Neurobiol *13*, 520-526.

Takamori, S., Rhee, J.S., Rosenmund, C., and Jahn, R. (2000). Identification of a vesicular glutamate transporter that defines a glutamatergic phenotype in neurons. Nature *407*, 189-194.

Tessier-Lavigne, M. (1995). Eph receptor tyrosine kinases, axon repulsion, and the development of topographic maps. Cell *82*, 345-348.

Torre, E.R., and Steward, O. (1996). Protein synthesis within dendrites: glycosylation of newly synthesized proteins in dendrites of hippocampal neurons in culture. J Neurosci *16*, 5967-5978.

Varoqueaux, F., Aramuni, G., Rawson, R.L., Mohrmann, R., Missler, M., Gottmann, K., Zhang, W., Sudhof, T.C., and Brose, N. (2006). Neuroligins determine synapse maturation and function. Neuron *51*, 741-754.

Varoqueaux, F., Sigler, A., Rhee, J.S., Brose, N., Enk, C., Reim, K., and Rosenmund, C. (2002). Total arrest of spontaneous and evoked synaptic transmission but normal synaptogenesis in the absence of Munc13-mediated vesicle priming. Proc Natl Acad Sci U S A *99*, 9037-9042.

Verhage, M., Maia, A.S., Plomp, J.J., Brussaard, A.B., Heeroma, J.H., Vermeer, H., Toonen, R.F., Hammer, R.E., van den Berg, T.K., Missler, M.*, et al.* (2000). Synaptic assembly of the brain in the absence of neurotransmitter secretion. Science *287*, 864-869.

Vignes, M., and Collingridge, G.L. (1997). The synaptic activation of kainate receptors. Nature *388*, 179-182.

Waites, C.L., Craig, A.M., and Garner, C.C. (2005). Mechanisms of vertebrate synaptogenesis. Annu Rev Neurosci *28*, 251-274.

Wang, H., Bedford, F.K., Brandon, N.J., Moss, S.J., and Olsen, R.W. (1999). GABA(A)-receptor-associated protein links GABA(A) receptors and the cytoskeleton. Nature *397*, 69-72.

Wang, J.W., Howson, J., Haller, E., and Kerr, W.G. (2001). Identification of a novel lipopolysaccharide-inducible gene with key features of both A kinase anchor proteins and chs1/beige proteins. J Immunol *166*, 4586-4595.

Wang, N., Wu, W.I., and De Lozanne, A. (2002). BEACH family of proteins: phylogenetic and functional analysis of six Dictyostelium BEACH proteins. J Cell Biochem *86*, 561-570.

Wang, X., Herberg, F.W., Laue, M.M., Wullner, C., Hu, B., Petrasch-Parwez, E., and Kilimann, M.W. (2000). Neurobeachin: A protein kinase A-anchoring, beige/Chediak-higashi protein homolog implicated in neuronal membrane traffic. J Neurosci *20*, 8551-8565.

Watanabe, E., and Akagi, H. (1995). Distribution patterns of mRNAs encoding glycine receptor channels in the developing rat spinal cord. Neurosci Res *23*, 377-382.

Wenthold, R.J., Petralia, R.S., Blahos J, II, and Niedzielski, A.S. (1996a). Evidence for multiple AMPA receptor complexes in hippocampal CA1/CA2 neurons. J. Neurosci. *16*, 1982-1989.

Wenthold, R.J., Petralia, R.S., Blahos, J., II, and Niedzielski, A.S. (1996b). Evidence for multiple AMPA receptor complexes in hippocampal CA1/CA2 neurons. J Neurosci *16*, 1982-1989.

Wenthold, R.J., Prybylowski, K., Standley, S., Sans, N., and Petralia, R.S. (2003). TRAFFICKING OF NMDA RECEPTORS1. Annu Rev Pharmaco Toxicol *43*, 335-358.

Williams, K., Russell, S.L., Shen, Y.M., and Molinoff, P.B. (1993). Developmental switch in the expression of NMDA receptors occurs in vivo and in vitro. Neuron *10*, 267-278.

Wojcik, S.M., and Brose, N. (2007). Regulation of membrane fusion in synaptic excitation-secretion coupling: speed and accuracy matter. Neuron *55*, 11-24.

Wojcik, S.M., Katsurabayashi, S., Guillemin, I., Friauf, E., Rosenmund, C., Brose, N., and Rhee, J.S. (2006). A shared vesicular carrier allows synaptic corelease of GABA and glycine. Neuron *50*, 575-587.

Wojcik, S.M., Rhee, J.S., Herzog, E., Sigler, A., Jahn, R., Takamori, S., Brose, N., and Rosenmund, C. (2004). An essential role for vesicular glutamate transporter 1 (VGLUT1) in postnatal development and control of quantal size. Proc Natl Acad Sci U S A *101*, 7158-7163.

Wong, W., and Scott, J.D. (2004). AKAP signalling complexes: focal points in space and time. Nat Rev Mol Cell Biol *5*, 959-970.

Wyszynski, M., Kim, E., Dunah, A.W., Passafaro, M., Valtschanoff, J.G., Serra-Pages, C., Streuli, M., Weinberg, R.J., and Sheng, M. (2002). Interaction between GRIP and liprin-alpha/SYD2 is required for AMPA receptor targeting. Neuron *34*, 39-52.

Xia, J., Zhang, X., Staudinger, J., and Huganir, R.L. (1999). Clustering of AMPA receptors by the synaptic PDZ domain-containing protein PICK1. Neuron *22*, 179-187.

Zamanillo, D., Sprengel, R., Hvalby, O., Jensen, V., Burnashev, N., Rozov, A., Kaiser, K.M., Koster, H.J., Borchardt, T., Worley, P.*, et al.* (1999). Importance of AMPA receptors for hippocampal synaptic plasticity but not for spatial learning. Science *284*, 1805-1811.

Zhai, R.G., Vardinon-Friedman, H., Cases-Langhoff, C., Becker, B., Gundelfinger, E.D., Ziv, N.E., and Garner, C.C. (2001). Assembling the presynaptic active zone: a characterization of an active one precursor vesicle. Neuron *29*, 131-143.

Zhao, H., Boissy, Y.L., Abdel-Malek, Z., King, R.A., Norlund, J.J., and Boissy, R.E. (1994). On the analysis of the pathophysiology of Chediak-Higashi syndrome. Defects expressed by cultured melanocytes. Lab Invest *71*, 25-34.

Zhong, H., Sia, G.M., Sato, T.R., Gray, N.W., Mao, T., Khuchua, Z., Huganir, R.L., and Svoboda, K. (2009). Subcellular dynamics of type II PKA in neurons. Neuron *62*, 363-374.

Zhu, J.J., Esteban, J.A., Hayashi, Y., and Malinow, R. (2000). Postnatal synaptic potentiation: delivery of GluR4-containing AMPA receptors by spontaneous activity. Nat Neurosci *3*, 1098-1106.

Zhu, J.J., Qin, Y., Zhao, M., Van Aelst, L., and Malinow, R. (2002). Ras and Rap control AMPA receptor trafficking during synaptic plasticity. Cell *110*, 443-455.

9 Curriculum Vitae

Personal information

Name:	Ramya Nair
Address:	Goethe Alle 7A, Goettingen D-37073, Germany
Telephone:	+4917666197650
Email:	ramyanair85@gmail.com
Date of birth:	19th September 1985
Nationality:	Indian

Education

Oct 2007-2010	Max Planck Institute for Experimental Medicine PhD at the Department of Molecular Neurobiology Under the supervision of Prof. Nils Brose and Dr. JeongSeop Rhee
Sept 2006-2007	International Max Planck Research School MSc/PhD Neuroscience Program St. Stephen's College, Delhi University BSc (Hons) Chemistry

Scholarships

2007-2010	IMPRS PhD stipend
2006-2007	IMPRS MSc stipend

Scientific Meetings and Courses

Gordon Research Conference 2008 Neurobiology of Brain Disorders (Oxford)

Society for Neuroscience 2009 (Chicago)

8th German Neuroscience Society Meeting 2009 (Goettingen, Germany)

Federation of European Neuroscience Meeting 2010 (Amsterdam)

5th Westerberger Herbsttagung and Molecular Neurobiology Meeting (Osnabruck; 2nd Poster Prize).

Advanced Microscopy Course Olympus 2009 (Goettingen Germany)

FENS Neurotrain Program: Neuroplasticity and Neurodegenerative Disorders: Dysfunction and Treatments 2008 (Innsbruck, Austria)

10 Publication list

1. **R. Nair**, J. Lauks, S. Jung, N. Brose, M.W. Kilimann, M. Verhage and J.S Rhee. Neurobeachin is a novel regulator of functional receptors. Review JCB.
2. E. Reisinger, C. Bresee, J.Neef, **R. Nair**, K. Reuter, A. Bulankina, R. Nouvian, M. Koch, L. Kastrup, I. Roux, C. Petit, S. Hell, N. Brose, J.S. Rhee, S. Kuegler, J. Brigande, and T. Moser. Probing the functional equivalence of otoferlin and synaptotagmin 1 in exocytosis. Accepted in Journal of Neuroscience.
3. J.Yang, J. Seo, **R. Nair**, S. Han, S. Jang, K. Kim, K. Han, S. K. Paik, J. Choi, S. Lee, Y. C. Bae, M. K. Topham, S. M. Prescott, J.S. Rhee, S. Y. Choi and E. Kim. DGKi regulates presynaptic release during mGluR-dependent LTD. EMBO J. 2011 Jan 5; 30(1): 165-80.